EUROPEAN ORGANIZATION FOR NUCLEAR RESEARCH

CERN-PPE/95-147
October 12, 1995

Physics of Tau Leptons

Simonetta Gentile
Università di Roma, La Sapienza, and INFN, Sezione di Roma, Italy

and

Martin Pohl
Labor für Hochenergiephysik, ETH Zürich, Switzerland

Abstract

We review the current status of τ physics from an experimental point of view. Results from all experiments that have observed $e^+e^- \to \tau^+\tau^-$, from threshold to LEP energies, are summarized and discussed. Recent results on static properties of the $\tau^\pm$ and the ν_τ, such as mass and spin, are reported. We then analyze the world data on the production of τ pairs by the electroweak neutral current interaction. Decay properties of the τ lepton by the weak charged current are discussed. For the electroweak sector, we compare the properties of the three lepton generations. Since the τ lepton also decays into hadrons, resonance production by the weak charged current is studied and information on final state strong interactions is achieved. Finally, we comment on the implications of τ physics results in the search for new particles and new interactions.

(Submitted to *Physics Reports*)

Contents

Chapter 1

Introduction

The physics of the third generation lepton family is a subject that combines simplicity in principle with complexity in practice. It is simple since the τ lepton and its neutrino appear to be elementary, sequential leptons just like the electron and the muon. Its analysis is rather complex because of its many decay modes and short lifetime.

A couple of intriguing questions immediately comes to mind when thinking about the objects of this review. The first one is the obvious question of why the third generation of elementary matter constituents exists at all, a question equally valid as for the second generation. And, as the measurement of the number of light neutrino families at LEP indicates, the τ family may well be the last one for which this question can be asked. In the approach to an answer, one faces a pair of related questions:

1. Are the τ and its neutrino truly elementary, i.e. pointlike and structureless?
2. Is the τ a sequential lepton, with the same vertices and couplings as the electron and the muon?

Should the answer to both of these questions really be yes, one would be dealing with just another lepton like the ones defined as the matter contents of the Standard Model [1], distinguished from the first two lepton generations only by its mass and its own conserved lepton number. Would a deviation from this baseline be observed one would hope that indeed progress could be made to find the raison d'être for a lepton almost twice as heavy as the proton. Even in the framework of the standard model, the asymmetry between leptons, whose mass eigenstates and weak eigenstates seem to coincide, and quarks, for which this is manifestly not the case, is most remarkable and disturbing.

Twenty years after its discovery [2], e^+e^- reactions have stayed the only abundant source of τ leptons to date. Four generations of experiments have been performed covering the energy region from threshold to the mass of the Z boson. The experimental approach to the above questions has stayed constant:

- to measure the static properties of the τ and its neutrino, especially their masses, with high precision;

- to study their production by the electroweak neutral current and their decay by the weak charged current;
- to search for interactions of τ neutrinos and possible oscillations between ν_τ and other neutrino species.

In addition to these rather classic features of experimentation with leptons, a new element enters in that the τ lepton is the only one heavy enough to decay hadronically. This opens the possibility to study the hadronic current at rather low momentum transfer in a simple experimental environment.

The history of τ physics has been reviewed elsewhere [3]. The purpose of this paper is to systematically collect the currently existing data and review them under the above aspects. Preference is given to recent results and, wherever possible, to published data; earlier τ results have been summarized in previous reviews [4–6]. The organization of the paper is as follows. We first summarize the experimental conditions for the four generations of τ lepton experiments, from threshold to the Z pole. We then review the current knowledge of the static properties of τ and ν_τ. The following two chapters are devoted to the measurements of the electroweak couplings of τ and ν_τ. Strong interactions in τ decay are then covered, both for exclusive charged hadronic currents and for inclusive final state interactions at low momentum transfer. A final chapter collects results of searches for new physics in which the τ lepton enters as a powerful tool.

Chapter 2

Experimental conditions for $e^+e^- \to \tau^+\tau^-$

Although τ leptons have been observed at hadron colliders [7–9], e^+e^- experiments remain the major contributors to the study of their properties and interactions.

An overview of e^+e^- experiments which have published results on τ leptons shows that they densely cover the energy range from threshold all the way to the Z pole. One can identify the following main energy domains:

1. Threshold region: SPEAR and BEPC
2. Heavy quark resonance region: CESR and DORIS
3. Electroweak interference region: PETRA, PEP and TRISTAN
4. Z region: SLC and LEP

Fig. 2.1 gives an overview of the τ production cross section in these energy regions, without showing enhancements by hadronic resonances such as the Υ. All data are radiatively corrected so that they can be directly compared to Born level Standard Model predictions. This procedure is not very accurate, especially close to the Z resonance, so that this only gives a qualitative picture. A more precise analysis, which does full justice to the impressive experimental accuracy at the Z pole, will be described in chapter 4.

The methods to separate $e^+e^- \to \tau^+\tau^-$ from concurrent e^+e^- reactions are based on

- apparent lepton number violation in the visible final state, such as $e^+e^- \to \tau^+\tau^- \to (e\nu\nu)\ (\mu\nu\nu)$ or $\to$ (h $n\pi^0\ \nu$) (e/μ $\nu\nu$);
- combinations of other specific decay modes in a single tag or double tag configuration;
- two low multiplicity, narrow jets of particles.

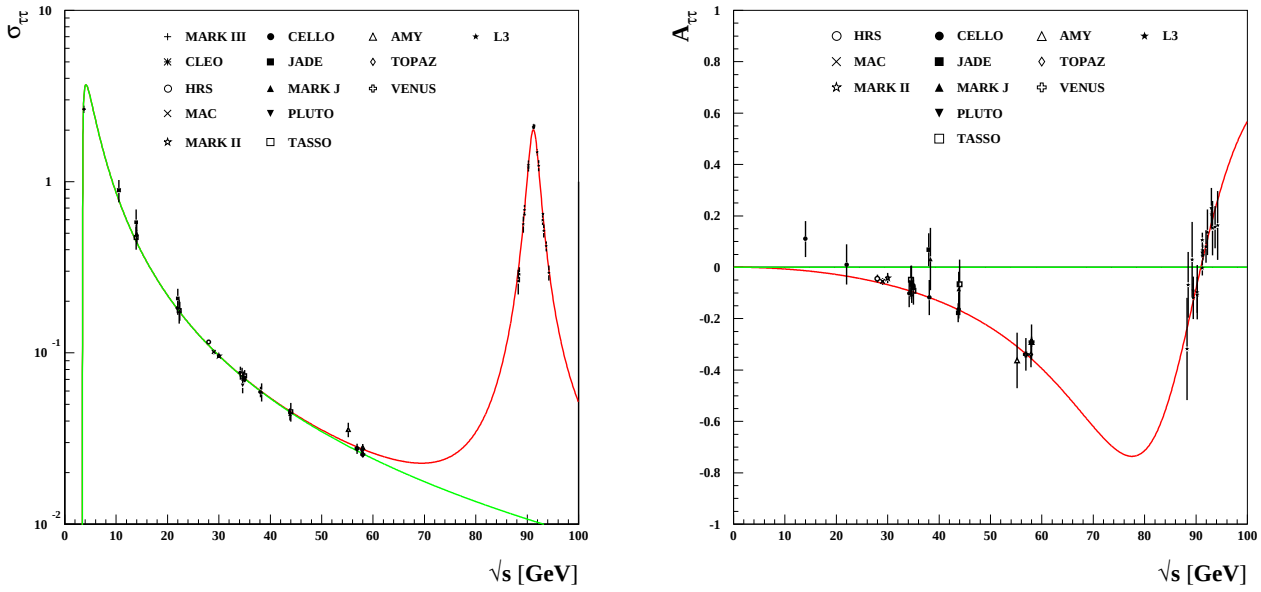

Figure 2.1: The center-of-mass energy dependence of the $\tau^+\tau^-$Born cross section and forward-backward charge asymmetry (without enhancements by heavy quark resonances). Also shown are experimental results covering the whole energy region from threshold to the mass of the Z boson [10–41]. All data have been radiatively corrected to allow for a qualitative comparison with electroweak theory at the Born level.

Main backgrounds to $e^+e^- \to \tau^+\tau^-$ are fluctuations towards low multiplicity in $e^+e^- \to$ hadrons, $e^+e^- \to e^+e^-(\gamma)$, $e^+e^- \to \mu^+\mu^-(\gamma)$, as well as the four fermion reactions $e^+e^- \to e^+e^-l\bar{l}$ and $e^+e^- \to e^+e^-$hadrons. Their relative importance varies considerably with energy. As a consequence, the τ decay modes amenable to a clean selection as well as the selection efficiency and purity are very much energy dependent. In general one can observe that the selection of tau lepton samples becomes more complete and purer with increasing energy.

Table 2.1 lists the pioneering experiments at SPEAR [2, 10, 42–52] and DORIS [53–62], at threshold and in the region of heavy quark resonances (3 to 11 GeV). Due to the fact that τ branching fractions were not very well established at the time, experiments usually restricted their analysis to the leptonic decay modes with apparent lepton flavor violation in the visible final state, like $e^+e^- \to \tau^+\tau^- \to (e\nu\nu)\ (\mu\nu\nu)$ or $\to (h\nu)\ (e/\mu\nu\nu)$. This resulted in high purity samples (55 to 94% depending on details of the selection), but at the expense of low detection efficiencies (15 to 2%).

Experiments in this energy region are still being continued very successfully at CESR [11, 63–83], at BEPC [84–87], and until recently at DORIS II [88–109]. Tab. 2.2 shows an overview of recent samples on which published analysis has been based. Clearly the CLEO experiment at CESR holds the world record in both produced and detected sample size. In the region of the Υ resonances, the boost of τ lepton decays is already sufficient and the multiplicity of hadronic background high enough to base a $\tau^+\tau^-$ event selection on topological criteria, which are less aimed at specific decay modes. Nevertheless, detection efficiencies are in the 15% region when a purity above 90% is required.

Experiment	$\sqrt{s}$ [GeV]	$\mathcal{L}$ [pb^{-1}]	$N_{\tau^+\tau^-}$
SLAC-LBL	3.8-7.8	16	86
MARK II	3.5-6.7	21	2150
DELCO	3.1-7.4		692
MARK III	3.77	9.4	500
DESY-Hdlb.	3.6-4.4	3	299
DASP	3.1-5.2	7	93

Table 2.1: Early experiments at τ threshold and in the resonance region at SPEAR [2,10,42–52] and DORIS [53–62]. The event samples consist predominantly of leptonic τ decays.

Experiment	$\sqrt{s}$ [GeV]	$\mathcal{L}$ [pb^{-1}]	$N_{\tau^+\tau^-}$
BES	3.5-3.6	5	1600
CLEO	10.6	2050	1870000
ARGUS	9.4-10.6	387	373000

Table 2.2: Recent experiments at τ threshold and in the resonance region at BEPC [84–87], CESR [11,63–83], and DORIS [88–106].

Experiment	$\sqrt{s}$ [GeV]	$\mathcal{L}$ [pb^{-1}]	$N_{\tau^+\tau^-}$
CELLO	14-47	137	4116
JADE	14-47	210	6182
MARK J	14-47	214	2197
PLUTO	35	42	419
TASSO	14-47	227	1310
MAC	29	216	7035
Mark II	29	220	8200
HRS	29	300	6507
TPC	29	140	5000
AMY	52-58	160	1310
TOPAZ	52-61	74	572
VENUS	50-61	27	283

Table 2.3: Experiments in the region of electroweak interference, at PETRA [16–31,110–122], PEP [12–15,123–161] and TRISTAN [32–36].

Due to the low total cross section, experimentation in the region of maximum electroweak interference (15 to 60 GeV) is difficult. However, τ events are rather easily recognized as low multiplicity, narrow back-to-back jets of particles. Separation of $\tau^+\tau^-$ final states from concurrent reactions becomes progressively easier with increasing energy, and substantial samples of $\tau^+\tau^-$ final states have been collected at PETRA [16–31,110–122], PEP [12–15,123–161] and TRISTAN [32–36] in this interesting energy domain. Tab. 2.3 shows an overview of published statistics. Already here, the large average multiplicities in $e^+e^- \to$ hadron background and the characteristic τ decay kinematics allow for 95% pure separation at efficiencies approaching 30 to 40%.

Experiment	$\sqrt{s}$ [GeV]	$\mathcal{L}$ [pb^{-1}]	$N_{\tau^+\tau^-}$
MARK II	92	0.2	21
SLD	92	2.2	4522
ALEPH	89-93	122	132000
DELPHI	89-93	77	45000
L3	89-93	118	105000
OPAL	89-93	121	127000

Table 2.4: Experiments in the region of the Z resonance, at SLC [245–248] and LEP [37–41, 162–244]. Note that DELPHI data are only included up to 1993, while the other experiments include preliminary 1994 data.

Since the charged multiplicity of $e^+e^- \rightarrow$ hadrons grows with $\log s$ and the tau decay multiplicity stays small, it is clear that a sample selection based just on topology must be very successful at high energies. As an example, fig. 2.2 shows the observed multiplicity distribution with the contributions of various final states from DELPHI at LEP [162]. Consequently, high efficiencies *and* purities can in fact be obtained simultaneously at energies around the Z pole. Tab. 2.4 shows an overview of published statistics for the LEP [37–41, 162–244] and SLC [245–248] experiments. Sample purities close to 100% and efficiencies of order 70% result. This is very important in that it not only provides high statistical accuracy to $\tau^+\tau^-$ data but that it also establishes samples with low bias on the decay channel and the decay kinematics. This matters especially for the study of high multiplicity τ decays and the measurement of τ polarization. Chapters 4 and 5 will provide details on these measurements. Moreover, the Z resonance sufficiently enhances the production cross section to allow for samples of order 100000 $\tau^+\tau^-$ final states to be collected and analyzed by each LEP experiment to date.

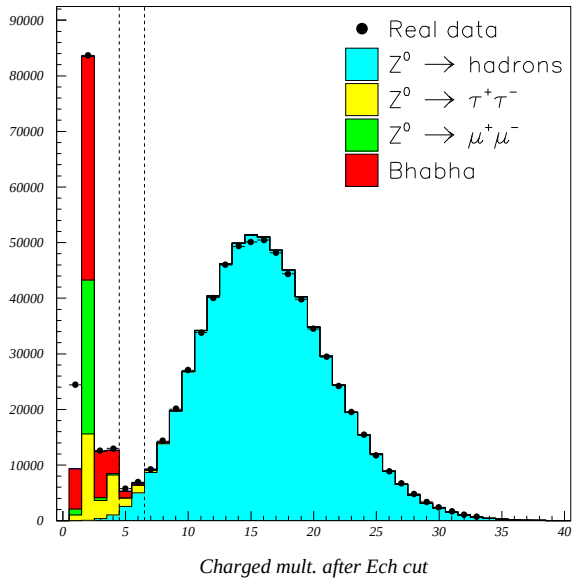

Figure 2.2: The observed multiplicity distribution of charged particles from DELPHI at LEP [162]. Also shown are the contributions of various final states as determined by Monte Carlo calculation.

Chapter 3

Static properties of τ leptons

3.1 The mass of the τ lepton

The masses of fundamental constituents of matter, leptons and quarks, are basic parameters of the Standard Model. They are not predicted by the model and have to be fixed experimentally. Masses are of fundamental importance since they distinguish between the generations. They are also of great practical importance, since they enter into all rate calculations through phase space factors with a high exponent. To a lesser extent, they are also important as arguments of the running coupling constants of the theory.

Probably the best example to show that precision measurements of the charged lepton masses are of prime importance is the consistency check on lepton universality by comparing the leptonic width of the muon and the tau (see section 5.1). In the calculation of the width for $\tau^- \to e^- \bar{\nu}_e \nu_\tau$, the tau mass enters as the fifth power, the results are thus very sensitive to the experimental uncertainty on this parameter. The measurement of the τ mass by DELCO in 1978 [47], later corrected by the Particle Data Group to take into account a precise recalibration via the $\psi(2S)$ mass from resonant depolarisation [249,250], dominated the world average for over a decade until 1992. The DELCO result, $m_\tau = 1783^{+3}_{-4}$ MeV, was extracted from an analysis of the $e^+e^- \to \tau^+\tau^-$ excitation curve at threshold. The limited statistics of the measurement and the non-optimum distribution of energy points in the threshold scan severely limited the accuracy of the mass measurement. However, the rather wide range in energy covered by the experiment allowed to unambiguously conclude that the tau spin is 1/2.

As the accuracy of the ingredients into the measurement of the tau leptonic width increased, an apparent violation of leptonic universality at the level of two standard deviations started to appear (see e.g. [251]). In addition, and equally importantly, the large uncertainty in the tau lepton mass limited the obtainable accuracy in upper limits to the tau neutrino mass.

The mass accuracy for the three lepton families has reached a precision of $\Delta m/m$ of 10^{-7} for electron and muon [252]. Only recently, the tau mass measurement has entered into the sub-permill region. In the following, the most recent and most accurate measurements will be discussed. ARGUS, and later CLEO, have used the kinematics of hadronic tau decays to obtain a mass value with high statistics, high accuracy measurements far above threshold. The

threshold scan has been repeated with a stepwise refinement method in a dedicated experiment by the BES collaboration at BEPC.

3.1.1 Excitation curve at threshold

This method is based on the measurement of the $e^+e^- \to \tau^+\tau^-$ cross section in the region most sensitive to m_τ, a few MeV around threshold. The energy dependence of the total or visible cross section is interpreted in the Standard Model to derive the τ mass. This method, pioneered at SPEAR by DELCO to obtain the first accurate mass value [47], has recently been repeated at BEPC with the BES detector [84,86,87]. In their threshold scan, a data driven scan strategy was used to adjust the center of mass energy of each scan point in order to reach maximum sensitivity on the tau lepton mass. The sensitivity is amplified by the fact that the $\tau^+\tau^-$ cross section has a finite step at threshold, due to Coulomb interactions [253,254].

The first BES measurement, based on a small event sample of the type $\tau^+\tau^- \to e\mu + 4\nu$ [84], was restricted to the $e\mu$ topology to guarantee an essentially background free sample. The data were collected at ten different energies within a range of 24 MeV around threshold, with an integrated luminosity of $\simeq 4.3$ pb^{-1}. The selected sample consisted of 14 $e\mu$ events with a negligible background of 0.12 events. This background, crucial to the accuracy of the mass measurement, was estimated by applying the same selection to a sample taken at the J/ψ energy. Measurements of the J/ψ peak were also used to calibrate the beam energy scale.

The likelihood function used to estimate m_τ is the product of Poisson probabilities, defined at each center of mass energy, to obtain the observed number of events given a mass dependent prediction. The predicted number of events is

$$N = \mathcal{L}[\epsilon B \sigma(\sqrt{s}, m_\tau) + \sigma_B] \tag{3.1}$$

where $\mathcal{L}$ is the integrated luminosity, B the product of semileptonic branching fractions corresponding to the signature, ϵ the signal detection efficiency and σ_B the accepted part of the background cross-sections. The function $\sigma(\sqrt{s}, m_\tau)$ is the Standard Model cross section for $\tau^+\tau^-$production including radiative corrections and integrated over the spread in the center of mass energy, $\sqrt{s}$, $\sigma_{\sqrt{s}} \simeq 1.4$ MeV.

With a two dimensional maximum likelihood fit, the values of m_τ and ϵ, the overall absolute efficiency to detect $\tau^+\tau^-$events, are determined. Thus, uncertainties in the luminosity scale, the trigger and detector efficiencies are implicitly taken into account. The value of ϵ is then fixed to the fit result and a value for m_τ obtained from a one parameter fit, its error is included in the systematics. As independent sources of systematic error were considered: uncertainties in the product $\epsilon B\mathcal{L}$, that contributed $\Delta m_\tau = ^{+0.16}_{-0.20}$ MeV, the absolute beam energy scale ($\Delta m_\tau = \pm 0.09$ MeV), the uncertainty in the beam energy spread ($\Delta m_\tau = \pm 0.02$ MeV) and the background ($\Delta m_\tau = \pm 0.01$ MeV). Combining these systematic error in quadrature, the BES result on the mass of τ lepton from dilepton events was $m_\tau = 1776.9^{+0.4}_{-0.5} \pm 0.2$ MeV, where the first error is statistical and the second systematic.

Recently, a re-analysis of the full data sample yielded an improved final result [86,87]. It uses a sample of dilepton as well as lepton-hadron events to obtain larger statistics. These events are

distributed in different decay categories as: ee(4), eμ(18), eπ(19), eK(2), $\mu\mu$(3), $\mu\pi$(5), μK(3), $\pi\pi$(4) and πK(6), for a total of 64 events. Using the same procedure as described above, BES finds a final result of

$$m_\tau = 1776.96^{+0.18+0.20}_{-0.19-0.16}\ \text{MeV} \tag{3.2}$$

The efficiency corrected cross section as function of center of mass, and the result of the likelihood fit are shown in Figure 3.1.

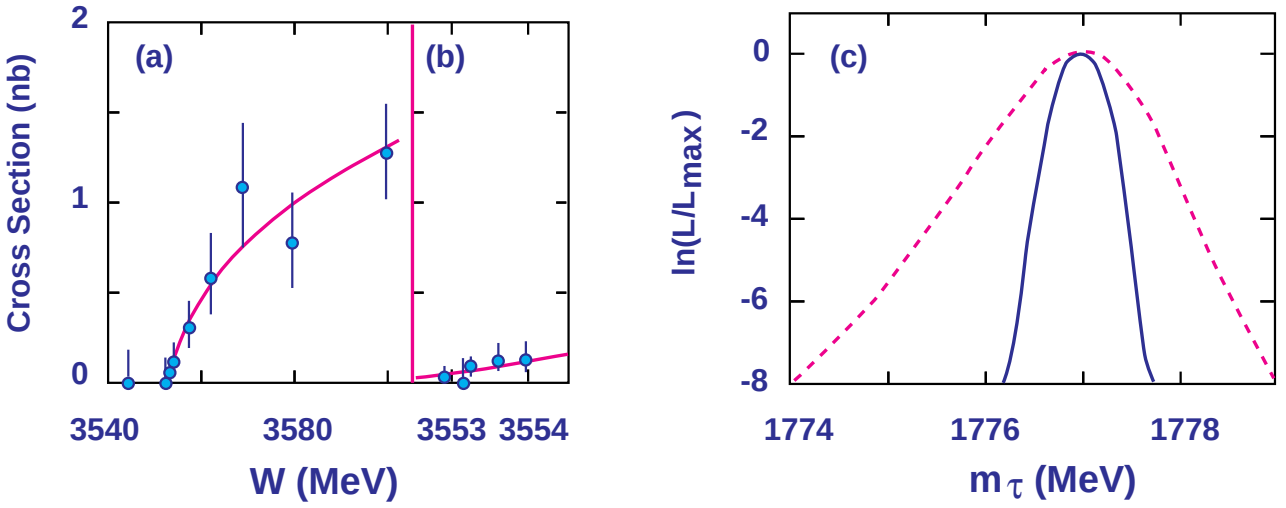

Figure 3.1: a) The center-of-mass energy dependence of the $\tau^+\tau^-$cross section as measured by BES [86] (dots), compared to the result of the likelihood fit (curve). b) An expanded view of the region in the immediate vicinity of the $\tau^+\tau^-$threshold. c) The dependence of the log likelihood on the tau mass, solid curve for the final BES result [87], dashed curve for the result from eμ events alone [84].

3.1.2 Decay kinematics

Another method to measure the tau mass, based on kinematics properties of hadronic τ decays, has been applied by the ARGUS and CLEO collaborations.

The ARGUS Collaboration [101] used a large sample (11K events) of taus decaying into three charged pions, $\tau^- \to \pi^-\pi^-\pi^+\nu_\tau$. The other tau in the event was required to decay in one prong mode. Since the neutrinos escape detection, the event kinematics cannot be completely reconstructed. Nevertheless, approximating the tau direction by the direction of the charged particles, a so-called pseudomass m^*_τ can be defined

$$m^*_\tau = 2(E_\tau - E_{3\pi})(E_{3\pi} - p_{3\pi}) + m^2_{3\pi} \tag{3.3}$$

where $E_\tau \simeq E_b$ is the τ energy, $E_{3\pi}$, $p_{3\pi}$, and $m_{3\pi}$ are the energy, momentum and mass of the three pion system. This quantity tends towards the real tau mass as the neutrino energy goes to zero. The pseudomass spectrum, shown in Figure 3.2 has a sharp cut-off on the high mass side. The position of this edge is directly related to m_τ. The background has only a very slight slope in this area.

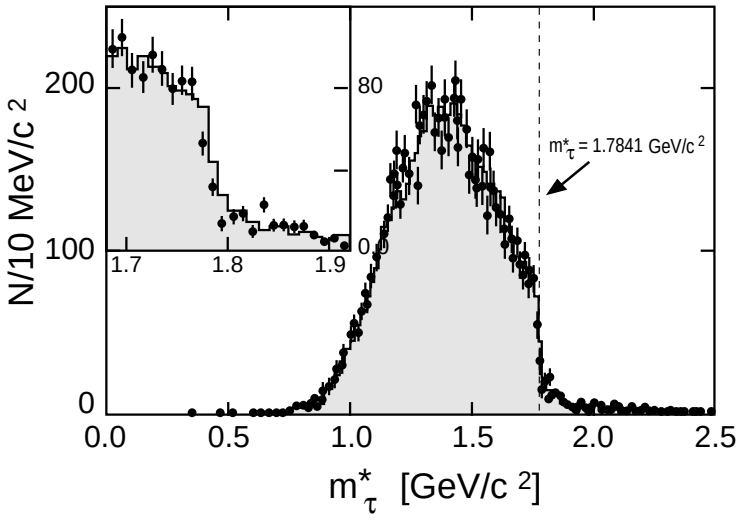

Figure 3.2: Pseudomass distribution from $\tau^- \to \pi^-\pi^-\pi^+\nu_\tau$ showing data (points with error bars) and Monte Carlo simulation (shaded histogram) [101] for a tau mass of 1784.1 MeV. The insert shows an enlarged view of the region at the kinematic limit.

The τ mass has been obtained fitting the measured m_τ^* spectrum using a model function with a sigmoid shape. This shape has been obtained from a Monte Carlo simulation of the measurement at a reference mass of 1784.1 MeV. The measurement was thus reduced to obtaining a small shift with respect to this reference value. In addition, an almost constant background must be added to the fit function. Figure 3.3 shows the data in the region of the kinematic limit, together with the fit result.

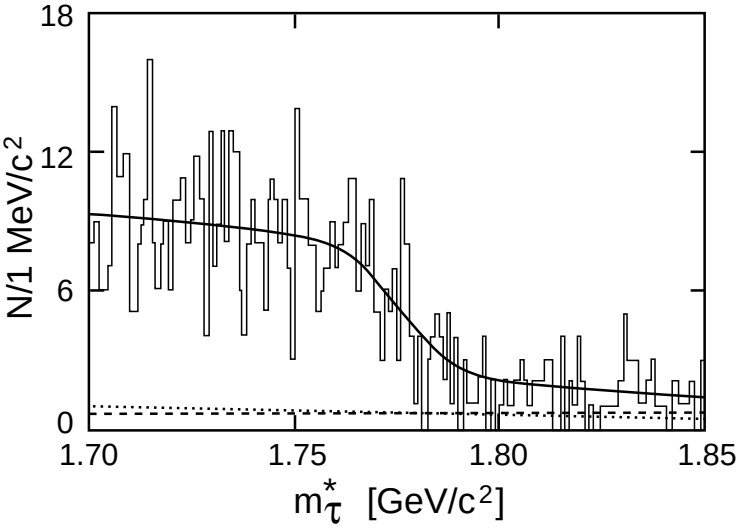

Figure 3.3: m_τ^* distribution from data ARGUS data in the vicinity of the kinematic limit (histogram), together with the result of the fit (solid line) and the background contributions (dashed and dotted curve. [101]

The result obtained from this method is:

$$m_\tau = 1776.3 \pm 2.4 \pm 1.4 \text{ MeV} \tag{3.4}$$

with the first error representing the statistical, the second one systematic uncertainties. The systematic error includes the contribution from uncertainties in the absolute beam energy ($\Delta m_\tau = 0.5$ MeV), the assumption of zero neutrino mass ($\Delta m_\tau = 0.3$ MeV), the absolute momentum scale of the apparatus ($\Delta m_\tau = 1.2$ MeV), and the modeling of the 3π spectra ($\Delta m_\tau = 0.5$ MeV). This result in fact gave the first indication that m_τ is significantly below the previous best value measured by DELCO. Preliminary results from DELPHI [255], using a similar technique, have yielded a mass value of $1778.7 \pm 3.1 \pm 1.3$ MeV.

Using a similar kinematic approach, but with a differently defined sample of decay modes, CLEO obtained a precise value of m_τ soon after [75]. The decay sample consisted of one prong decays. Since the two tau leptons in an event have to be emitted back to back up to radiative corrections, the tau direction can be reconstructed up to a two fold ambiguity just from the two charged tracks and four-momentum conservation. The two tau directions are constrained to lie on cones around the charged particle direction (see Figure 3.4), the opening angle $\cos\theta^\pm$ of the cones depends on the tau mass

$$\cos\theta^\pm = \frac{1}{2p_\tau p_{h^\pm}}\left(m_{\nu_\tau}^2 - m_\tau^2 - m_{h^\pm}^2 + 2E_\tau E_{h^\pm}\right) \tag{3.5}$$

The intersections of one cone with the parity inverted second one thus define the two kinematically allowed tau directions. Varying the mass of the tau, one can determine a lower limit per event, M_m, which is reached when the two cones just touch each other. At CESR energies, the half-angles are small ($\sim 8^\circ$) and the value of M_m is close to m_τ. The M_m distribution shows a characteristic edge, the position of this edge again gives the tau mass.

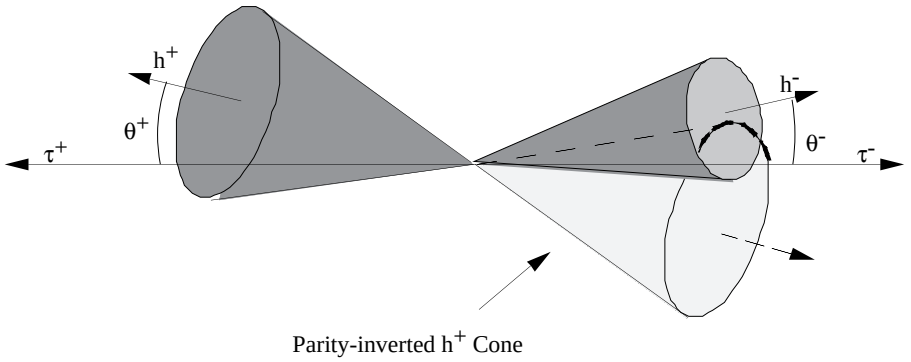

Figure 3.4: The kinematics of $\tau^+\tau^- \to \mathrm{h}^+\bar{\nu}_\tau\mathrm{h}^-\nu_\tau$ [75].

The CLEO sample consists of τ decaying hadronically into one charged particle and 0, 1, or 2 π^0's. Inclusion of additional π^0's reduces the dependence of the result on the absolute knowledge of the momentum scale, but introduces an additional dependence on the energy scale. At least one π^0 is required in the event to reduce background. The value of M_m for each event is calculated from measurements of charged tracks and calorimetric showers, as well as the beam energy. The distribution is shown in Figure 3.5 and indeed shows the expected pile up just below m_τ and a sharp drop beyond. Monte Carlo and experimental M_m distributions are fitted with an empirical shape to extract a mass value. The result is

$$m_\tau = 1777.8 \pm 0.7 \pm 1.7 \text{ MeV} \tag{3.6}$$

where the first error is statistical and the second systematic. The systematic error comes from uncertainties in the momentum scale ($\Delta m_\tau = 0.8$ MeV), the calorimeter energy scale

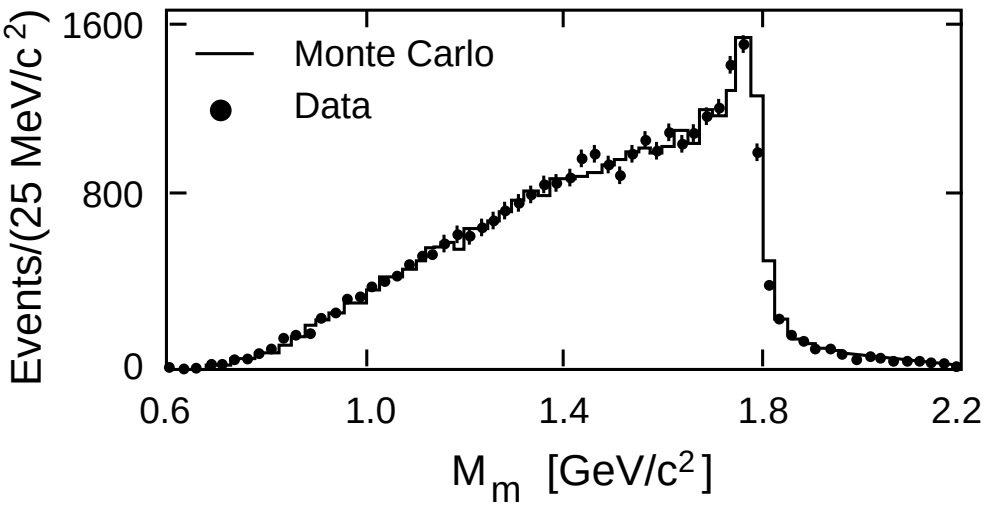

Figure 3.5: The M_m distribution in the data and in the simulation for a tau mass of 1784.1 MeV [75].

(Δm_τ = 1.2 MeV), the beam energy (Δm_τ = 0.1 MeV), simulation statistics (Δm_τ = 0.8 MeV), the cuts and the fit itself (Δm_τ = 0.5 MeV).

Clearly both kinematical methods have to assume that the mass of the tau neutrino is zero, while the result from the threshold scan is insensitive to small neutrino masses. ARGUS takes this into account in the systematic error. A finite neutrino mass would increase the CLEO result by $m^2_{\nu_\tau}/1100$ MeV.

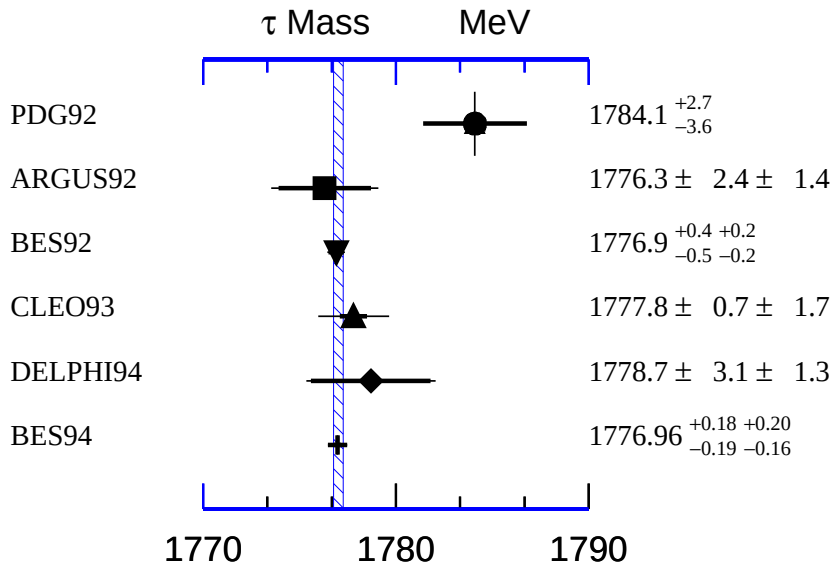

Figure 3.6: The value of m_τ obtained from recent experiments, compared to the 1992 world average of the Particle Data Group. Note that the final result from BES [86,87] supersedes the previous BES result [84]. The band indicates the current world average and its error, $m_\tau = 1777.02^{+0.26}_{-0.24}$ MeV.

In summary, the recent accurate measurements of the tau mass, listed in Fig. 3.6, correct its value downwards to an new world average of

$$m_\tau = 1777.02^{+0.26}_{-0.24}\ \text{MeV} \tag{3.7}$$

and reduce its error by more than an order of magnitude compared to the 1992 world average. Even with respect to the 1994 average of the Particle Data Group, which contained the result of the early BES analysis, their final result improves the error by almost a factor of two.

3.2 Limits on the τ neutrino mass

The kinematic properties of the observed final state in hadronic τ decays also give the possibility to estimate the tau neutrino mass. It is obvious that the best decay channels for a missing mass measurement will be those with a high hadronic mass, where the least energy is available for the missing neutrino. Thus high multiplicity decays are selected for this analysis. The endpoint of the visible hadronic mass spectrum, compared to the tau mass, then gives a limit on the ν_τ mass. It is also clear that this measurement is simpler when the tau leptons are produced with a low momentum, thus with a low boost factor. However, the distinction between a high multiplicity tau decay and a low multiplicity event from $e^+e^- \to$ hadrons becomes a lot easier with increasing center of mass energy. Recent precision limits on the ν_τ mass thus come from ARGUS and CLEO at $\sqrt{s} \simeq 10$ GeV and, surprising at first sight, from OPAL and ALEPH at $\sqrt{s} \simeq 91$ GeV. The recent results are summarized in Tab. 3.1 and shortly extended on in the following.

Experiment characteristics	CLEO	ARGUS	OPAL	ALEPH
Produced $\tau^+\tau^-$	1.77 M	325 K	36 K	76 K
Signal	$3\pi^\pm\pi^0/5\pi^\pm$	$5\pi^\pm$	$5\pi^\pm(\pi^0)$	$5\pi^\pm/5\pi^\pm\pi^0$
2^{nd} τ	$\mu^\pm e^\pm$	$\mu^\pm e^\pm h^\pm$	1 prong	$<$ 4 prongs
Number events	53/60	20	5	23/2
Method	1-D	1-D	2-D	2-D
$m_{\nu_\tau} <$ (95% CL)	32.6	31	74	23.8

Table 3.1: Limits on the tau neutrino mass in MeV.

3.2.1 Low energy measurements

In low as well as high energy experiments it is extremely important to have an event sample as clean as possible, since a background event near the endpoint of the visible mass spectrum can produce an artificially low upper limit for m_{ν_τ}. This aim is reached at low center of mass energies [76,92,101] by selecting one τ decaying into a high multiplicity final state, the other decaying leptonically (CLEO) or into a single charged particle (ARGUS).

ARGUS [92,101] used τ's decaying into 5 pions, $\tau^- \to \pi^-\pi^-\pi^-\pi^+\pi^+\nu_\tau$, recoiling against a single charged particle. 20 candidates were found in this category, with an estimated background of much less than one event. The visible hadronic mass of the 5π system is shown in Fig. 3.7

and compared to what one expects from a tau decay into 5 pions according to phase space, assuming $m_{\nu_\tau} = 0$. Within statistics, the spectra agree in shape and peak position, such that a zero mass cannot be excluded. An upper limit on m_{ν_τ} is defined by the event with the highest visible hadronic mass. To account for possible uncertainties in the background determination, ARGUS conservatively disregards the event with the highest observed mass and extracts a limit from the masses (and errors) of the remaining 19 events, compared to their own result for m_τ (see section 3.1). The result is $m_{\nu_\tau} < 31$ MeV at 95% confidence level.

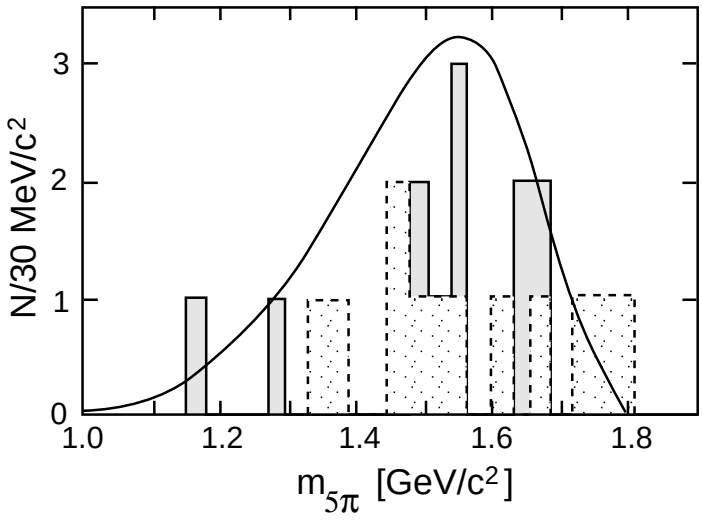

Figure 3.7: Measured invariant mass spectrum of the 5 pion system in events $\tau^- \to 5\pi\nu_\tau$ from ARGUS [101]. The light histogram corresponds to the distribution observed in an earlier study [92]. The curve is the expected shape for a phase-space decay with zero neutrino mass.

For a similar analysis, CLEO [76] selected high multiplicity tau decay modes with charged as well as neutral pions, namely $\tau^- \to 2h^-h^+2\pi^0\nu_\tau$ and $\tau^- \to 3h^-2h^+\nu_\tau$. The size of their event sample is 60 events of the first and 53 events of the second category, with a total background of less than half an event including feed up from lower multiplicity tau decays. 12 events with a mass of the hadronic system larger than 1.65 GeV were observed. The distribution of the invariant mass for all candidates is shown in Fig. 3.8; no event above m_τ was observed. The agreement to the expected spectrum with $m_{\nu_\tau} = 0$ is good.

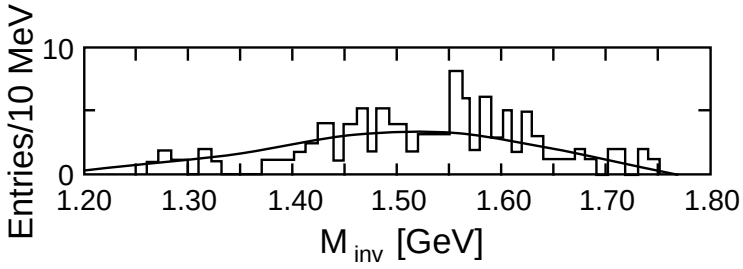

Figure 3.8: Distribution of invariant masses of five pion tau decays from CLEO [76]. The superimposed curve is the expected distribution for $m_{\nu_\tau} = 0$.

An upper limit for m_{ν_τ} is obtained from a likelihood function calculated event by event as a function of m_{ν_τ}, taking into account the observed mass and the theoretical mass spectrum

convoluted with detector resolution and acceptance. The limit on m_{ν_τ} obtained from both decay modes is $m_{\nu_\tau} < 32.6$ MeV at 95% CL. It is dominated by the sample with neutral pions. This limit include the effects of systematic errors such as uncertainties in acceptance, mass scale, mass resolution, distortion from backgrounds, the model of τ decays used and m_τ, which was taken from an early BES measurement [84].

3.2.2 High energy measurements

The kinematic disadvantage of high boost factors for high energy measurements of this kind is counterbalanced by the diminishing multihadron background and the excellent momentum and energy resolution of LEP detectors. Also, statistics is not necessarily an issue, since a single event at high visible mass suffices to give a stringent limit. Moreover, the correlation between visible mass and visible energy in a tau decay allows to enhance the sensitivity to a non-zero m_{ν_τ}, as first shown by OPAL [234].

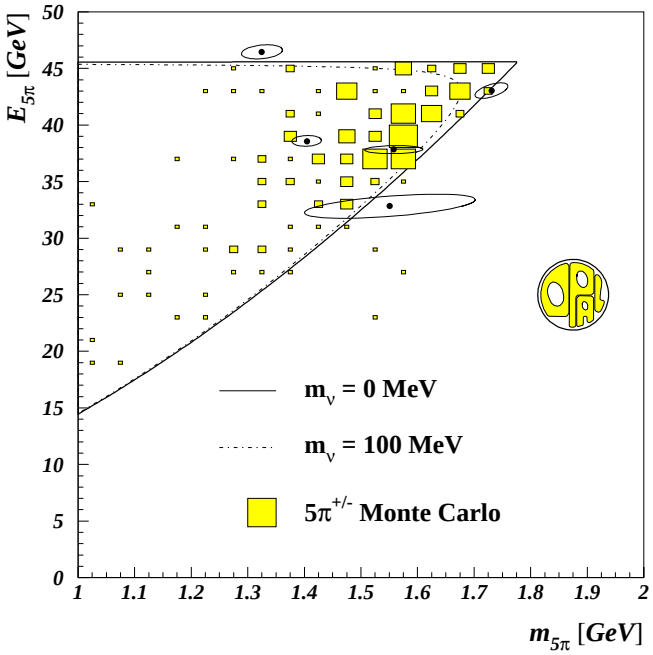

Figure 3.9: Selected $\tau \to 5\pi\nu_\tau$ data from OPAL [234], with 1σ ellipses indicating the experimental resolution. The Monte Carlo events (m_{ν_τ}=0), with a statistics eight time higher, are plotted with boxes. The lines show the kinematically allowed range for $m_{\nu_\tau} = 0$ and $m_{\nu_\tau} = 100$ MeV.

In the OPAL analysis, five tau decays into a final state with five charged pions were selected, recoiling against a one prong tau decay. The estimated background is less than 0.1 event in this category. The events were studied in the plane defined by the total hadronic energy and the total hadronic mass, as shown in Fig. 3.9. Again, the "best event", with a mass of 1.731 ± 0.023 GeV and an energy of 43.03 ± 0.81 GeV dominates the mass limit, which is obtained from a maximum likelihood method analogous to the one dimensional analysis. The result of the fit is $m_{\nu_\tau} < 74$ MeV at 95% CL [234]. A recent update [243], exploiting the high statistics sample of events where both tau leptons decay into three charged hadrons, yields the preliminary limit $m_{\nu_\tau} < 29.9$ MeV at 95% CL [234], including the earlier result quoted above.

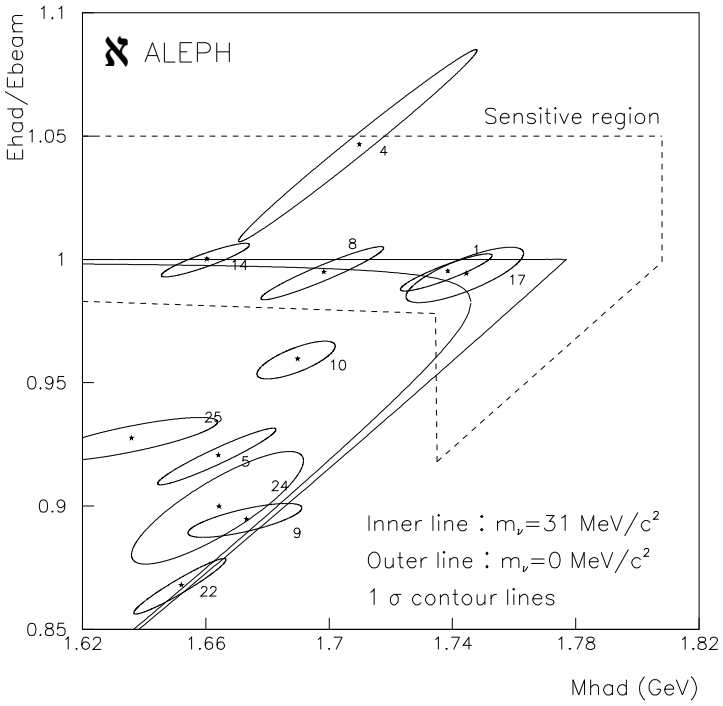

Figure 3.10: The observed mass and energy of the hadrons in $\tau \to 5\pi\nu_\tau$ from ALEPH data [184, 188]. The events labeled as 4 and 25 are identified as $\tau \to 5\pi\pi^0\nu_\tau$. The kinematic boundaries for a zero and non-zero neutrino mass are indicated, as well as the region most sensitive to small neutrino masses.

The same analysis technique has been used by ALEPH [184,188], based on a larger event sample. The decay modes used are $\tau \to 5\pi\nu_\tau$ and $\tau \to 5\pi\pi^0\nu_\tau$. In the opposite hemisphere, a τ decaying into three or less charged particles is admitted. The data sample consists of 23 events identified as 5π and 2 as $5\pi\pi^0$ decays. There is nearly no background other than cross feed among the two signal channels. The total background in the region sensitive to the neutrino mass is estimated to be 0.04 ± 0.03 events. The characteristics of the candidates closest to the kinematic boundary are displayed in Fig. 3.10.

The method used to extract an upper bound on the neutrino mass is analogous to the OPAL method. The 2-dimensional likelihood analysis yields $m_{\nu_\tau} < 23.8$ MeV at the 95% confidence level, including systematic errors. As expected, the upper limit is dominated by the events labeled 1 and 17 in Fig. 3.10. Using a one dimensional likelihood analysis instead, a weaker limit of $m_{\nu_\tau} < 40.6$ MeV would have been set.

3.3 Oscillations of the τ neutrino

The existence of the ν_τ as a light, only weakly interacting particle distinct from ν_e and ν_μ has been confirmed by the precision measurements at LEP [163,189,203,217] and SLC [246], measuring the number of the light neutrino families, $N_\nu = 2.988 \pm 0.023$ [256]. The experimental

proof that ν_τ is indeed the weak isospin partner of the τ, for instance with the observation of inverse τ decay, $\nu_\tau e^- \to \tau^- \nu_e$, has not yet been accomplished. Neither has an interaction with a nucleus, $\nu_\tau + \mathcal{N} \to \tau^- + X$, ever been observed. Although it has been shown to be light, ν_τ may well be the heaviest neutrino if neutrinos are not strictly massless. The search for a massive ν_τ is thus of great interest, not only from the point of view of particle physics, but also for its impact on cosmology and astrophysics. This impact has been extensively reviewed elsewhere [257–261] and we restrict our discussion to the arguments directly relevant for particle physics.

In a cosmological model with a flat universe, the universe must be filled with dark matter that accounts for most of its mass. The τ neutrino may be considered a likely candidate, among the known particles, to be a constituent of dark matter. The expected mass value for such a neutrino should then be of order 10 eV [261–263], too low to be observed directly in the decay kinematics (see section 3.2). But also a more massive neutrino, in the MeV range, can be accommodated in cosmological models [264,265].

If any or all of the three neutrino species have a finite mass, hadronic and leptonic charged currents could also share the distinction between weak eigenstates and mass eigenstates. Neutrinos could mix in a way analogous to quark mixing by the CKM mechanism. Indirect evidence for low mass neutrinos could then be found through the observation of oscillations between neutrino states. This idea of neutrino oscillations was originally proposed by Pontecorvo [266–268] in analogy with K^0 mesons. The mechanism of oscillation is also a possible solution to the long standing problem of solar and atmospheric neutrinos (see sections 3.3.1 and 3.3.2).

The neutrino mass eigenstates, (ν_1, ν_2, ν_3), can be linked to the weak interaction eigenstates, $(\nu_e, \nu_\mu, \nu_\tau)$, with a three by three unitary matrix similar to the CKM matrix for quarks. There are then at least three angle parameters, $(\theta_{e\mu}, \theta_{\mu\tau}, \theta_{e\tau})$, that govern neutrino mixing. Neutrino oscillations could transform an originally pure weak eigenstate into a mixture, if the mass eigenstates evolve differently with time, i.e. if the masses are not degenerate. In the simplified case of two-neutrino mixing, such as $\nu_\mu \leftrightarrow \nu_\tau$, the probability P of finding, after a path L, a ν_τ which started as a ν_μ is given by

$$P = \sin^2 2\theta \sin^2 \frac{2\pi L}{\lambda} \tag{3.8}$$

where θ $(= \theta_{\mu\tau})$ is the mixing angle between the two neutrino species, and L is the distance between source and detection point. The oscillation length is $\lambda = 5E_\nu/\Delta m^2$, with the mass difference parameter $\Delta m^2 = |m^2_{\nu_\mu} - m^2_{\nu_\tau}|$.

Since neutrino masses are small, the mass difference parameter must also be small. The observation point should thus be installed far from the neutrino source and small neutrino energies are favored. The ranges accessible to different types of oscillation experiments are summarized in Fig. 3.11. Since the oscillation probability contains two unknown parameters, experimental results are expressed as limits in the plane of Δm^2 versus $\sin^2 2\theta$.

There is little theoretical guidance on the values that neutrino masses or mixing angles might have [269]. In extensions to the Standard Model, like Supersymmetric Grand Unified Theories [270], the so-called see-saw mechanism [271,272] may generate neutrino masses from couplings of Dirac neutrinos with Majorana neutrinos. This leads to a mass hierarchy such

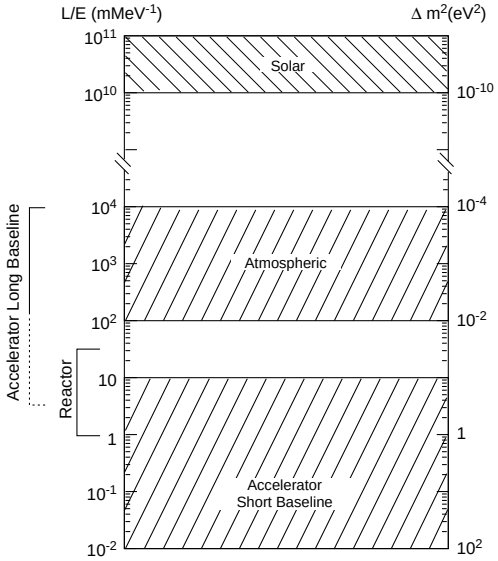

Figure 3.11: The sensitivity regions in L/E and Δm^2 for different neutrino sources in oscillation experiments.

that $m_{\nu_e} \ll m_{\nu_\mu} \ll m_{\nu_\tau}$ [271,272], with mass ratios proportional to a power of the quark mass ratio [262, 269, 270] or the charged lepton mass ratio [263]. The neutrino masses predicted in such models are usually too small [270] or too large [262] to respect cosmological limits on dark matter properties [263–265, 273]. However, due to the mass hierarchy, it can still be concluded that only the tau neutrino mass can lead to observable oscillations. To this extent even the relatively weak upper bound on the tau neutrino mass from direct observation ($m_{\nu_\tau} < 23.8$ MeV, see section 3.2) has a larger impact on cosmological models [274] than the more stringent limits on the other neutrino families ($m_{\nu_\mu} < 0.16$ MeV at 90% CL, $m_{\nu_e} < 5.1$ eV at 95% CL [252]).

Even less is known about expected values for the mixing angles. A reasonable guideline would be that the structure of the neutrino mixing matrix would follow the pattern seen in the CKM matrix [263]. Thus, the diagonal elements would be almost one, and the elements be smaller and smaller the more off-diagonal they are. The mixing angles might then range from 10^{-1} to 10^{-4}, with $\sin^2 2\theta_{e\tau} \ll \sin^2 2\theta_{\mu\tau}$. Mixing would thus be mainly restricted to neighboring generations.

3.3.1 Solar Neutrinos

Based on the argument discussed in the beginning of this section, the sun constitutes an ideal source for the study of possible neutrino oscillations. It abundantly produces low energy electron neutrinos, such that about 10^{10} impinge on the earth's surface per square cm and per second [258, 261, 269]. Its large distance, 149×10^6 km, satisfies the requirement for the study of very small Δm^2.

Many experiments have studied the rate of solar neutrinos reaching the earth, for detailed reviews see [258,259,261,275,276]. The aim of the experiments is to look for the disappearance

of solar neutrinos on the way from the center of the sun to the surface of the earth. Given the neutrino energy spectrum and the source-target distance, these experiments are sensitive to regions of Δm^2 above 10^{-11} eV^2.

The detection strategy for electron neutrinos is twofold. Radiochemical experiments study the inverse beta decay reaction induced by neutrinos on massive underground targets, detected by a small number of converted nuclei. This category includes the pioneering experiment Homestake [277,278], using a chlorine target, as well as recent experiments with a using gallium target, like Sage [279–281] and Gallex [282–286]. Underground Cerenkov detectors, on the other hand, like Kamiokande [287–289] detect the quasi-elastic scattering of neutrinos off electrons (see Fig. 3.12). All these experiments indicate, that the flux of electron neutrinos from the sun is lower than expected from the Standard Solar Model [290–293]. The radiochemical experiments are sensitive to electron neutrinos only, while the Cerenkov experiments have a reduced efficiency also for ν_μ and ν_τ, through the neutral current contribution to the cross section.

The lack of solar electron neutrinos on the earth can be explained by either modifying the Standard Solar Model [258,290–292], or by postulating that electron neutrinos disappear on the way. The more interesting latter possibility would mean that either the electron neutrino is not stable, or that it oscillates into another flavor that the experiments are not (or less) sensitive to. There is no evidence for radiative neutrino decay [294] and supernova data indicate a very long lifetime [295].

Thus if there is no deficiency in the calculated solar neutrino flux, electron neutrinos might oscillate, either inside solar matter or on the way from the sun to the earth. The first mechanism, oscillations in matter, could be amplified by the fact that the total cross section for low energy electron neutrinos with ordinary matter is higher than for any other neutrino species (see Fig. 3.12). This difference in interaction probability could lead to an increase in oscillation probability through resonance effects [296]. As a consequence, even small mixing angles could give rise to appreciable oscillation effects. Of course, the same argument applies to interactions inside the earth.

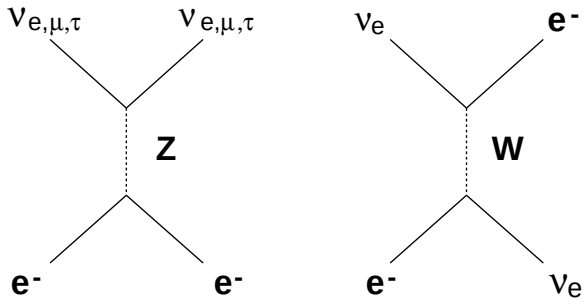

Figure 3.12: Low energy neutrino interactions in solar matter. The neutral current process (left) is available to all neutrino species, while at very low neutrino momenta the charged current channel (right) exists only for electron neutrinos.

The results of solar neutrino experiments, interpreted in terms of oscillations between ν_e and either ν_μ or ν_τ are summarized in Fig. 3.13, as an allowed zone in the plane of Δm^2, $\sin^2 2\theta$ [258]. The regions of maximum probability are situated between $\Delta m^2 \simeq 3 \times 10^{-6}$ eV^2

and 10^{-5} eV^2. From the mass hierarchy argument one can estimate that $\Delta m^2 \simeq m^2_{\nu_\mu} \simeq 10^{-5}$ eV^2, and a muon neutrino mass of order 2 meV results. Using a proportionality of the neutrino masses to the square of quark masses, one can thus predict a mass for the tau neutrino of

$$m_{\nu_\tau} \simeq m_{\nu_\mu} \left(\frac{m_t}{m_c}\right)^2 \tag{3.9}$$

Using the known quark masses (m_c = 1.5 GeV [252], $m_t \simeq$ 174 GeV [297, 298]), one thus arrives at a tau neutrino mass between 30 and 40 eV, which is in the right range required for tau neutrinos to form dark matter. The tau neutrino oscillation length would be of order 60 m, sufficiently short to be observed by an accelerator experiment (see Section 3.3.3).

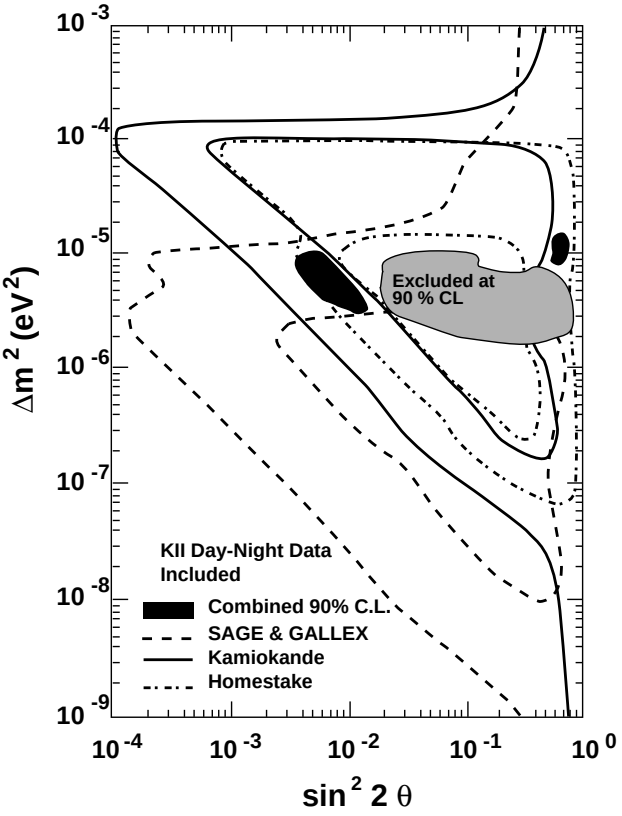

Figure 3.13: Regions of parameter space allowed by recent experiments on solar electron neutrinos [258]. The band between the lines is allowed by the experiments at 90% CL. The grey area is excluded by the combined results. The black regions correspond to the best fit to all experiments.

It is clear, however, that this interpretation depends heavily on the correctness of the neutrino flux predicted by the Standard Solar Model. The next generation of solar neutrino experiments thus aims at measuring the rate of all neutrino types simultaneously. Such measurements would thus be less dependent on absolute flux predictions. Experiments under construction are SNO [299] and Super-Kamiokande [269, 300]; the detectors for Icarus [269, 301] and Borexino [302] are in a prototype stage.

3.3.2 Atmospheric Neutrinos

The other source of information on possible neutrino oscillations, in particular for ν_τ, are atmospheric neutrinos. The neutrino spectrum on earth above a neutrino energy of about 100 MeV [258] is dominated by ν_μ and ν_e produced in cosmic ray interactions inside the atmosphere. These neutrinos come from the decay of pions and kaons present in air showers. The basic production and decay scheme is

$$\begin{aligned} P + \mathcal{N} &\rightarrow \pi's + K's \\ (\pi^\pm/\mathrm{K}^\pm) &\rightarrow \mu^\pm + (\nu_\mu/\bar{\nu}_\mu) \\ \mu^\pm &\rightarrow \mathrm{e}^\pm + (\nu_e/\bar{\nu}_e) + (\bar{\nu}_\mu/\nu_\mu) \end{aligned} \tag{3.10}$$

From this decay chain, the expected flavor ratio in the atmospheric neutrino flux can be simply estimated: one expects about twice as many muon neutrinos as electron neutrinos and as many neutrinos as antineutrinos. Calculation of electron and muon neutrino fluxes [303, 304] have an uncertainty of 25%, whereas the ratio between these fluxes is determined to better than 5%. The neutrino flux is approximately isotropic. In the presence of neutrino oscillations, the detected neutrino fluxes will differ from expected ones and be different in the upwards and downwards direction due to interactions inside the earth. While the electron neutrino rates are quite consistent with prediction, there appears to be a significant deficit in muon neutrinos. The rate is usually expressed in terms of the double ratio $R = (\mu/\mathrm{e})_{\mathrm{data}}/(\mu/\mathrm{e})_{\mathrm{MC}}$, comparing the observed ratio of electron to muon events with the expected ratio. Kamiokande recently published a result [305] based on a reanalysis of events with energies less than 1.33 GeV, which gives $R = 0.60^{+0.06}_{-0.05}(\mathrm{stat}) \pm 0.05(\mathrm{syst})$. The same technique gives $R = 0.57^{+0.08}_{-0.07}(\mathrm{stat}) \pm 0.07(\mathrm{syst})$ for high energy events. IMB3 [306, 307] finds a comparable deficit, $R = 0.54 \pm 0.05(\mathrm{stat}) \pm 0.12(\mathrm{syst})$, which is also shown by the lower statistics Soudan2 [308], $R = 0.64 \pm 0.17(\mathrm{stat}) \pm 0.09(\mathrm{syst})$. No evidence for a deficit has been found by Frejus [309, 310], $R = 0.87 \pm 0.16 \pm 0.12$ [258], and Nusex, $R = 0.96^{+0.32}_{-0.28}$ [258, 311].

Again, this data has been interpreted in terms of neutrino oscillations [258, 260, 261, 312] between ν_μ and ν_τ. A summary is reproduced in Fig. 3.14 [258, 305]. Although the evidence cannot be considered conclusive, hints from solar and atmospheric neutrino experiments indicate that neutrino oscillations might indeed exist, consistent with an meV muon neutrino mass and a 10 to 100 eV tau neutrino mass.

3.3.3 Accelerator neutrinos

Since the current data allow oscillations of the ν_τ with a reasonable oscillation range, it is a challenge to confirm their existence with an accelerator neutrino experiment. Experiments with a short distance from source to target (baseline) would be sensitive to larger Δm^2 values, those with a long baseline to smaller ones. Experiments in muon neutrino beams and beam dumps have searched for interactions of the type $\nu_\tau \mathcal{N} \rightarrow \tau^- X$, with the τ lepton identified by its decay. None such interactions were found. At present the most stringent limit reached in $\nu_e \rightarrow \nu_\tau$ oscillations and in $\nu_\mu \rightarrow \nu_\tau$ was obtained from the E531 collaboration, a hybrid emulsion spectrometer in the Fermilab wide-band neutrino beam. Figures 3.15 quotes the

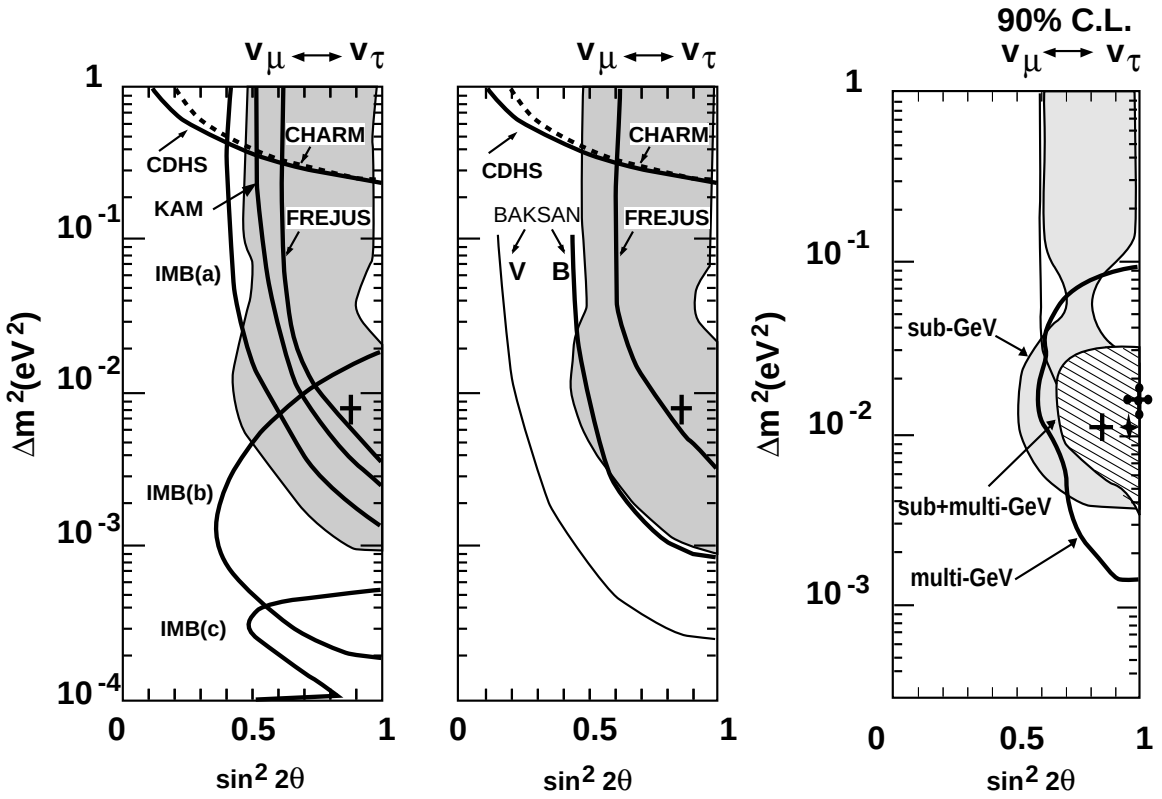

Figure 3.14: a) and b): Regions of parameter space for tau neutrino oscillations, allowed (shaded) or excluded at 90% CL (above lines) by experiments [258]. The shaded area corresponds to the regions allowed by earlier Kamiokande results. c) The recent Kamiokande results [305]. The thick curve encloses the allowed region (90% CL) for neutrino oscillation parameters obtained from high energy data. The hatched region combines results from high and low energy data. The best fit values are shown by the crosses.

resulting limits for $\nu_e \to \nu_\tau$ and $\nu_\mu \to \nu_\tau$ oscillation parameters, together with earlier results from BEBC [313,314], CCFR [315], CDHS [316], CHARM [317] and CHARM II [318].

There are currently two new experiments running at an accelerator, CHORUS [320,321] and NOMAD [322,323], both at CERN. A third one, E803 [324] will be taking data at Fermilab before the turn of the century. Two further, long baseline experiments far from the neutrino beam's source project to use the Fermilab neutrino beam with the Soudan 2 detector [325,326], and the Brookhaven beam with E889 [327]. All these experiments aim at being sensitive to neutrino oscillation parameters far beyond the current limits (see Figures 3.15).

The CERN experiments [328] aim at observing a ν_τ appearance in a ν_μ beam, through a charged current interactions $\nu_\tau \mathcal{N} \to \tau^- X$. The ν_τ contents in these beams is negligible (10^{-7}). The ν_μ beam is derived from 450 GeV protons of the CERN SPS. It has a mean energy of $E_\nu \simeq 27$ GeV and a small contamination from $\bar{\nu}_\mu$ (6%), ν_e (0.7%) and $\bar{\nu}_e$ (0.2%).

The two experiments NOMAD [322] and CHORUS [320] are situated at $L \simeq 800$ m away from the neutrino source. They are sensitive to the range $10 \leq m_{\nu_\tau} \leq 20$ eV. The principle used by NOMAD [322,323,328] is to separate ν_τ interactions statistically on the basis of kinematic quantities like the missing transverse momentum of the reaction. To obtain a high detection

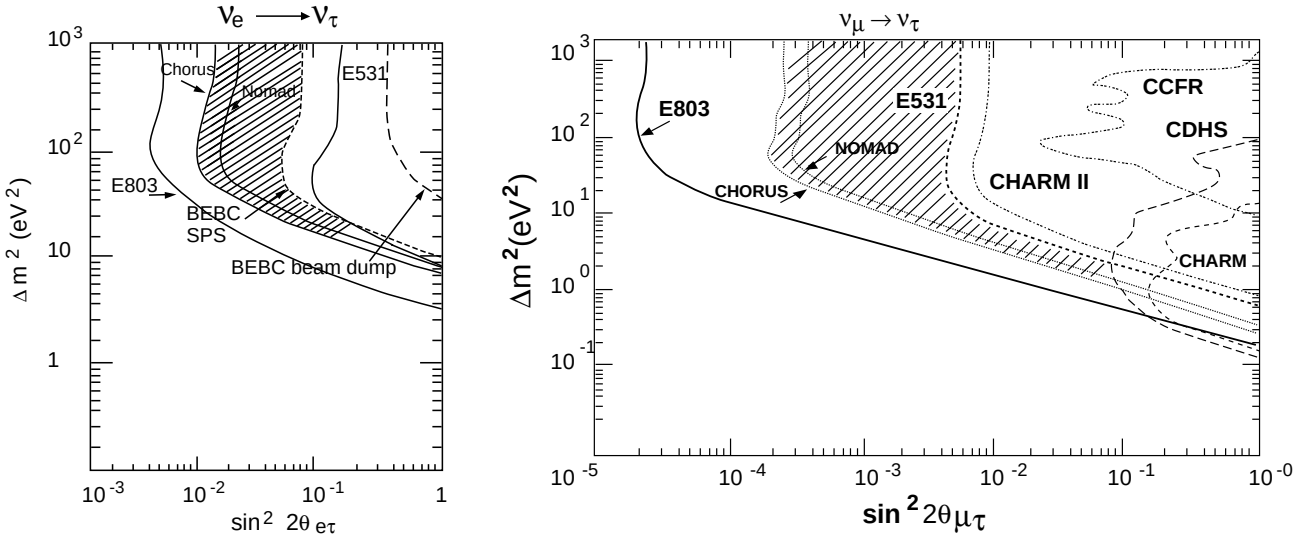

Figure 3.15: Left: Existing limits for $\nu_e \rightarrow \nu_\tau$ oscillations at the 90 % confidence level, from BEBC at the SPS [313], the BEBC beam dump experiment [314] and E531 [319]; the expected limits for CHORUS [320,321], NOMAD [322,323] and E803 [324] are also presented. Right: Existing limits for $\nu_\mu \rightarrow \nu_\tau$ oscillations at the 90%confidence limit, from CCFR [315], CDHS [316], CHARM [317], CHARM II [318] and E531 [319]; the expected limits for CHORUS [320, 321], NOMAD [322, 323] and E803 [324] are also represented. The hatched area emphasizes the expected improvement.

efficiency, very good energy, momentum and angular resolution are needed. The NOMAD detector (see fig 3.16) is installed, with the exception of the forward veto plane and the rear muon chamber, inside a 0.4T magnetic field perpendicular to the beam axis. It is similar to a classical fixed target neutrino detector, except for a transition radiation detector to enhance electron recognition. The target consists of the walls of drift chambers used for the momentum measurement. The main characteristics of the detector are summarized in Tab. 3.2.

Experiment characteristics	NOMAD	CHORUS	E803
Number of CC interactions	1.1×10^6	5×10^5	6×10^6
Expected running time [y]	2+(2)	2+(2)	4
τ decay mode	e, μ	μ	e
	$\pi^- + (n\pi^0)$	$\pi^- + (n\pi^0)$	$\pi^- + (n\pi^0)$
	$\pi^+\pi^-\pi^- + (n\pi^0)$	$\pi^+\pi^-\pi^- + (n\pi^0)$	-
Sensitivity at largeΔm^2			
$\sin^2\theta_{\mu\tau}$	3.8×10^{-4}	2.8×10^{-4}	2.8×10^{-5}
$\sin^2\theta_{e\tau}$	2.7×10^{-2}	1.6×10^{-2}	5.0×10^{-3}
Energy	30 GeV	30 GeV	wideband $\simeq$ 10 GeV
Distance	800 m	800 m	470 m
Starting Time	1994	1994	1998

Table 3.2: Summary of characteristics of NOMAD, CHORUS, E803

The detection principle used by CHORUS, see Fig. 3.17 [320,321,328], is to recognize the presence of a $\tau^\pm$ lepton before its decay. The τ decay path expected at these energies should be

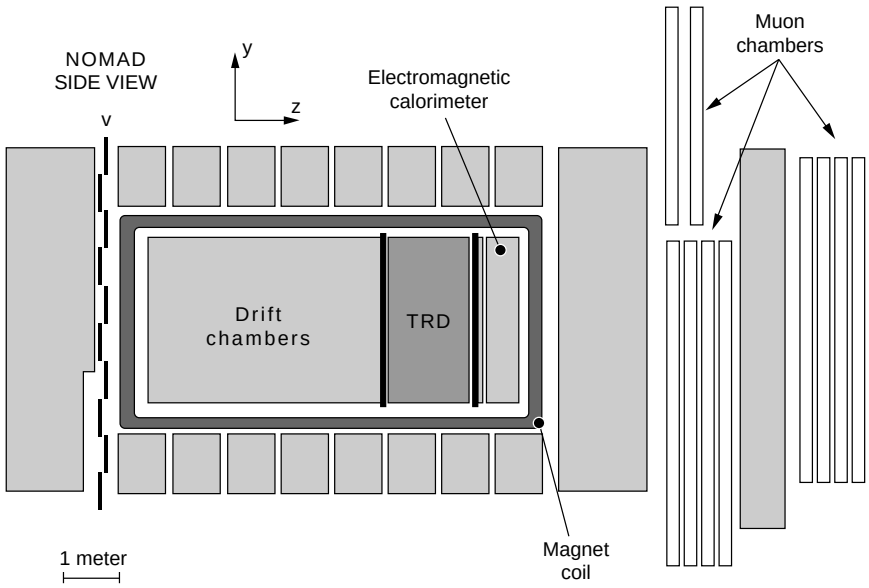

Figure 3.16: Side view of the NOMAD detector. The neutrino beam enters from the left.

shorter than 1 mm. Thus a track sensitive target made of an emulsion stack and a scintillating fiber tracker forms the core of the apparatus, followed by a spectrometer. A detailed view of the target is shown in fig 3.18. The bulk of the emulsion stack remains in place for the whole duration of the experiment, followed by a sheet changed more often to have less occupancy.

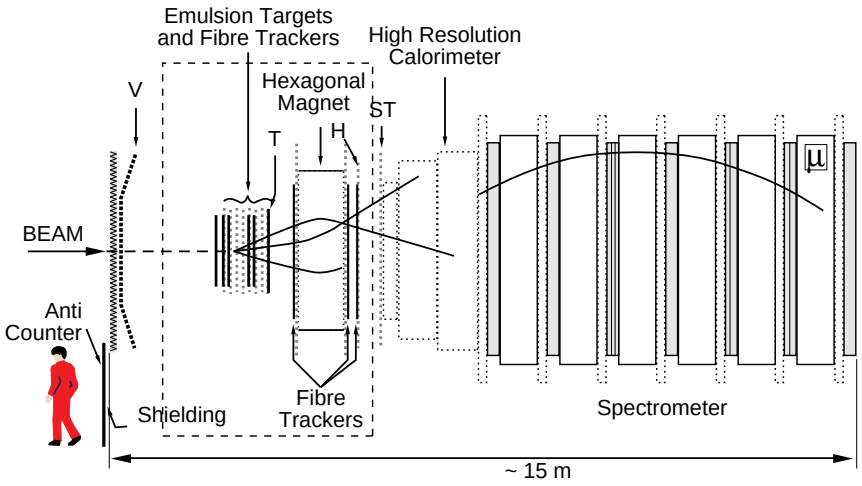

Figure 3.17: Lay-out of the CHORUS detector.

The CHORUS tracker is installed inside a 0.17T toroidal field to form a magnetic spectrometer. It is followed by an electromagnetic calorimeter and a muon detector. Using a kinematic event selection, vertex locations for about 50.000 events, i.e. about 10% of the full event sample, would be predicted and scanned for in the emulsion. Tracks emerging from the vertex are then inspected for kinks to single out τ decays. A similar experiment, E803 [324], has recently been approved at Fermilab to start taking data in 1998. The main characteristics of the three experiments are compared in Table 3.2.

Sensitivity to long oscillation lengths and thus small Δm^2 can be gained by installing detec-

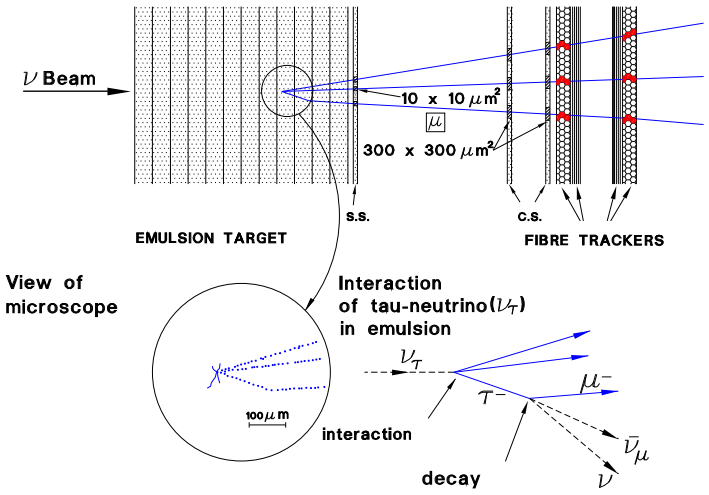

Figure 3.18: The CHORUS track sensitive target

tors far away from the neutrino source, outside the limits of the laboratory site. Fermilab plans to construct a neutrino beam aimed at a massive detector, P822 [326], in a distant underground laboratory, for example a new 15 KTon detector, 730 Km away in the Soudan laboratory. The experiment plans to start by the end of this century. The approved E803 (see previous paragraph) would occupy an underground experimental hall in the same beam. Both long and short base line experiments could detect the oscillations of $\nu_\mu \rightarrow \nu_\tau$, but in different regions. One would cover the region of interest for cosmology; the other the region pointed at by solar and atmospheric neutrinos experiments. Another project along the same lines is E889 [327]. The experiment intends to use a ν_μ beam produced by the Brookhaven AGS. It would use 3 detectors 1, 3, and 24 km away from the neutrino source. Each detector consists of a tank of water viewed by photomultipliers. The principle of the experiment is to look for the disappearance of ν_μ by comparing the normalized rate of $\nu_\mu \mathrm{n} \rightarrow \mu \mathrm{p}$ in the three detectors. The experiment can also look for the appearance of ν_e through the reaction $\nu_e \mathrm{n} \rightarrow \mathrm{e}^- \mathrm{p}$. It is thus not necessary to know the absolute neutrino flux at the three different locations. The $\nu_\mu \rightarrow \nu_e$ oscillations would be observed by a decrease in the ν_μ rate, with a corresponding increase in the ν_e rate. The signal for $\nu_\mu \rightarrow \nu_\tau$ oscillations would be just the ν_μ disappearance not accompanied by a corresponding increase in the ν_e rate.

Most oscillation experiments rely on a detection of tau neutrino charged current interactions, which has never been observed. So far, the low fraction of tau neutrinos in ordinary neutrino beams has prevented experiments from observing its interactions. A dedicated experiment for the observation of ν_τ interactions has been proposed at Fermilab, E872 [329]. Using the Fermilab 800 GeV proton beam to produce $\mathrm{D_s}$ mesons in a beam dump, a reasonably large flux of ν_τ may be expected. The interaction of neutrinos would be observed in an emulsion target with a subsequent spectrometer.

3.4 Electric and magnetic moment of the τ

Form factors at the $\gamma\tau\tau$ vertex can be used to parameterize non standard electromagnetic interactions of the tau lepton. The general electromagnetic amplitude, including magnetic and electric form factors, can be written as [330,331]

$$< p_2|J^{\mu}_{em}(0)|p_1 >= e\bar{u}(p_2)[F_1\gamma^{\mu} + (\frac{i}{2m_{\tau}}F_2 + \gamma_5 F_3)\sigma^{\mu\nu}q_{\nu}]u(p_1) \tag{3.11}$$

where p_1 and p_2 are the four-momenta of the incoming and outgoing leptons, $q = p_2 - p_1$ is the photon momentum, and F_i are the form factors of the interaction vertex. In the static limit, these form factors are related to the static properties of the tau lepton

$$q_{\tau} = eF_1(q^2 = 0) \tag{3.12}$$
$$a_{\tau} = F_2(q^2 = 0) \tag{3.13}$$
$$d_{\tau} = eF_3(q^2 = 0) \tag{3.14}$$

with the charge q_{τ}, the anomalous magnetic moment a_{τ} and the electric dipole moment d_{τ}. The matrix element describing the $Z\tau\tau$ vertex is analogous to Equ. 3.11, with $(C_V - C_A\gamma_5)$ replacing the second term [332].

Electromagnetic form factors can be measured either with the cross section for $e^+e^- \rightarrow \tau^+\tau^-$ or using real final state bremsstrahlung in the process $e^+e^- \rightarrow \tau^+\tau^-\gamma$. Both the total cross section, the angular distribution and the energy distribution of final state photons depend on the form factors. To give an example, the differential cross section as a function of the scattering angle [333] depends on F_2 by linear and a quadratic term, and on F_3 by a quadratic term.

The magnetic moment of the τ lepton

$$\mu = g_{\tau}\frac{e}{2m_{\tau}} \tag{3.15}$$

depends on the gyromagnetic ratio g_{τ} which, at Born level, is equal to two for a pointlike fermion. Deviations from this value are described by the anomalous magnetic moment, $a_{\tau} = (g_{\tau} - 2)/2$, thus by the anomaly quoted above. Analogous to the properties of the electron and muon, non-zero values of a_{τ} in the Standard Model are due to higher order processes [334]. They can be grouped into three categories according to their origin: a_{τ}^{QED} for higher order QED contributions, $a_{\tau}^{hadronic}$ for hadronic effects and a_{τ}^{weak} for weak effects. The expected contributions are [334]:

$$a_{\tau}^{QED} = (117.319 \pm 0.001) \times 10^{-5} \tag{3.16}$$
$$a_{\tau}^{hadronic} = (3.5 \pm 0.3) \times 10^{-6} \tag{3.17}$$
$$a_{\tau}^{weak} = (5.560 \pm 0.002) \times 10^{-7} \tag{3.18}$$

and sum up to a total expected value of $a_{\tau} = (11773 \pm 3) \times 10^{-7}$. The gyromagnetic ratio should thus be $g_{\tau} = 2.0023556 \pm 0.0000006$, only slightly higher than the corresponding one for electron and muon, $g_e = 2.002319304280 \pm 0.000000000056$ and $g_{\mu} = 2.00233183804 \pm 0.00000000154$. Because of the high tau lepton mass, the contributions of hadronic and weak corrections to the anomalous magnetic moment are significantly higher than for e and μ. The $a_{\tau}^{hadronic}$ is even 50

times larger than $a_\mu^{hadronic}$, a_τ^{weak} is enhanced by a factor $(m_\tau/m_\mu)^2$. Still these anomalies are tiny on an absolute scale and it is very difficult to observe them experimentally.

This is even more so since the classical method for the measurement of this quantity, precession of the spin vector in a magnetic field, is not available because of the short tau lepton lifetime. However, an analysis of the production cross section and final state bremsstrahlung at least gives a limit on unusually high values of a_τ. The results are summarized in Table 3.3. An analysis of data collected at PETRA [335], where the influence of Z exchange is limited to electroweak interference, gives a limit of $a_\tau < 0.02$ at 95% CL. The high statistics data at LEP, dominated by Z exchange, give a better limit from the analysis of the Z width into tau pairs [330,331]. Using the LEP I data, m_W measured at $p\bar{p}$ colliders and the CDF top quark mass, the authors find $a_\tau < 0.0062$ at 68% CL. However, their method of using an effective Lagrangian approach instead of a form factor restricts the validity of the result to a gauge invariant extensions of the Standard Model [330,331].

A more direct method to obtain a limit on anomalous electromagnetic moments is to study final state radiation of real photons from a tau pair [336] (see Fig. 3.19). Using data from L3 at LEP [204], Grifols and Mendez first looked for anomalous production of photons in the total rate of $e^+e^- \to \tau^+\tau^-\gamma$ and found $a_\tau < 0.11$ at 68% CL. This limit was later revised by L3 itself, which found a slightly stronger limit of $a_\tau < 0.14$ at the 90% confidence level [337].

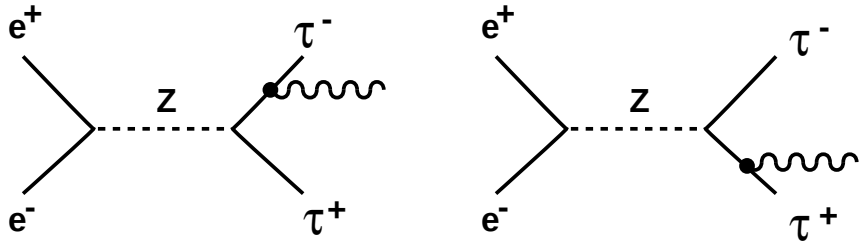

Figure 3.19: Contribution of final state bremsstrahlung to the process $Z \to \tau^+\tau^-\gamma$

a_τ	CL	Reference	Method
0.0011778 ± 0.0000003		[334]	theoretical expectation
0.39 ± 0.30	68%	[338]	PEP, PETRA τ asymmetry
< 0.02	95%	[335]	total cross section at PETRA
< 0.11	68%	[336]	anomalous hard photon production at LEP
< 0.14	90%	[337]	anomalous hard photon production at LEP
< 0.0062	68%	[331]	electroweak data at LEP

Table 3.3: Expected value and experimental upper limits (90 % CL) for the τ anomalous magnetic moment.

These limits are still far above the Standard Model expectations for the anomaly. A recent calculation [339] gives a weak contribution of $a_\tau^{weak}(m_Z^2) = -(2.10 + 0.61i) \times 10^{-6}$ at $q^2 = m_Z^2$. This level of accuracy is unreachable even with the full data sample ultimately expected at LEP.

As the magnetic moment, the electric dipole moment is experimentally accessible via the search for anomalies in $e^+e^- \to \tau^+\tau^-$. As before the observables would be the total and the differential cross section. The results are summarized in Tab. 3.4. A more powerful alternative is, however, to use the fact that the third term in equation 3.11 is CP violating and thus extremely small in the SM. CP violating observables can thus be constructed to single out terms of this kind with high sensitivity. This method will be treated in chapter 7.

Again, the most stringent limits come from PETRA and LEP data. CELLO at PETRA [332] analyzed possible deviations in the τ angular distribution and found a limit of $d_\tau < 1.4 \times 10^{-16}$ e cm at the 68% CL. The electroweak data at LEP give [331] $d_\tau < 3.4 \times 10^{-17}$ e cm at 68% confidence, when only gauge invariant extensions are considered. Analogous to the magnetic case, the lack of anomalous final state radiation from the τ can be interpreted in terms of a limit on the dipole moment [336]; the authors find $d_\tau \leq 6 \times 10^{-16}$ e cm at 68% CL.

d_τ [e cm]	CL	Reference	Method
$< 6 \times 10^{-16}$	68%	[336]	Anomalous hard photon production at LEP
$< 3.4 \times 10^{-17}$	68%	[331]	Electroweak data at LEP
$< 1.4 \times 10^{-16}$	68%	[332]	Angular distribution at PETRA

Table 3.4: Upper limits on the τ electric dipole moment.

Clearly, the existing limits for the tau electric dipole moment are far above those set for electron and muon [252], $d_\mu = (-3.7 \pm 3.4) \times 10^{-19}$ e cm and $d_e = (-2.7 \pm 8.3) \times 10^{-27}$ e cm. A sign of new physics will, however, often manifest itself in interactions preferentially involving heavier quarks or leptons such as the τ. The sensitivity of anomalous couplings may then be enhanced by a power of the lepton mass ratio, which is very large [340]. If one assumes an enhancement by e.g. $(m_\tau/m_e)^3 \approx 3 \times 10^{10}$, the sensitivity of current limits on the tau moments to new physics is already competitive to the much higher accuracies reached in electron and muon properties.

3.5 Electric and magnetic moment of the ν_τ

If neutrinos have a finite mass, they are expected to also have an induced magnetic moment. This dipole moment is predicted in the Standard Model framework to be, for a massive Dirac neutrino [341]

$$\mu_\nu = \frac{3eG_F}{8\sqrt{2}\pi^2} m_\nu = 3.2 \times 10^{-19} \mu_B \left(\frac{m_\nu}{1 \text{ eV}}\right)$$

in units of the Bohr magneton $\mu_b = e/2m_e$. Given current limits for the neutrino masses, this seems definitely out of experimental reach. On the other hand, a closed universe can be achieved (see Section 3.3) with a tau neutrino which has an abnormally high magnetic moment, $\mu_\nu \simeq 10^{-6}\mu_B$ [265]. Such a massive neutrino (m_{ν_τ} =1 to 35 MeV) could then be a cold dark matter candidate. However, it is not even necessary for a particle to have mass in order to have a magnetic or electric dipole moment [342].

Experimentally, it is impossible to distinguish between electric, δ_ν, and magnetic moment, μ_ν, of a relativistic neutrino since only $(\delta_\nu^2 + \mu_\nu^2)^{\frac{1}{2}}$ appears in the Lagrangian. Thus bounds

on magnetic moments can be translated into bounds on the electric dipole moment. In analogy to the τ coupling in Equ. 3.11, the electromagnetic interaction of its neutrino can be written as [331]:

$$< p_2|J^{\mu}_{em}(0)|p_1 >= \bar{u}(p_2)[(iF_2\mu_B + eF^{\nu}_3\gamma_5)\sigma^{\mu\nu}q_{\nu}]u(p_1) \tag{3.19}$$

The magnetic moment of the neutrino is (in units of μ_B)

$$k_{\nu} = F^{\nu}_2(q^2 = 0) \tag{3.20}$$

and the electric dipole moment is:

$$d_{\nu} = eF^{\nu}_3(q^2 = 0) \tag{3.21}$$

The analysis of electroweak data at LEP I, in this case the information on the invisible width of the Z boson, gives [331] $a_{\nu_\tau} < 3.6 \times 10^{-6}$ and $d_{\nu_\tau} < 6.9 \times 10^{-17}$ e cm at 90% CL. For comparison, bounds coming from astrophysics [265, 343] are reported in Tables 3.5 and 3.6 These tighter limits are derived in the hypothesis of $m_{\nu_\tau} \leq \mathcal{O}(10)$ keV, using red giant evolution. Heavier neutrinos cannot be produced in stellar cores. Again, neutrino experiments give additional limits. The BEBC beam dump experiment [344] set an upper limit of $\mu_{\nu_\tau} < 5.4 \times 10^{-7}$ μ_B. This limit is based on assumptions about the D_s production cross section in hadronic processes and its branching ratio into $\tau\nu_\tau$.

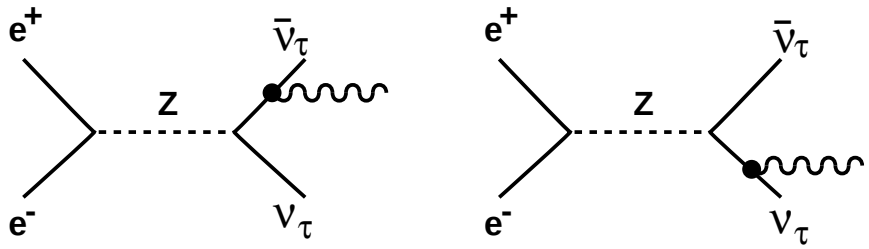

Figure 3.20: Anomalous contributions to the process Z$\rightarrow \nu\bar{\nu}\gamma$.

$a_\tau[\mu_B]$	CL	Reference	Method
$< 1 \times 10^{-6}$		[265]	Cosmology, $m_{\nu_\tau} = 1 - 35$ MeV
$< 2 \times 10^{-12}$		[343]	Astrophysics, $m_{\nu_\tau} \leq \mathcal{O}(10$ keV)
$< 5.4 \times 10^{-7}$	90%	[344]	Beam dump BEBC
$< 5.6 \times 10^{-6}$	90%	[345]	Neutrino counting at PEP
$< 4.6 \times 10^{-6}$	90%	[346]	Neutrino counting at PEP and PETRA
$< 3 \times 10^{-6}$	68%	[331]	Electroweak data at LEP
$< 5.5 \times 10^{-6}$	90%	[347]	Differential photon cross section at LEP
$< 4.1 \times 10^{-6}$	90%	[213]	Differential Photon cross section L3

Table 3.5: Limits on the anomalous magnetic moment of the ν_τ.

Electromagnetic moments would also lead to anomalous contributions to $e^+e^- \rightarrow \nu\bar{\nu}\gamma$, which have been searched for at low and high energies. PEP and PETRA data give [345,346] $\mu_{\nu_\tau} < 4 \times 10^{-6}$ μ_B at 90% CL. Near the Z pole, non vanishing moments can lead to anomalous contributions to the so-called neutrino counting channel, as indicated in Fig. 3.20 [347]. Using early data from ALEPH and L3, one finds [347] $\mu_{\nu_\tau} \leq 5.5 \times 10^{-6}$ μ_B at 90% CL. A more stringent limit has recently been obtained by L3 [213] analyzing single photon data. Requiring high

d_τ [e cm]	CL	Reference	Method
$< 3.9 \times 10^{-23}$		[343]	Astrophysics, $m_{\nu_\tau} \leq \mathcal{O}(10$ keV)
$< 6.9 \times 10^{-17}$	68%	[331]	Electroweak data at LEP

Table 3.6: Limits on the electric dipole moment of the ν_τ.

energy γ rays seen in the detector, no excess indicating the presence of additional contributions was observed. This sets a limit of $\mu_{\nu_\tau} \leq 4.1 \times 10^{-6}\ \mu_B$ at 90% CL. This result is competitive (see Tab. 3.5) with limits from low energy experiments and from the Z invisible width. It is one order of magnitude weaker those derived from the beam-dump experiment, but doesn't rely on assumptions about the hadronic processes and or branching ratios.

Chapter 4

Production of τ leptons by electroweak neutral current interactions

The production cross section, angular distribution and polarization of τ leptons from e^+e^- annihilation are used to study its neutral current couplings. Sufficiently far above threshold, the Born level total cross section for $e^+e^- \to \tau^+\tau^-$ can be decomposed into three terms

$$\sigma^0(s) = \sigma^0_\gamma + \sigma^0_Z + \sigma^0_{\gamma Z} \tag{4.1}$$

The purely electromagnetic contribution is σ^0_γ

$$\sigma^0_\gamma = \frac{4\pi\alpha^2}{3s} \tag{4.2}$$

with the fine structure constant α and the square of the center of mass energy s. The contribution σ^0_Z due to Z exchange can be written in terms of the Z partial widths into electrons, Γ_e, into tau leptons, Γ_τ, and the total width, Γ_Z

$$\sigma^0_Z = \frac{12\pi}{M_Z^2}\frac{\Gamma_e}{\Gamma_Z}\frac{\Gamma_\tau}{\Gamma_Z}\frac{s\Gamma_Z^2}{(s-M_Z^2)^2 + M_Z^2\Gamma_Z^2} \tag{4.3}$$

The multiplicative pole term is obviously small for center of mass energies sufficiently far below the Z mass, $s << M_Z^2$.

The partial decay widths of the Z to a fermion f can be expressed via its vector- and axialvector couplings $g_V(f)$ and $g_A(f)$

$$\Gamma_f = \frac{G_F M_Z^3}{6\pi\sqrt{2}}\left(g_V^2(f) + g_A^2(f)\right) \tag{4.4}$$

In standard electroweak theory, these are universal constants depending only on the fermion charge, Q_f, and the third component, T_3, of the weak isospin

$$g_V = T_3(f) - 2Q_f \sin^2\theta_W \tag{4.5}$$
$$g_A = T_3(f) \tag{4.6}$$

The interference term $\sigma^0_{\gamma Z}$

$$\sigma^0_{\gamma Z} = \frac{4\pi\alpha^2}{3} J_f \frac{s - M_Z^2}{(s - M_Z^2)^2 + s^2\Gamma_Z^2/M_Z^2} \tag{4.7}$$

with $J_f \simeq (G_F M_Z^2/\sqrt{2}\pi\alpha) g_V^2$, gives only a small contribution to the total cross section at essentially all energies.

We now specialize the discussion to charged leptons, like the tau, with $T_3 = -1/2$ and $Q = -1$. The distribution of the scattering angle θ, defined as the angle between the incoming e^- and the outgoing τ^-, can be written (at the Born level) as

$$\frac{d\sigma}{d\Omega} = \frac{\alpha^2}{4s}\left[a_0(1 + \cos^2\theta) + a_1 \cos\theta\right] \tag{4.8}$$

with a symmetric term a_0 and an asymmetric one a_1

$$a_0 = 1 + 2\mathrm{Re}(\chi) g_V(e) g_V(\tau) + |\chi|^2 \left(g_V^2(e) + g_A^2(e)\right)\left(g_V^2(\tau) + g_A^2(\tau)\right) \tag{4.9}$$

$$a_1 = 4\mathrm{Re}(\chi) g_A(e) g_A(\tau) + 8|\chi|^2 g_V(e) g_V(\tau) g_A(e) g_A(\tau) \tag{4.10}$$

Their properties depend on a pole term χ

$$\chi = \frac{G_F}{\sqrt{8}\pi\alpha} \frac{s M_Z^2}{(s - M_Z^2) + i M_Z \Gamma_Z} \tag{4.11}$$

which comes from the ratio of the γ and Z propagators. It is essentially real for $s << M_Z^2$ and purely imaginary at the Z pole. Integration over the solid angle yields the total cross section $\sigma_{tot} = a_0 \sigma^0_\gamma$. Electroweak interference in the angular distribution is negligible only very far below the Z mass. Already at PETRA and PEP energies, it leads to a sizeable forward backward asymmetry A_{FB}

$$A_{FB} \equiv \frac{\int_0^{+1} d\sigma/d\Omega \; d\cos\theta - \int_{-1}^0 d\sigma/d\Omega \; d\cos\theta}{\int_0^{+1} d\sigma/d\Omega \; d\cos\theta + \int_{-1}^0 d\sigma/d\Omega \; d\cos\theta} \tag{4.12}$$

which is a measure of the relative strength of the asymmetric and symmetric part of the cross section

$$A_{FB} = \frac{3a_1}{8a_0} \tag{4.13}$$

On the Z pole we find

$$A_{FB}(s = M_Z^2) = \frac{3}{4} A_e A_\tau \tag{4.14}$$

with the coupling parameters A_f of the neutral current

$$A_f = \frac{2 g_V(f) g_A(f)}{g_V^2(f) + g_A^2(f)} \tag{4.15}$$

for each lepton species, $f = e, \mu, \tau$.

As a rule of thumb one can summarize that for PETRA and PEP energies, $s << M_Z^2$, the total cross section measures g_V^2, the angular asymmetry g_A^2. At the Z pole, $s \simeq M_Z^2$, the total cross section will be proportional to $(g_V^2 + g_A^2)$, the angular asymmetry to g_V^2/g_A^2.

Since the Lorentz structure of the standard electroweak theory involves different left and right handed couplings to the Z, parity will be violated in neutral current processes. In processes dominated by Z exchange, parity is in fact violated twice, both in Z production and in Z decay. As a consequence, the final state τ leptons will be polarized, even when produced by unpolarized electrons and positrons. Their degree of polarization will depend on the relative strength of vector and axial vector couplings as well as on the scattering angle. One defines, at each scattering angle θ, a helicity asymmetry $A_\tau(\theta)$

$$A_\tau(\theta) \equiv \frac{\sigma^{h_\tau=+1/2}(\theta) - \sigma^{h_\tau=-1/2}(\theta)}{\sigma^{h_\tau=+1/2}(\theta) + \sigma^{h_\tau=-1/2}(\theta)} \tag{4.16}$$

which measures the relative production rate τ leptons with helicity $h_\tau = \pm 1/2$. Again at Born level we have

$$A_\tau(\theta) = \frac{A_\tau(1+\cos^2\theta) + 2A_e\cos\theta}{(1+\cos^2\theta) + 2A_eA_\tau\cos\theta} \tag{4.17}$$

The two parity violations can even be distinguished from each other. Integrating $A_\tau(\theta)$ over the scattering angle yields the average final state polarization $\mathcal{P}_\tau$

$$\int_{-1}^{+1} A_\tau(\theta)\ d\cos\theta \equiv -\mathcal{P}_\tau = A_\tau \tag{4.18}$$

which depends only on the τ lepton couplings to the Z. Integrating over the forward and backward hemispheres separately and forming an asymmetry yields

$$\frac{\int_0^{+1} A_\tau(\theta)\ d\cos\theta - \int_{-1}^0 A_\tau(\theta)\ d\cos\theta}{\int_0^{+1} A_\tau(\theta)\ d\cos\theta + \int_{-1}^0 A_\tau(\theta)\ d\cos\theta} \equiv A_{pol}^{FB} = -\frac{3}{4}A_e \tag{4.19}$$

which depends only on the electron couplings. For an axialvector dominated neutral current, like in the Standard Model, both polarization asymmetries will be essentially linear in g_V/g_A and measure their relative sign. It is worth noting that the forward-backward asymmetry is $A_{FB} = -A_{pol}^{FB} \cdot A_\tau$ and thus does not separate the two parity violation effects. Polarization asymmetries, in contrast to the angular asymmetry, vary slowly with s and are not small even at $s \simeq M_Z^2$.

The quantity A_e can also be measured using longitudinally polarized electron beams which are available at SLC. The asymmetry between the total cross sections of left-handed (σ_L) and right-handed electrons (σ_R) and unpolarized positrons is

$$A_{LR} \equiv \frac{\sigma_L - \sigma_R}{\sigma_R + \sigma_L} = A_e \tag{4.20}$$

Like the polarization forward backward asymmetry, Equ. 4.19, A_{LR} is a very sensitive measure of A_e. Its power is greatly enhanced by the fact that it is not necessary to select a certain final state for the measurement.

Beyond this simple Born level picture, radiative corrections are clearly important [348–352]. They fall into two general categories:

- Real photon bremsstrahlung: These corrections, dominated by initial state photon radiation in the case of τ production, are large, $\mathcal{O}(25\%)$, and experiment dependent. Their effect is essentially to shift the effective center of mass energy in each event to lower values.

- Propagator and vertex corrections: These are much smaller, $\mathcal{O}(1\%)$, and experiment independent, since they do not modify the event kinematics. They are also more interesting since heavy fermion and boson loops appear and since genuine weak corrections contribute.

The approach to radiative corrections varies from experiment to experiment and with the required accuracy. At energies below the Z pole, where cross section and asymmetry measurements are statistics limited, a correction of the experimental results with

$$d\sigma_{corr} = \frac{d\sigma_{obs}}{\delta_{RC}} \tag{4.21}$$

where σ_{obs} is the observed cross section after acceptance and background corrections, is appropriate. A radiative correction factor

$$\delta_{RC} = \frac{d\sigma_{theo}}{d\sigma_0} \tag{4.22}$$

where σ_{theo} is the cross section including higher orders, thus converts the observed cross section into one that can be directly compared to the Born level theory. This approach is adopted by the experimental groups up to and including TRISTAN energies.

At the Z pole, where the experimental accuracy is high and higher order electroweak effects themselves are a subject of study, this procedure must be replaced by a more elaborate one. Fortunately, in the vicinity of the Z pole, vertex and propagator corrections factorize such that a replacement of the bare electroweak couplings (g_V and g_A) by effective ones ($\bar{g}_V$ and $\bar{g}_A$) gives an accurate result without changing the simple Born level picture [348, 352]. This does not mean, however, that these corrections are negligible, they are in fact clearly required by the data. Real photon bremsstrahlung, on the other hand, can be corrected for with a convolution integral over the photon spectrum, thus including the correction in the theoretical prediction rather than correcting the data. This procedure has been adopted by the LEP and SLC collaborations.

The differences in the radiative correction scheme make it difficult to directly compare results from the two energy domains, since this would require detailed knowledge of the experimental cuts. In figure 2.1, cross section data spanning the whole available energy domain have therefore only been presented to give a qualitative impression. Also, since radiative corrections using the PETRA/PEP/TRISTAN method have been applied, only the data from one high energy experiment have been included. For quantitative conclusions, it is therefore best to base oneself on the comparison of the extracted electroweak parameters, rather than the cross section and asymmetry data themselves. This will be done in the following sections, together with a short overview of the experimental methods and errors.

4.1 τ Production and Electroweak Interference

Many experiments have observed τ production in the energy domain from 10 to 60 GeV, where the production mechanism is dominated by photon exchange and γ-Z interference is observed.

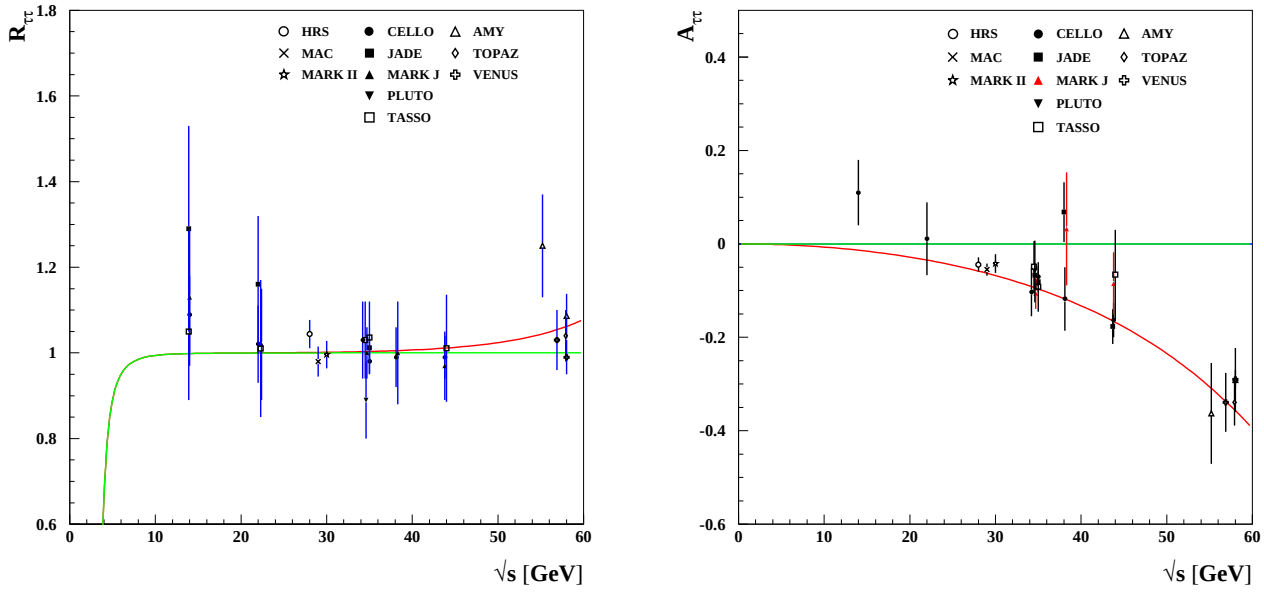

Figure 4.1: The center-of-mass energy dependence of the $\tau^+\tau^-$cross section and forward-backward charge asymmetry from experiments in the region of electroweak interference [12–36]. All data have been radiatively corrected to allow for a comparison with electroweak theory at the Born level, which is indicated by the curve.

Figure 4.1 gives an overview of the measured total cross-sections and forward-backward asymmetries as a function of the center-of-mass energy. As pointed out earlier, radiative corrections in this energy domain are dominated by initial state photon bremsstrahlung and corrected by applying a multiplicative factor to the measured data. Since the cross-section varies slowly in this energy range, this is accurate enough a method and allows direct comparison of the experimental results to the Born-level formulae. The data are thus compared to electroweak theory at this level, taking the "bare" values of electroweak parameters as measured at the Z resonance.

It is evident that the cross-section, expressed here as the ratio

$$R_{\tau\tau} = \frac{\sigma_{\tau\tau}}{\sigma^0_\gamma} \tag{4.23}$$

follows the expected energy dependence for pointlike fermions with unit charge. It agrees perfectly in magnitude with the cross-section for muon pair production. In this energy range, weak neutral current couplings come in only proportional to g_V^2 and the Z pole term. Sizeable deviations from pure QED in the total cross-section are thus only observed as one approaches the Z pole. Indeed, at the highest PETRA energies and more pronouncedly at TRISTAN, a slow rise of the cross section is observed.

Deviations of the cross-section from its expected behavior are traditionally parametrized [353] by a form-factor applied at the $\gamma\tau^+\tau^-$ vertex. Given a dipole form of the form-factor, the cross section would then be modified as

$$\sigma_{\tau\tau} = \sigma^0_{\tau\tau}\left(1 \mp \frac{s}{s - \Lambda^2_\mp}\right) \tag{4.24}$$

Experiment	Λ_- [GeV]	Λ_+ [GeV]
CELLO [17]	231	318
JADE [19]	210	285
MARK J [24]	205	235
PLUTO [26]	101	107
TASSO [30]	169	161
HRS [13]	284	129
TOPAZ [34]	208	134
VENUS [36]	225	234

Table 4.1: 95% CL lower limits on the scale parameter of a hypothetical dipole form-factor at the $\gamma\tau^+\tau^-$ vertex.

Experiment	g_V^2	g_A^2
CELLO [17]	0.04 ± 0.07	0.22 ± 0.06
JADE [354]	0.03 ± 0.04	0.26 ± 0.04
MARK J [25]	0.04 ± 0.03	0.27 ± 0.02
TASSO [31]	0.04 ± 0.04	0.26 ± 0.03
MARK II [15]	0.03 ± 0.04	0.23 ± 0.05
HRS [12]		0.23 ± 0.07
AMY [33]	0.00 ± 0.18	0.23 ± 0.05
VENUS [36]		0.23 ± 0.03

Table 4.2: Results on the vector and axialvector neutral current couplings to leptons from PETRA, PEP and TRISTAN experiments, assuming lepton universality

with a scale parameter Λ in momentum space. Since the non pointlike nature of the vertex will start to be resolved at momentum transfers much below this scale, the good agreement of the data translates into limits on Λ of several hundred GeV. Results are summarized in Table 4.1. More specific models of compositeness, which predict larger cross-section modifications at low energies due to contact terms can also be tested [19,33,35,36].

In contrast to the total cross section, the forward-backward asymmetry shows measurable electroweak interference effects already at moderate center of mass energies. Figure 4.1 lists a compilation of data from PETRA, PEP and TRISTAN. Careful control of systematic errors allows to observe a non-zero asymmetry already at about 30 GeV. Since the asymmetry in this energy region mainly depends on g_A^2, the cross-section on g_V^2, these data give an error in these quantities of order 5%. The sensitivity of the measurements is not sufficient to draw separate conclusions for each lepton species, one has to assume lepton universality of neutral current couplings. Table 4.2 compiles such results from the PEP, PETRA and TRISTAN experiments.

Although not very accurate, these data clearly show that the weak neutral current is dominated by its axialvector component, i.e. $|g_V| \ll |g_A|$. They thus solve a two-fold ambiguity in the neutral current couplings left over from the measurement of the cross sections for $\nu_\mu e^-$, $\bar{\nu}_\mu e^-$, $\nu_e e^-$ and $\bar{\nu}_e e^-$ scattering. This is shown in Figure 4.2 [355,356], which summarizes the status of leptonic neutral current couplings before the start of the TRISTAN, LEP and SLC experiments.

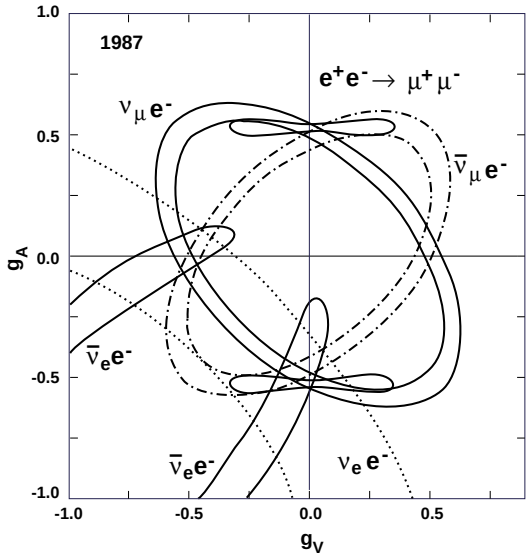

Figure 4.2: Allowed region of g_V and g_A for leptonic neutral currents [355, 356] before the Tristan, LEP and SLC experiments, assuming lepton universality. Neutrino-electron cross sections correspond to ellipses in this plane. Electroweak interference measurements solve the ambiguity in favor of an axialvector dominated neutral current.

4.2 Z-τ Interactions

4.2.1 Cross section and forward-backward asymmetry

Clearly, experiments at the Z pole are best suited to measure the couplings of the weak neutral current to leptons. The cross-section is enhanced by the Z pole such that rates are high and the relative contribution of QED is small. The cross section at $\sqrt{s} = M_Z$ can be expressed as the product of the Z partial widths to electrons and a given fermion species (see Equation 4.3), compared to the total width which is measured independently by the width of the excitation curve. Thus the cross-section, forward-backward asymmetry and polarization all carry information about the neutral current couplings. For more detailed reviews of the electroweak LEP data on tau production, see e.g. [357,358].

Figures 4.3 and 4.4 show the dependence of the total cross section and forward-backward asymmetry (extrapolated to 4π solid angle) for $e^+e^- \rightarrow \tau^+\tau^-$ on the center of mass energy $\sqrt{s}$, as published by the four LEP experiments. The overlayed curve, calculated with ZFITTER [359–361], corresponds to the result of a fit to all electroweak LEP data as compiled by the LEP Electroweak Working Group [256, 362]. It is convenient to choose the quantities $R_l = \Gamma_{had}/\Gamma_l$, the ratio of the Z width into hadrons and lepton species l, and A^l_{FB}, the forward-backward asymmetries at $\sqrt{s} = M_Z$, as observables, since this choice gives minimum correlations among the parameters. Figure 4.5 shows the latest preliminary results of the four LEP experiments collected by the LEP Electroweak Working group [362], as 68% CL contours in the R_l-A^l_{FB} plane for each lepton species. For electrons, a correction is applied to account for the influence of t-channel Bhabha scattering. It is evident that the observables are compatible with being the same to high precision among the lepton species, the shape of the Z excitation

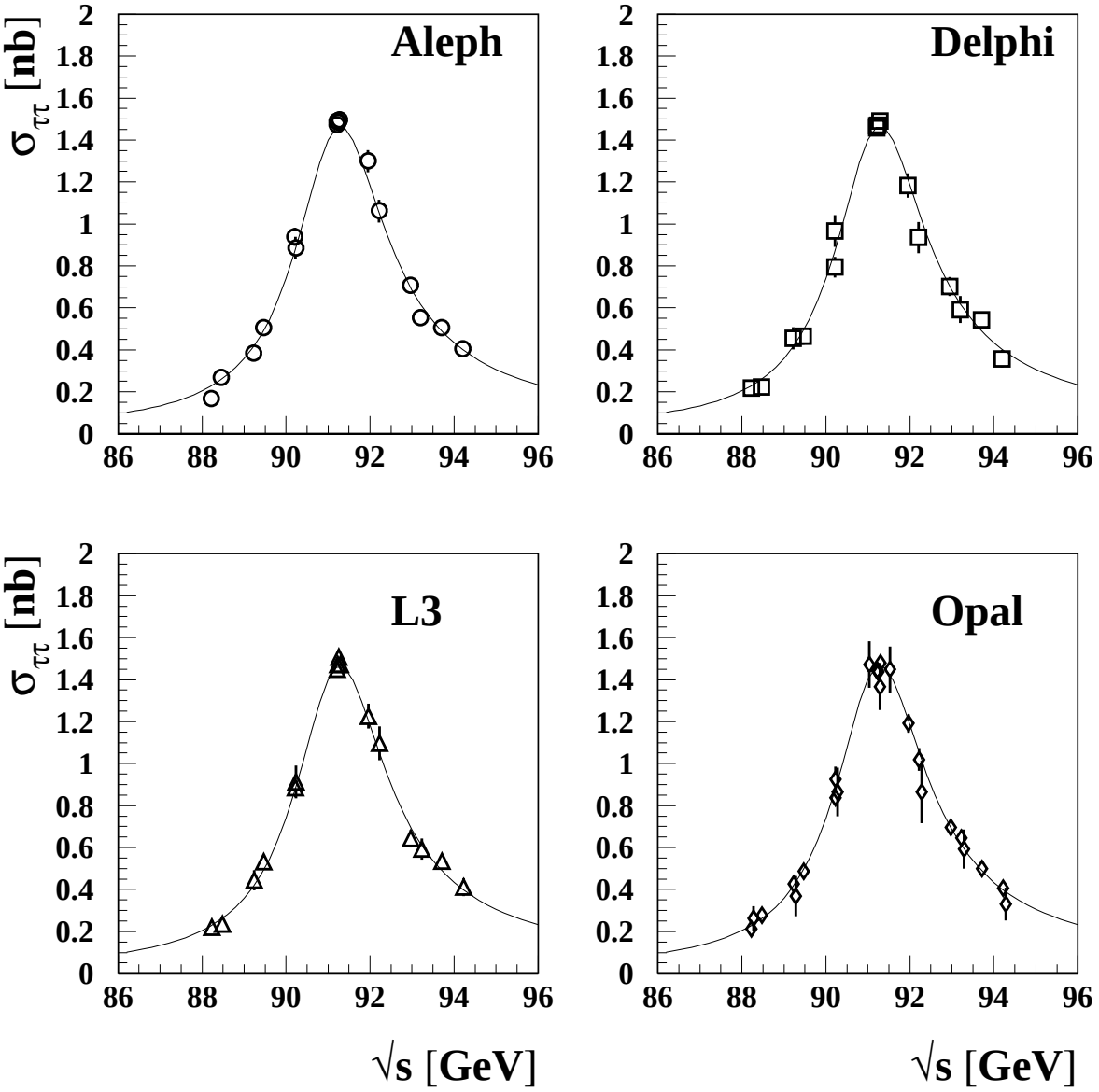

Figure 4.3: The center-of-mass energy dependence of the $\tau^+\tau^-$cross section from experiments in the region of the Z resonance [41,162,178,180,197,221,229,232]. The solid line corresponds to the prediction of the Standard Model, with parameters derived from the combined electroweak results and assuming lepton universality.

curves and the angular distribution is thus independent of the lepton flavor. For a more quantitative analysis, the combined preliminary LEP results [362] are summarized in Tab. 4.3. In addition to the relative decay widths and asymmetries for the three lepton species, it specifies the combined values for the Z mass, the total width and the hadronic peak cross section σ_h^0. From these data one can determine the partial width of the Z into the three lepton species to be 83.92 ± 0.17 MeV, 83.92 ± 0.23 MeV and 83.85 ± 0.29 MeV, for electrons, muons and taus, respectively. Evidently this is in excellent agreement with the assumption of lepton universality

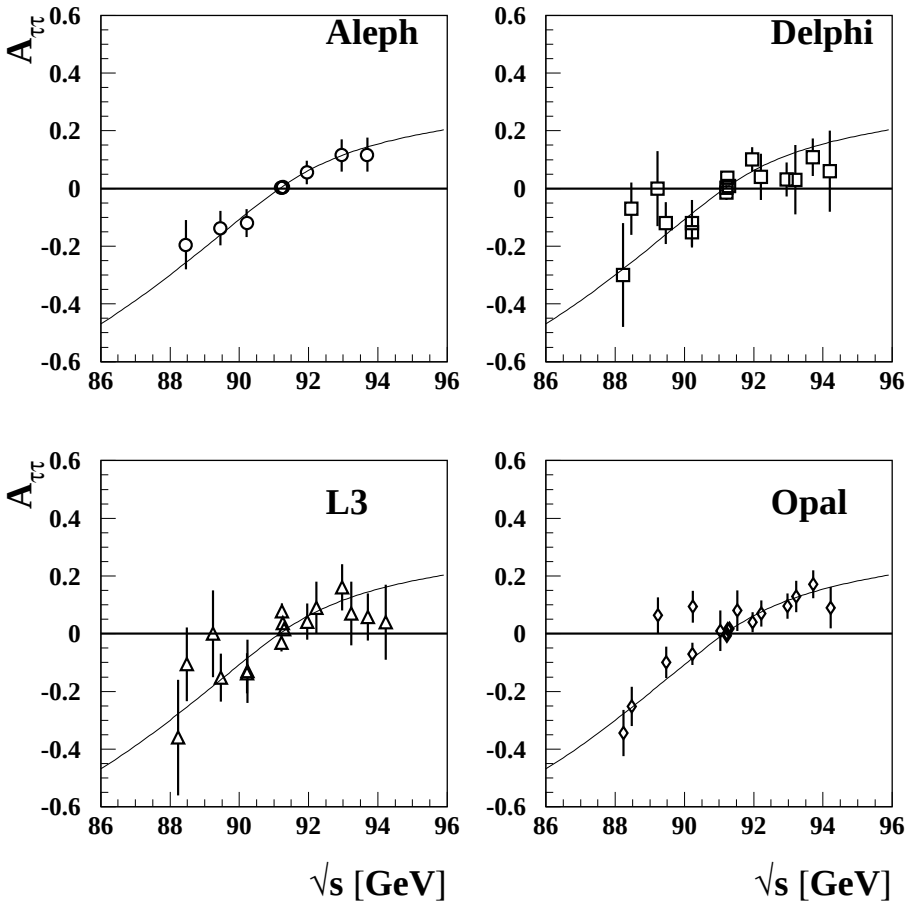

Figure 4.4: The center-of-mass energy dependence of the $\tau^+\tau^-$forward-backward asymmetry from experiments in the region of the Z resonance [41, 162, 178, 180, 197, 221, 229, 232]. The apparent differences in accuracy are mainly due to different binning of the data. The solid line corresponds to the prediction of the Standard Model, with parameters derived from the combined electroweak results and assuming lepton universality.

Parameter	Average Value
M_Z (GeV)	91.1885 ± 0.0022
Γ_Z (GeV)	2.4963 ± 0.0032
σ_h^0 (nb)	41.488 ± 0.078
R_e	20.797 ± 0.058
R_μ	20.796 ± 0.043
R_τ	20.813 ± 0.061
A_{FB}^e	0.0157 ± 0.0028
A_{FB}^μ	0.0163 ± 0.0016
A_{FB}^τ	0.0206 ± 0.0023

Table 4.3: Average Z line shape and asymmetry parameters (at $Q^2 = M_Z^2$) from preliminary data of the four LEP experiments [362]. The χ^2 per degree of freedom for the average is 36.1/27.

in neutral currents.

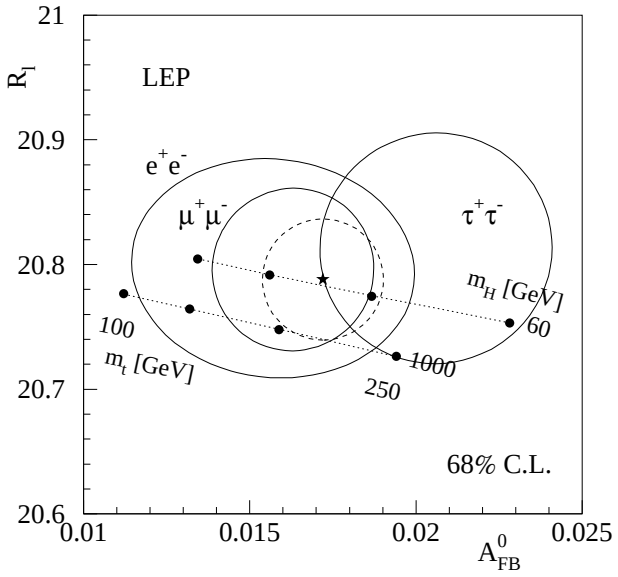

Figure 4.5: 68% CL contours for the pole forward-backward asymmetries for $e^+e^- \to e^+e^-$, $\mu^+\mu^-$ and $\tau^+\tau^-$ versus the peak cross section ratio $R_l = \Gamma_{had}/\Gamma_l$ as measured at LEP. The dashed contour gives the allowed region assuming lepton universality. The dotted lines correspond to the prediction of the Standard Model for top quark masses between 100 and 250 GeV with two different Higgs boson masses, 60 and 1000 GeV.

4.2.2 Tau polarization in Z decays

Z decays into τ leptons are the only ones where final state polarization is observable in addition. Since the couplings of the τ to the charged current are compatible with being a pure $V-A$ interaction (see Chapter 5), one assumes maximum parity violation, such that τ^- decays only to lefthanded ν_τ and the τ^+ only to righthanded $\bar{\nu}_\tau$. The τ helicity then determines the direction of the neutrino emission as illustrated in Fig. 4.6. In the massless limit, the τ^- and τ^+ helicities are completely anticorrelated.

Since the neutrino escapes detection, its direction of emission must be inferred from the observable final state. In the simplest case of the decay $\tau^- \to \pi^-\nu_\tau$, all information is contained in the decay angle θ^*, the angle between the τ line of flight and the pion in the τ rest frame. In the laboratory system, this angle is measured by the ratio of the pion energy to the τ energy, the latter one being approximated by the beam energy. This is also the only polarization sensitive observable in three-fermion decays, $\tau \to e/\mu\nu\nu$, where a lot of sensitivity is lost by the additional neutrino. As an example, Figure 4.7 shows the charged particle spectra from $\tau \to e\nu\nu$, $\mu\nu\nu$ and $\pi\nu$ as measured by ALEPH [187] in terms of the scaled energy $x = E/E_b \simeq E/E_\tau$. Also shown are the spectra expected for positive and negative helicity and for the background, as well as the combination of them that best fits the data. It is this combination that determines the average polarization.

For decays into vector mesons, $\tau \to \rho\nu_\tau$ and $\tau \to a_1\nu_\tau$, the spin orientation of the decay

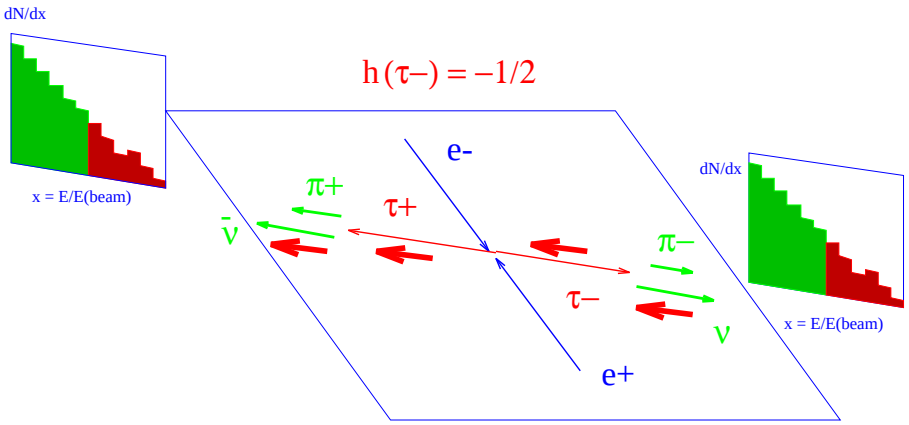

Figure 4.6: Use of the simplest τ decay into pion and neutrino to statistically determine the degree of polarization from the pion momentum distribution. Thin arrows indicate particle momenta, thick arrows indicate the spin orientation. Negative helicity for the τ^- leads to a linearly falling pion energy distribution, positive helicity to a linearly rising one.

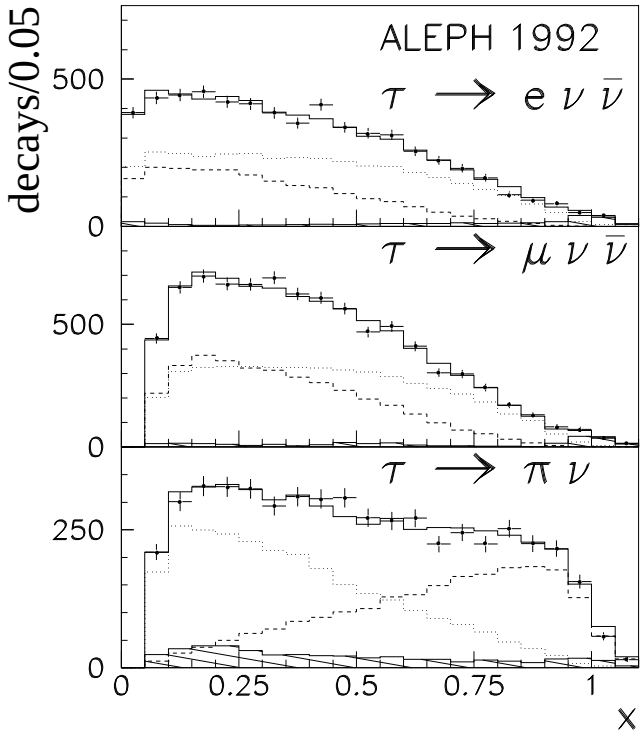

Figure 4.7: The distributions of the scaled energy $x = E/E_b$ in $\tau \to e\nu\nu$, $\mu\nu\nu$ and $\pi\nu$ as measured by ALEPH [187]. Also shown are the Monte Carlo best fit (solid histogram), the contributions from positive helicity (dotted histogram), negative helicity (dashed histogram) and the non-τ background (hatched area).

hadron can be transverse or longitudinal. Thus, there are more observables that carry helicity information. For the ρ decay, these are [363,364]: θ^*, the angle between the ρ and the τ line of flight in the tau rest frame, and ψ^*, the angle between the π and the ρ line of flight in the ρ rest frame. For the a_1 decay, an additional angle is defined using the orientation of the three-pion

system with respect to its decay plane. These angles and their correlation can be used in a multidimensional fit or combined to form an optimum observable [365]. As an illustration, Figure 4.8 shows the distributions of ψ^* in bins of $\cos\theta^*$ for $\tau \to \rho\nu$ as measured by L3 [211]. Figure 4.9 shows the distribution of optimal observables ω for $\tau \to \rho\nu$ and $\tau \to a_1\nu$ as measured by ALEPH [187]. Again, the helicity and background components as well as the best fit to the data are also shown.

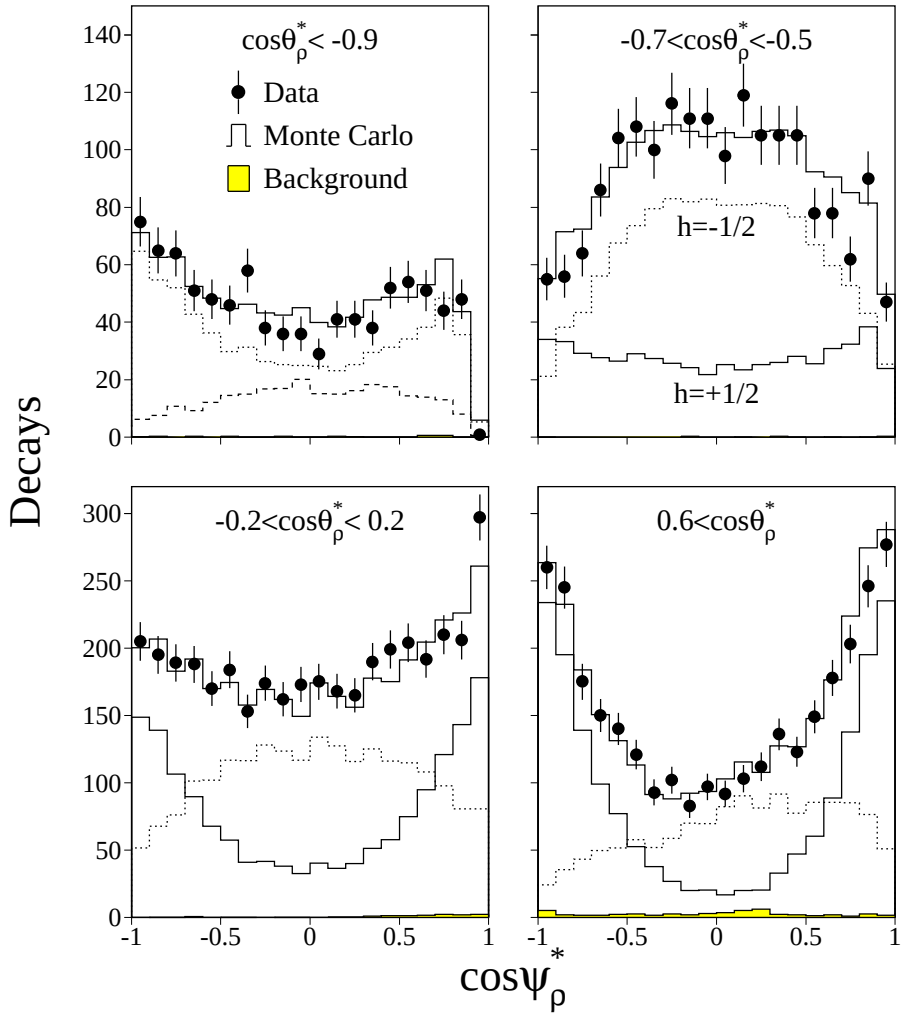

Figure 4.8: The distributions for $\tau \to \rho\nu$ of ψ^* in four ranges of $\cos\theta^*$ from L3 [211]. Also shown are the Monte Carlo best fit (solid histogram), the contributions from positive helicity (dashed histogram), negative helicity (dotted histogram) and the non-τ background (shaded area).

It is in fact beneficial, but not really necessary to completely identify the tau decay mode in order to measure its polarization. One can thus also do an inclusive measurement that mixes several decay modes together [199]. Since the helicities of τ^+ and τ^- are anti-correlated, correlation observables, like the acollinearity of charged decay products, can be used in addition. Figure 4.10 shows the acollinearity distribution of $\tau\tau \to \pi X$ final states (where X is any one prong τ decay) from L3 [211], with the contributions from helicities and background indicated.

Putting together results from all channels and all methods as a function of the scattering angle $\cos\theta$, one arrives at the angular dependence of the mean polarization as shown in

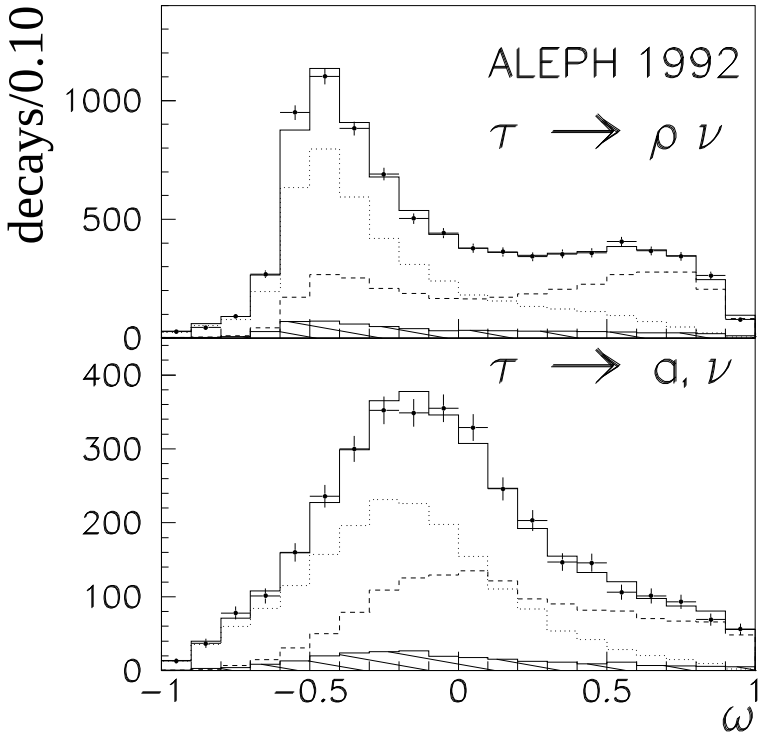

Figure 4.9: The distributions of optimal variables for the decays $\tau \to \rho\nu$ and $a_1\nu$ as measured by ALEPH [187]. Also shown are the Monte Carlo best fit (solid histogram), the contributions from positive helicity (dotted histogram), negative helicity (dashed histogram) and the non-τ background (hatched area).

Figure 4.11. Analyzing this dependence as indicated in Equ. 4.17, one obtains the results summarized in Table 4.4 for the asymmetry parameters A_e and A_τ of electron and τ lepton. The combined preliminary results of the LEP collaborations yield [362]

$$A_e = 0.139 \pm 0.009 \tag{4.25}$$
$$A_\tau = 0.142 \pm 0.008 \tag{4.26}$$

This measurement, with percent precision, is again in excellent agreement with lepton universality of neutral currents. As mentioned earlier, the total cross section asymmetry A_{LR} (see Equ. 4.20) observed with polarized beams at SLC is an alternative way to measure the asymmetry parameter A_e. One obtains [247,248]

$$A_e = 0.155 \pm 0.004 \tag{4.27}$$

in agreement with the LEP measurement within errors.

Using all electroweak results from LEP and SLC, Figure 4.12 summarizes the latest results on the effective neutral current couplings to leptons [357,362]. Quantitative results are shown in Tab. 4.5. The sign of g_V is chosen to agree with the results of neutrino electron scattering (see Section 4.1). Universality of the leptonic neutral current is clearly confirmed by these data, the couplings are compatible with being independent of lepton flavor with permill precision. The impressive improvement obtained from the LEP/SLC experiments with respect to previous results is obvious from a comparison to Figure 4.2.

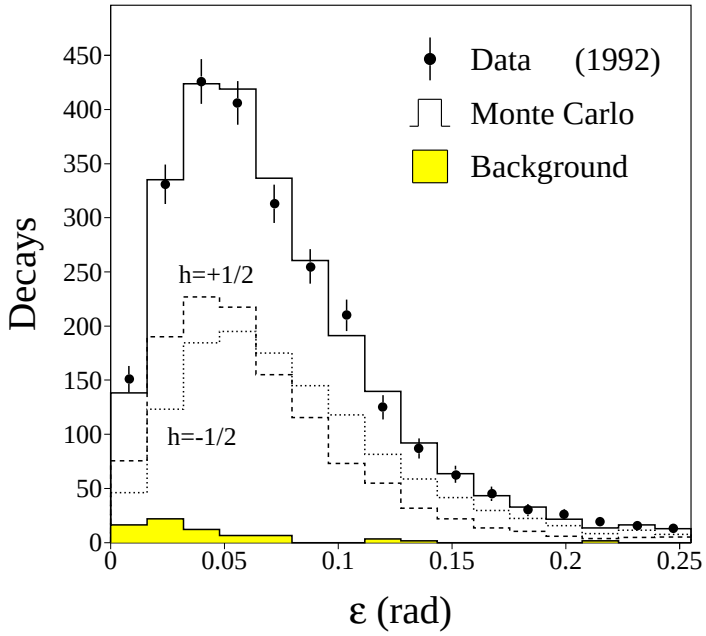

Figure 4.10: The distributions of the acollinearity angle ϵ for $\tau\tau \to \pi X$ from L3 [211]. Also shown are the Monte Carlo best fit (solid histogram), the contributions from positive helicity (dashed histogram), negative helicity (dotted histogram) and the non-τ background (shaded area).

Experiment	A_e	A_τ
ALEPH [187]	$0.129 \pm 0.016 \pm 0.005$	$0.136 \pm 0.012 \pm 0.009$
DELPHI [199]	$0.136 \pm 0.027 \pm 0.003$	$0.148 \pm 0.017 \pm 0.014$
L3 [215]	$0.156 \pm 0.016 \pm 0.005$	$0.152 \pm 0.010 \pm 0.009$
OPAL [244]	$0.134 \pm 0.015 \pm 0.004$	$0.134 \pm 0.010 \pm 0.009$

Table 4.4: Results on the asymmetry parameter of electrons and τ leptons from the LEP experiments' analysis of τ polarization. The L3 [215] and OPAL [244] results are preliminary and replace the published ones [211,235]. The first error is statistical, the second systematic.

Coupling	Combined Result (LEP+SLC)
$\bar{g}_V(\mathrm{e})$	-0.0385 ± 0.0009
$\bar{g}_V(\mu)$	-0.0354 ± 0.0036
$\bar{g}_V(\tau)$	-0.0369 ± 0.0018
$\bar{g}_A(\mathrm{e})$	-0.5010 ± 0.0005
$\bar{g}_A(\mu)$	-0.5012 ± 0.0008
$\bar{g}_A(\tau)$	-0.5015 ± 0.0009

Table 4.5: Results for the effective vector and axial vector couplings derived from the combined LEP and SLC data without the assumption of lepton universality [362].

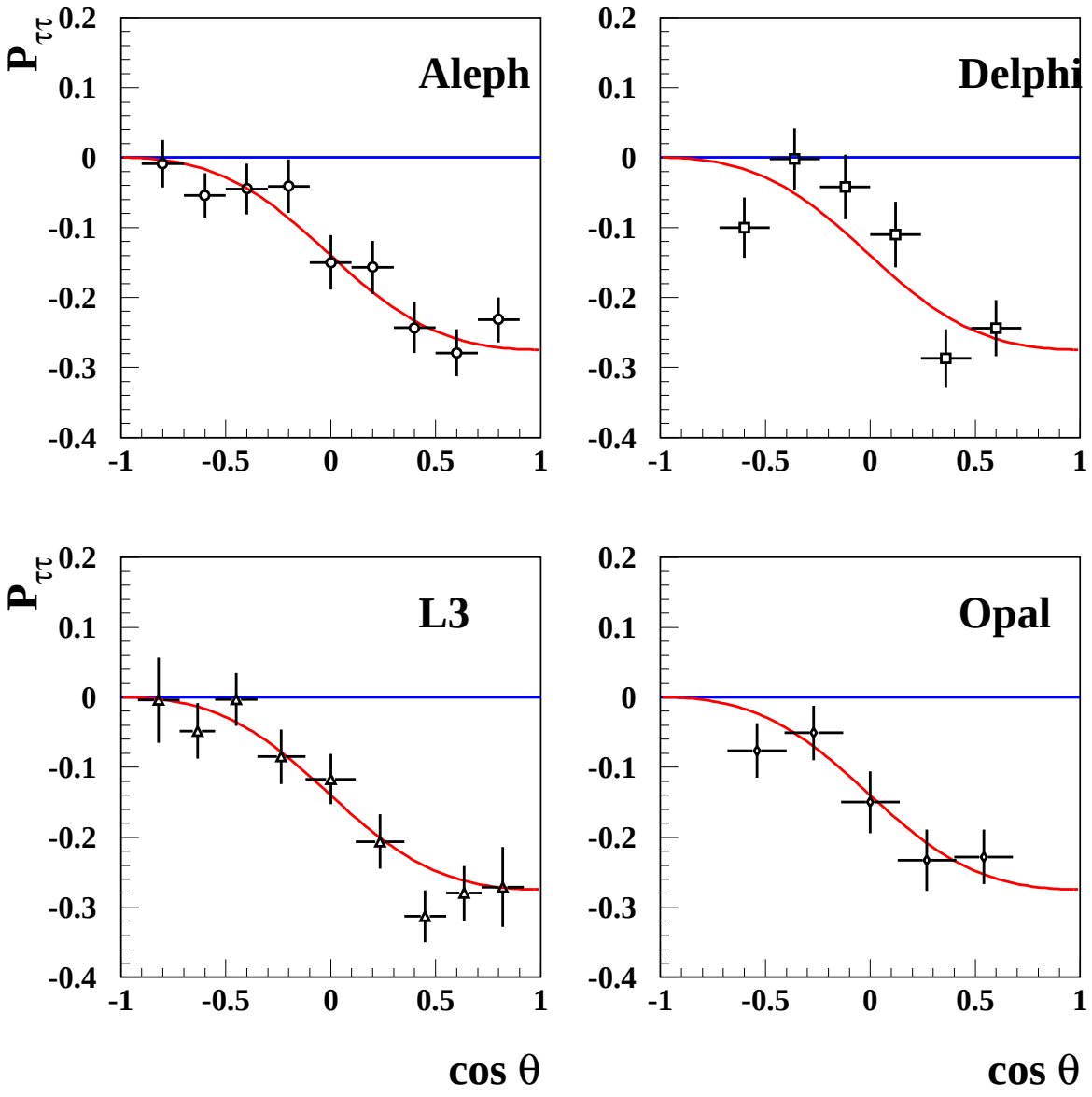

Figure 4.11: The dependence of the τ polarization on the scattering angle at the Z resonance [187, 199, 211, 235]. The solid line corresponds to the prediction of the Standard Model, with parameters derived from the combined electroweak results and assuming lepton universality.

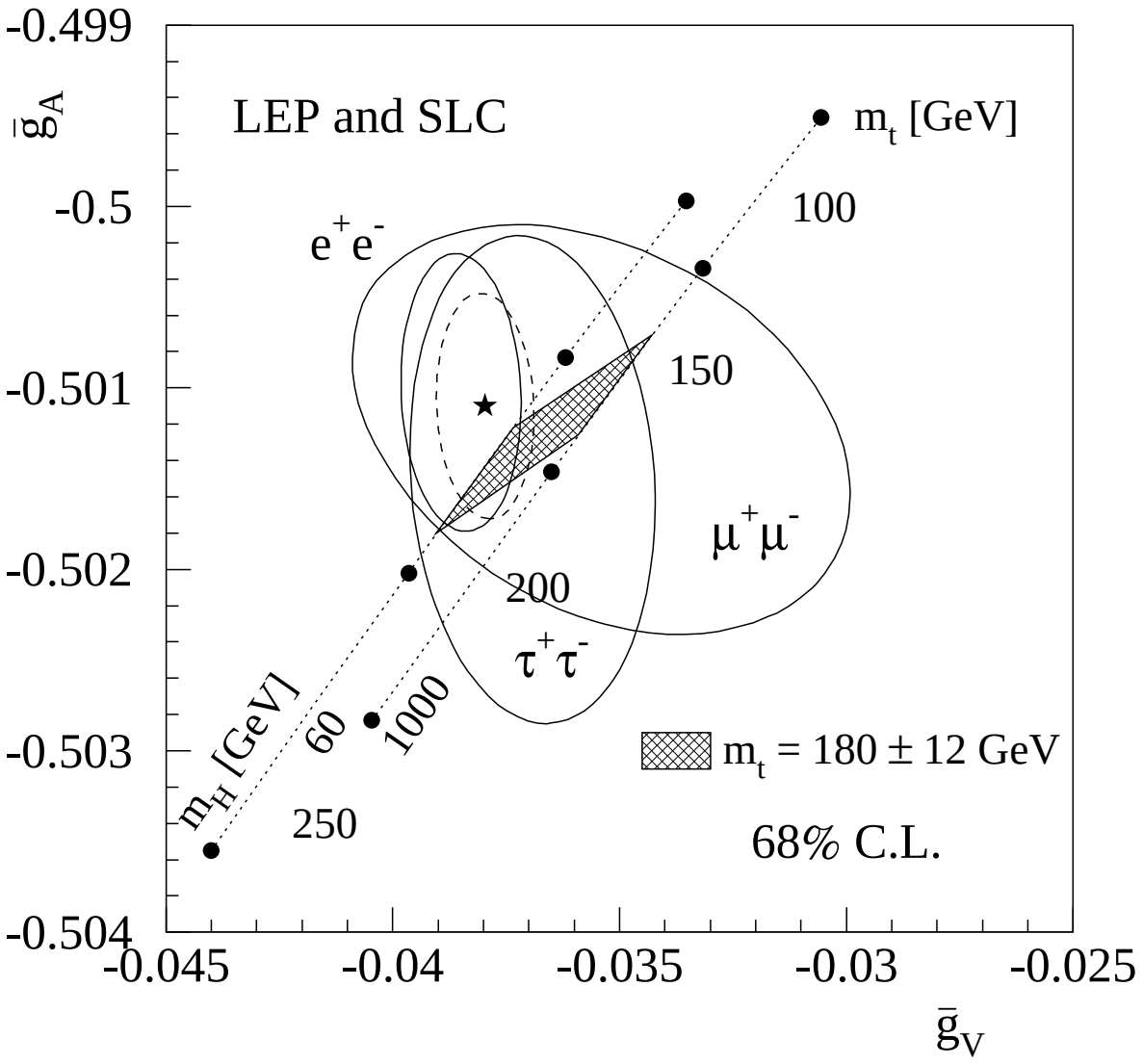

Figure 4.12: Allowed region of $\bar{g}_V$ and $\bar{g}_A$ for the three lepton generations. The graph shows combined LEP and SLC results from 1995. The star and dashed ellipse gives the best fit and 68% CL contour assuming lepton universality of neutral current couplings. The dotted lines correspond to the prediction of the Standard Model for top quark masses between 100 and 250 GeV with two different Higgs boson masses, 60 and 1000 GeV. The shaded area delimits the predictions for currently prefered values of the top mass [366,367].

Chapter 5

Decays of τ leptons by weak charged current interactions

The weak decays of tau leptons are of special interest because of the specific range of momentum transfer that they allow to study. On one hand, the mass of τ, which limits phase space, is high enough to allow for hadronic decays, which are absent for the light leptons. On the other hand, the mass is low so that the decay final states are of low multiplicity. Thus, the interesting process of hadronic resonance production by the weak charged current becomes experimentally accessible. In this region of momentum transfer, the only other ways of studying the hadronic charged current are charm decays [368] and low energy neutrino nucleon scattering [369], where the conclusions are limited by the complications of hadronic structure in the initial state.

However, the first task in the study of tau lepton decays is to understand in detail the leptonic currents. The study of tau production properties concludes that it can be regarded as a pointlike lepton up to the highest momentum transfers probed so far. Thus according to the Standard Model, which imposes lepton universality of charged as well as neutral couplings, the charged weak current in tau decays should be identical to the one in muon decays up to mass effects. Since the total muon decay rate defines the effective leptonic charged current coupling strength G_F, the Fermi constant, the decays width of $\mu^- \to e^- \bar{\nu}_e \nu_\mu$ should be related to $\tau^- \to e^- \bar{\nu}_e \nu_\tau$ by a simple phase space factor. The space-time structure of the decay, as measured by e.g. the Michel parameters, should be $V - A$. Maximum parity violation in the decay should lead exclusively to lefthanded tau neutrinos in the final state.

When studying hadronic tau decays, it is primordial to observe a maximum of all decay channels in order to make sure that no unusual final states pass unobserved. Since the q^2 region in question falls into the domain of single π/K and low mass hadronic resonances, multiparticle decay amplitudes can be related to amplitudes of weak meson decay as well as low energy e^+e^- experiments by current algebra techniques. Tau decays into pions and kaons, non-strange and strange resonances can thus provide valuable information on the mechanism by which a virtual W turns into hadrons at low q^2.

5.1 Total and leptonic decay width

The first test in search for a deviation from universality of the leptonic charged current is the comparison of the total coupling strength of electron, muon and tau to the W boson. The total muon decay rate [370]

$$\Gamma(\mu^- \to \mathrm{e}^- \bar{\nu}_\mathrm{e} \nu_\mu) = \frac{G_F^2 m_\mu^5}{192\pi^3} \left[1 + \delta_m(y_e)\right] (1 + \delta_W) (1 + \delta_{rad}) \tag{5.1}$$

in fact defines the total coupling strength, measured by the Fermi constant G_F. The first explicitly written term specifies the Born level result for a point-like $V - A$ four-fermion interaction with a massless final state. The correction δ_m takes into account the finite mass of the charged lepton in the final state

$$\delta_m(y_e) = -8y_e + 8y_e^3 - y_e^4 - 12y_e^2 \ln y_e \tag{5.2}$$

with $y_e = m_e^2/m_\mu^2 \simeq 2 \times 10^{-5}$, such that this correction is 0.2 permill for muon decays, negligible for $\tau^- \to \mathrm{e}^- \bar{\nu}_e \nu_\mu$ and 2.7% for $\tau^- \to \mu^- \bar{\nu}_\mu \nu_\mu$. The W propagator effects lead to a correction

$$\delta_W = +\frac{3}{5}\frac{m_\mu^2}{m_W^2} - 2\frac{m_e^2}{m_W^2} \tag{5.3}$$

which is negligible for muon as well as tau decays. QED radiative corrections introduce the largest correction for muon decays

$$\delta_{rad} = -\frac{\alpha(m_\mu)}{2\pi}\left(\pi^2 - \frac{25}{4}\right) \tag{5.4}$$

which is almost 5 permill. For the muon, the total decay rate is equal to the one into this particular decay channel to better than one part in 10^{10}; the leptonic width is thus simply the inverse of the muon lifetime.

The vertex factor for tau decays and muon decays is the same under the hypothesis of lepton universality in charged currents. Thus, the width of $\tau^- \to \mathrm{e}^- \bar{\nu}_e \nu_\tau$ can be obtained from the above formulae with the replacement $m_\mu \to m_\tau$. Since QCD corrections to the total tau decay width are non-negligible (see chapter 6), one does not directly compare the total widths of muon and tau. Instead, one uses the lifetime and the leptonic branching ratio to obtain the partial width of the tau into electrons

$$\Gamma(\tau^- \to \mathrm{e}^- \bar{\nu}_\mathrm{e} \nu_\tau) = \Gamma_\tau \ \mathrm{BR}(\tau^- \to \mathrm{e}^- \bar{\nu}_\mathrm{e} \nu_\tau) = \frac{\mathrm{BR}(\tau^- \to \mathrm{e}^- \bar{\nu}_\mathrm{e} \nu_\tau)}{\tau_\tau} \tag{5.5}$$

Given a precisely measured mass of the τ lepton, universality in the leptonic charged current thus requires that the leptonic branching fraction and the lifetime be proportional; the proportionality constant, including radiative corrections, is known to high precision.

Early tests of this universality relation [251], based on the 1990 Review of Particle Properties [371] as well as preliminary CLEO and LEP data, indicated a rather serious deviation: the lifetime appeared high and/or the electronic branching fraction low. With the now much more precisely known tau mass (see chapter 3), the universality test can be repeated with high sensitivity.

5.1.1 The tau lifetime

The first ingredient, the tau lifetime, τ_τ, giving the total decay width, has seen important experimental improvements since the availability of high precision silicon vertex detectors in collider experiments. The lifetime is short, such that the tau decays inside the beam pipe. Thus, the decay vertex cannot be directly observed, the lifetime must be inferred from the decay secondaries. The principles of the measurement and its observables are visualised in Fig. 5.1. The measurement is usually done in projection onto the plane perpendicular to the beam axis. The decay length is thus $L = \gamma\beta\tau_\tau \sin\theta$, with the boost factor $\gamma\beta = p_\tau/m_\tau$ and the polar production angle θ. The impact parameter $\delta = \gamma\beta\tau_\tau \sin\theta \sin\phi$, with the projected decay angle ϕ in the laboratory system, allows to have a measure of the lifetime transverse to the flight direction.

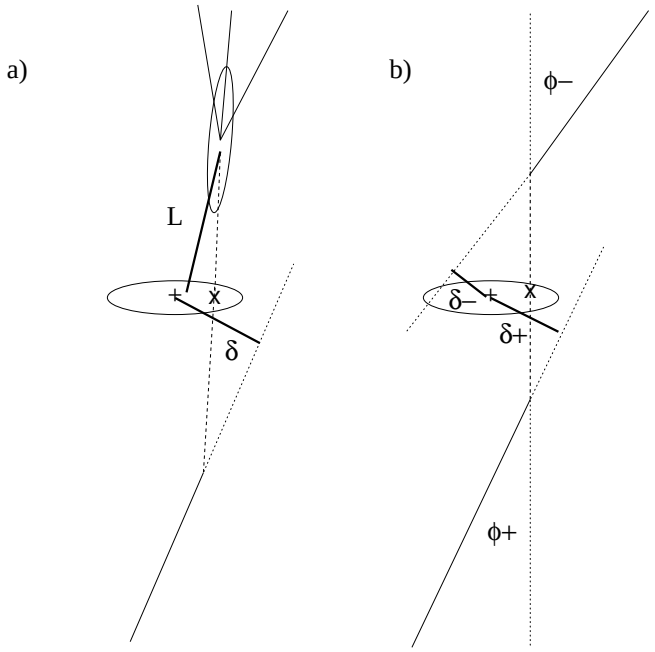

Figure 5.1: Schematic drawing to show the different observables used for the tau lifetime measurement. The beam spot is shown as an ellipse, the assumed production point as a plus, the actual tau production point as a cross. a) Definitions of the decay length L and the impact parameter δ. b) Correlation of the two observed impact parameters in an event with two 1-prong decays with the decay angle ϕ.

Since no tracks emerge from the e^+e^- vertex, the tau production vertex can only be determined on average, from the position of the luminous region. Its position and profile are measured using simultaneously taken e^+e^- annihilations into hadrons. The size of this luminous region depends on the accelerator and its optics, typical values for LEP (SLC) are $\sigma_y \simeq 5\mu$m (0.8μm) in the vertical plane and $\sigma_x \simeq 150\mu$m (2.6μm) in the horizontal plane. Since the beam profile is gaussian in shape, the size of the luminous region enters as a gaussian error into the decay length measurement. For three prong tau decays, the decay vertex can be determined from the charged final state (decay length method, see upper part of Fig. 5.1a). Its covariance matrix can be estimated using single track measurement errors as well as multiple scattering errors influencing the backward extrapolations towards the decay vertex. From the positions and covariance matrices for the two vertices, a most likely decay length (and its error)

can be extracted event by event. Since the tau momentum is equal to the beam energy up to radiative corrections, thus almost constant, the observed decay length distribution gives a true representation of an exponential when measured with sufficient precision. Fig. 5.2 shows an example from OPAL at LEP [236]. The observed distribution is well described by the convolution of an exponential with the experimental resolution function, tails are understood down to the level of a few events in several thousands. The distribution can be analysed in terms of a moments or maximum likelihood method to extract a tau lifetime. Recent preliminary results from this method are summarised in Fig. 5.3 and compared to the 1994 Review of Particle Properties [252]. The results of the experiments are consistent within errors and not yet dominated by systematics.

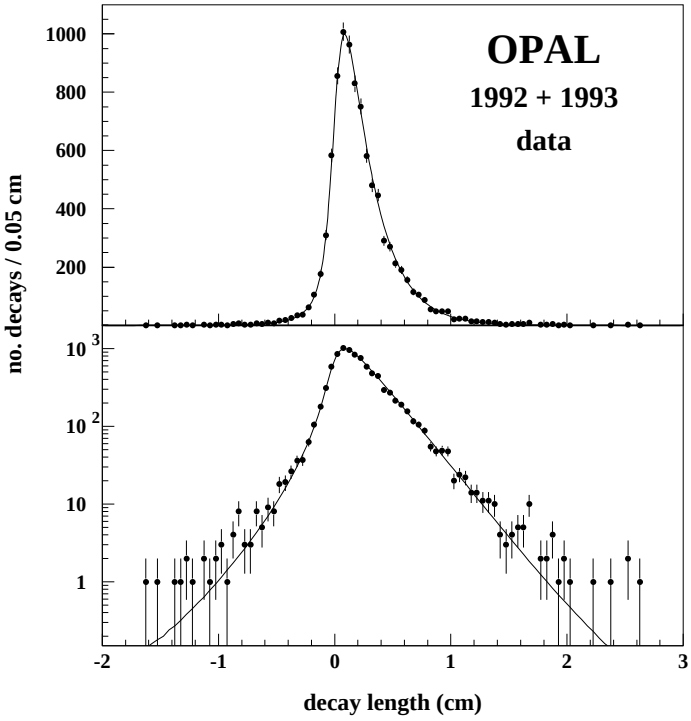

Figure 5.2: Decay distance distribution in linear and logarithmic scale from OPAL [236]. The data (dots) are compared to the result of the maximum likelihood fit, convoluting the decay distribution with the experimental resolution function.

The transverse distance of tau decay products to the average production vertex, the impact parameter (see lower part of Fig. 5.1a), is also a sensitive measure of the tau lifetime. It has the advantage that 1 prong decays can be used, thus the statistical accuracy is good. Clearly for an optimum measurement the position of the tau production vertex and the tau direction of flight would have to be known. While the former is approximated by the e^+e^- beam spot just as in the decay length measurement, the latter needs to be estimated from e.g. the thrust axis direction in the event. The transverse distance of closest approach is then given a sign depending on where the track appears to be crossing the estimated line of flight of the tau lepton. This introduces an additional uncertainty, essentially on the sign of the impact parameter. The impact parameter as such has recently been used by L3 [378], OPAL [236] and CLEO [372] to extract an updated tau lifetime value. As an example, Fig. 5.4 shows the impact parameter distribution from L3; overlaid is the result of a maximum likelihood fit.

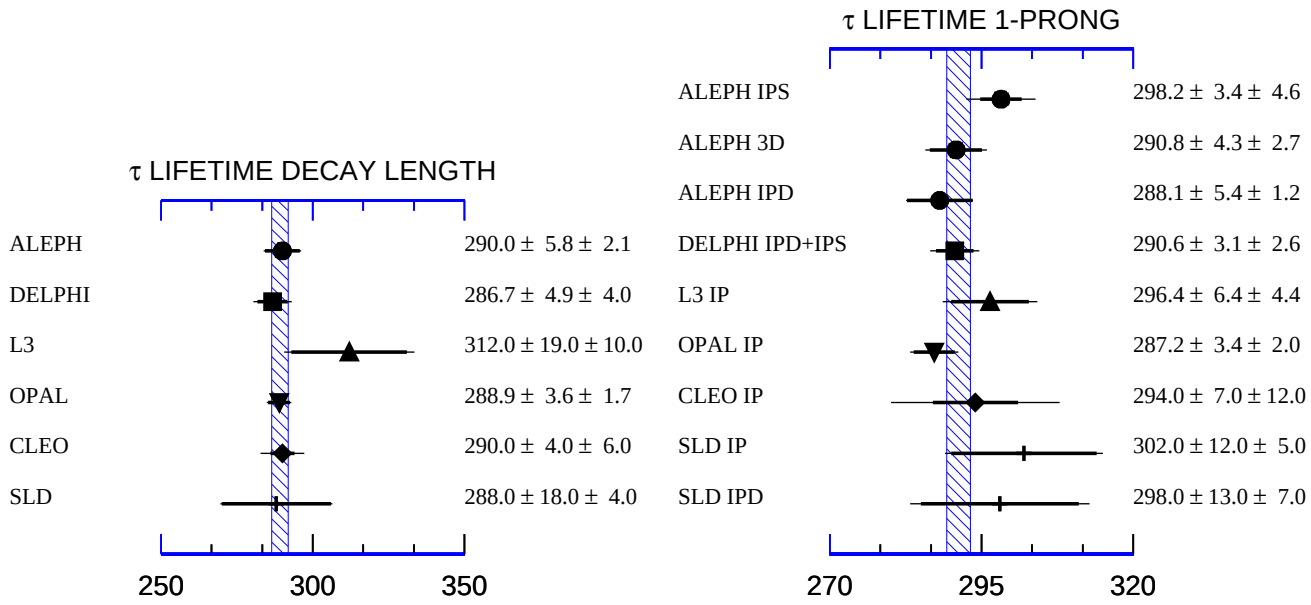

Figure 5.3: Left: Recent results from CLEO [372], SLD [373] and the LEP experiments [205, 209, 236, 374, 375] on the tau lifetime (in fs) from three-prong decays. Right: Recent results from CLEO [372], SLD [373] and the LEP experiments [236, 373, 376–378] on the tau lifetime (in fs) using impact parameter methods. IPS and IPD stand for impact parameter sum and difference, 3D for three dimensional impact parameter. Other measurements use single impact parameter distributions.

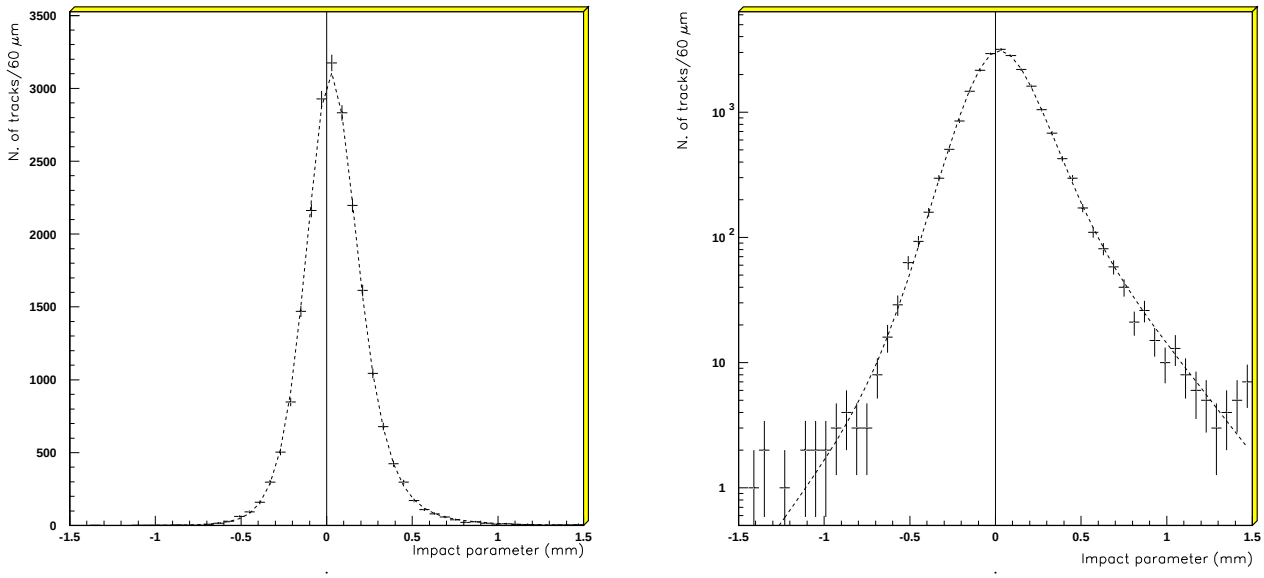

Figure 5.4: Impact parameter distribution in linear and logarithmic scale from L3 [378]. The data (dots) are compared to the result of the maximum likelihood fit, convoluting the decay distribution with the experimental resolution function.

It is rather easy to see (see Fig. 5.1b) that the sum and difference of the two impact parameters in an event where there are two one prong tau decays (1-1 topology) separates uncertainties from the production vertex and the tau direction. While the sum of impact parameters (also called the miss distance) is insensitive to the production point, their difference is insensitive to the tau direction of flight. Both quantities are thus used in recent measurements by ALEPH and DELPHI [376,377]. Again, the observed distributions are analysed by a moments method or subjected to a maximum likelihood fit, using an underlying physics function (basically exponential) folded with the experimental resolution function. The example in Fig. 5.5 shows the mean impact parameter difference as a function of the projected acoplanarity between the two tau decay tracks. The slope of the line is directly related to the lifetime.

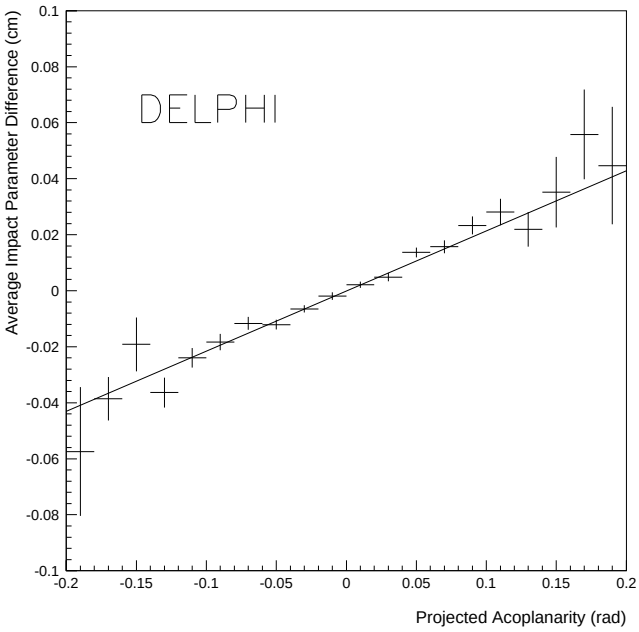

Figure 5.5: The mean impact parameter difference as a function of the projected acoplanarity from DELPHI [196]. The slope of the straight line is directly related to the tau lifetime.

It is well known [379–381] that even in a $\tau^+\tau^-$ event with two hadronic decays in the final state, where two neutrinos are unobserved, the tau direction can be reconstructed up to a two-fold ambiguity, when the constraints from energy-momentum conservation are used and radiative corrections are neglected. This fact has been used by ALEPH [376] to construct a three dimensional impact parameter, perpendicular to the plane going through the two solutions for the tau direction. This impact parameter can then be analysed as a function of the sum of the track angles with respect to the plane in order to extract a lifetime.

All recent, partially preliminary results on the tau lifetime from impact parameter methods are summarised in Fig. 5.3. The results from different methods and different experiments are consistent with each other.

The results evaluated inside one experiment can be correlated by partial overlap in the samples, common tracking uncertainties, bias corrections etc. Therefore, each experiment gives a best estimate of the tau lifetime using a combination of all results. On the other hand, correlations among different experiments can basically only come from the common use of Monte Carlo to evaluate background, the mixture of decays accepted and the decay kinematics

including radiative corrections. The systematic errors from such sources are small, thus it is reasonable to neglect correlations among experiments at this point. Fig. 5.6 shows a synopsis of all recent results, including preliminary ones, compared to the Particle Data Group's 1994 average. A new world average, taking into account partial correlations to earlier results within each experiment has been prepared by Wasserbaech [375,382]. The result is $\tau_\tau = 291.3 \pm 1.6$ fs, smaller than the previous world average [252] of $\tau_\tau = 296.6 \pm 3.1$ fs but not in disagreement with it. The error has shrunk by a factor of two, showing the impressive progress that is made by the introduction of silicon microvertex detectors.

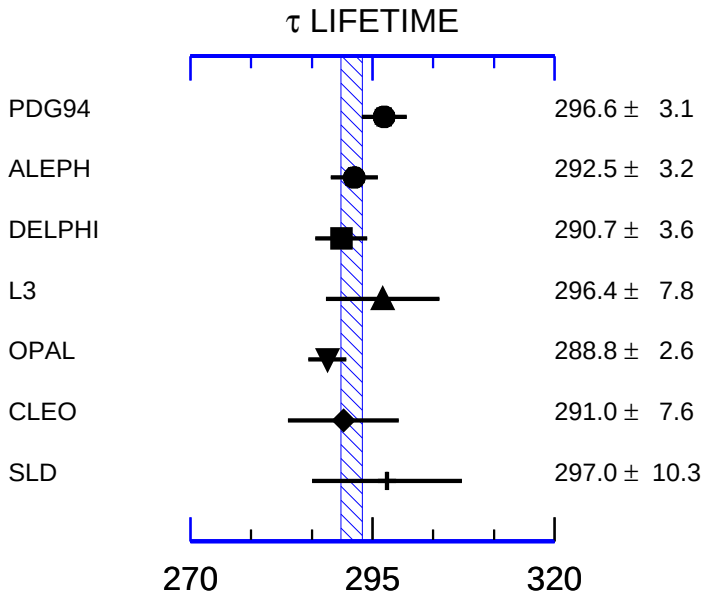

Figure 5.6: Recent preliminary results on the tau lifetime (in fs) from CLEO, SLD and the LEP experiments [375,382].

5.1.2 The leptonic branching fractions

The improvements in the measurement of the total tau decay width are matched by similar refinements in the measurement of the leptonic branching fractions. Important factors in these measurements are the good resolution, coverage and homogeneity of modern e^+e^- detectors. Redundant methods in particle identification also allow to reduce systematic errors. Electrons are usually identified by measuring dE/dx in a tracking device, requiring a short, slim and symmetric shower in the electromagnetic calorimeter and comparing tracking and calorimetric information, i.e. matching energy and momentum, impact point and shower center of gravity. Muons are singled out by observing a minimum ionising, long range particle in the hadronic calorimeter and/or an isolated track in the muon detection system.

The homogeneity of the detectors already ensures that the efficiency of lepton identification will not vary rapidly with solid angle or momentum. Nevertheless, in order to reach permill precision, an experimental cross check on the efficiency which is usually extracted from detailed Monte Carlo simulation, is necessary. Therefore, electrons or muons from $e^+e^- \to l^+l^-(\gamma)$ and

$e^+e^- \to e^+e^-l^+l^-$ are used as control samples to verify the absolute value and the momentum dependence of the efficiencies.

Latest, partially preliminary results from the LEP experiments [200,239,375,382–385] are shown in Fig. 5.7. The agreement of the new measurements among each other and to the previous world average [252], which contains earlier LEP results, is good. A new world average can be extracted [375], neglecting correlations among experiments and replacing superseded data, and one gets

$$\mathrm{BR}(\tau^- \to \mu^- \bar{\nu}_\mu \nu_\tau) = (17.33 \pm 0.09)\% \quad (5.6)$$

$$\mathrm{BR}(\tau^- \to \mathrm{e}^- \bar{\nu}_e \nu_\tau) = (17.79 \pm 0.09)\% \quad (5.7)$$

where statistical and systematic errors are added in quadrature. It is again observed that the new measurements substantially improve on previous ones, statistically as well as systematically. This new average is dominated by the LEP results.

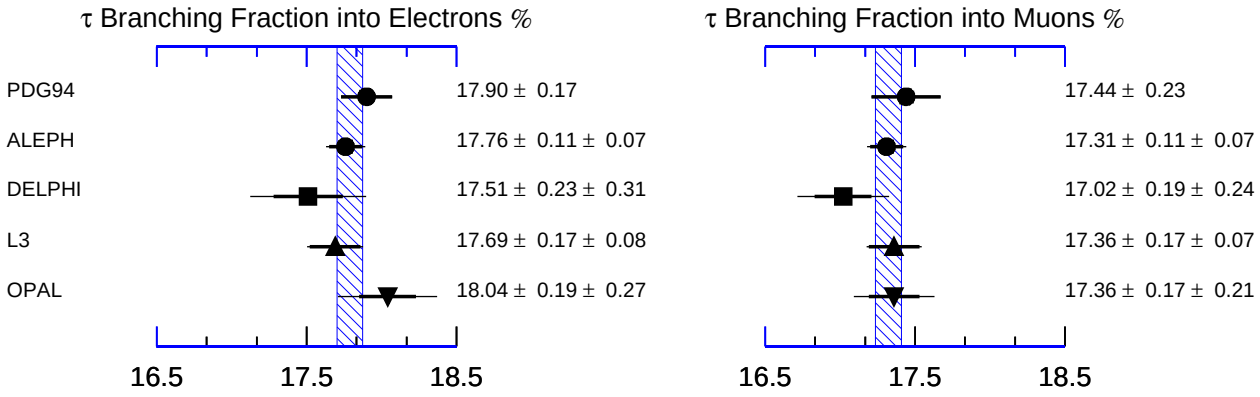

Figure 5.7: Recent, partially preliminary results on the leptonic branching fractions of the tau from the LEP experiments [200,239,375,382–385].

5.1.3 Universality of the leptonic charged weak current

Given all the ingredients we can now test the universality of the leptonic charged current interaction. If we factorize the Fermi constant G_F into effective couplings G_l for each lepton species, such that

$$G_F^2 \to G_\tau G_l \qquad (l = e, \mu) \quad (5.8)$$

$$G_l = \frac{g_l^2}{\sqrt{32} M_W^2} \qquad (l = e, \mu, \tau) \quad (5.9)$$

where g_l is the coupling at the W-l-ν_l vertex, we find that all three couplings can be tested for equality by looking at leptonic tau decays. First, the ratio of the branching fraction into muons and electrons

$$\frac{\mathrm{BR}(\tau^- \to \mu^- \bar{\nu}_\mu \nu_\tau)}{\mathrm{BR}(\tau^- \to \mathrm{e}^- \bar{\nu}_e \nu_\tau)} = \frac{1 + \delta_m(y_\mu)}{1 + \delta_m(y_e)} \frac{g_\mu^2}{g_e^2} \quad (5.10)$$

should be unity up to a phase space factor which makes it equal to 0.9726 in case of lepton universality. The experimental result is

$$\frac{\mathrm{BR}(\tau^- \to \mu^- \bar{\nu}_\mu \nu_\tau)}{\mathrm{BR}(\tau^- \to \mathrm{e}^- \bar{\nu}_e \nu_\tau)} = 0.9741 \pm 0.0071 \tag{5.11}$$

Translated into coupling constants, this gives

$$\left|\frac{g_\mu}{g_e}\right| = 1.001 \pm 0.004 \tag{5.12}$$

in excellent agreement with the hypothesis of e-μ universality. The accuracy of this measurement is still about a factor of two away from the best existing test, the comparison of $\pi^- \to \mu^- \bar{\nu}_\mu$ to $\pi^- \to \mathrm{e}^- \bar{\nu}_e$, which gives $g_\mu/g_e = 1.0012 \pm 0.0016$ [386–388].

Given the fact that the e and μ couplings are compatible, we are allowed to enhance the accuracy by forming a combined leptonic branching fraction of the tau

$$\mathrm{BR}(\tau^- \to l^- \bar{\nu}_l \nu_\tau) = \frac{1}{2}\left(\mathrm{BR}(\tau^- \to \mathrm{e}^- \bar{\nu}_e \nu_\tau) + \frac{\mathrm{BR}(\tau^- \to \mu^- \bar{\nu}_\mu \nu_\tau)}{0.9726}\right) = (17.80 \pm 0.06)\% \tag{5.13}$$

With these recent measurements of the leptonic branching fraction and the lifetime as quoted above, we find consistency with the linear relation predicted by the Standard Model as shown in Fig. 5.8. Extracting the partial width of tau decays to electrons and comparing to the total muon decay width, we find

$$\left|\frac{g_\tau}{g_\mu}\right| = 0.999 \pm 0.003 \tag{5.14}$$

in excellent agreement with μ-τ universality in the charged current sector. It must, however, be pointed out that our way of averaging experimental results is somewhat naive. Correlations among experiments do exist, for the LEP experiments the normalization to the number of produced tau leptons and the use of KORALZ [389] is an example of common elements in the analysis. A common effort to take these into account properly, in the style of the LEP Electroweak Working Group, would thus be welcome.

5.2 The Lorentz structure of charged currents

Once the overall coupling strength has been fixed to the Fermi constant, one can use the tau decay angles to investigate the Lorentz structure of the W-τ-ν_τ coupling. In the Standard Model, there is maximum parity violation and the structure is $V - A$ only. The invariant amplitude of the most general lepton number conserving four-fermion interaction for leptonic tau decays takes the form [390, 391]

$$\mathcal{M} = \frac{4G_F}{\sqrt{2}} \sum_{\gamma=S,V,T} \sum_{\alpha,\beta=R,L} g^\gamma_{\alpha\beta} \left(\bar{u}^\alpha_l \Gamma_\gamma v_{\nu_l}\right) \left(\bar{v}_{\nu_\tau} \Gamma_\gamma u^\beta_\tau\right) \tag{5.15}$$

where γ labels the transformation properties of the current (S, V, T = scalar, vector and tensor), α and β label the handedness (L, R = left-, righthanded) of the chiral spinors u for the charged

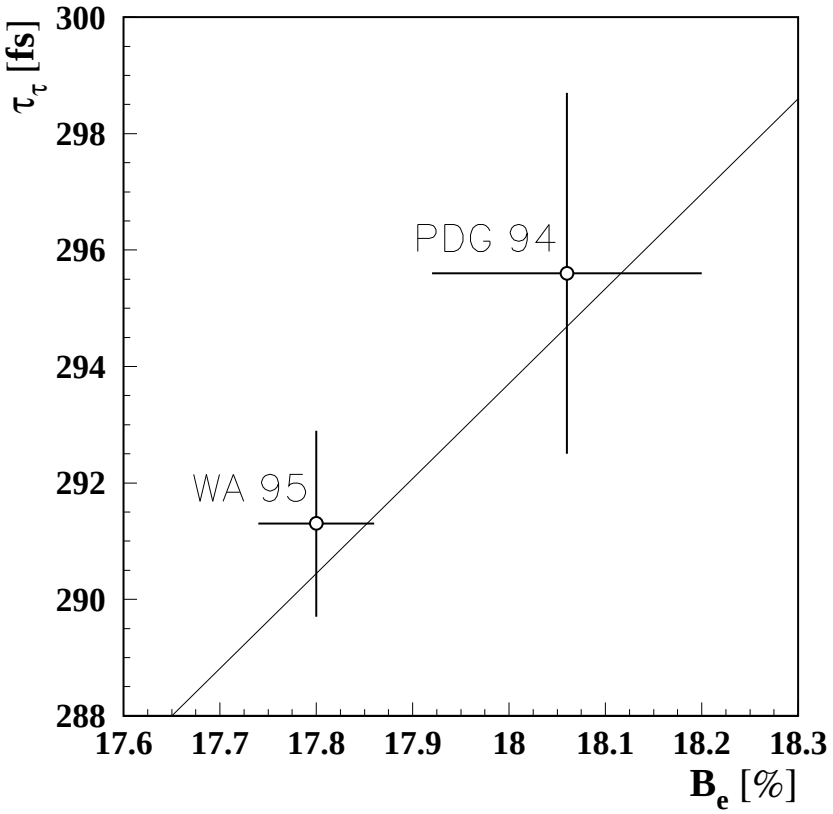

Figure 5.8: The new world average tau lifetime versus its leptonic branching fraction, compared to the previous world average [252] and the linear relation (sold line) predicted by the Standard Model using the new world average of the tau mass.

leptons. The helicity of the chiral neutrino spinor v is then given by the combination of γ, α and β together with conservation of angular momentum. In this representation, the pure $V-A$ case of the Standard Model corresponds to $g^V_{LL}=1$, with all other couplings zero. In the most general case, there are 10 complex couplings g to be determined by experiment. Since a four-fermion interaction does not require factorisation at two separate vertices, the couplings could in principle also depend on the final state, i.e. they could be different for $\tau^- \to \mu^- \bar{\nu}_\mu \nu_\tau$ and $\tau^- \to e^- \bar{\nu}_e \nu_\tau$.

It has been shown [391,392] that without information on the polarization of the final state particles, the combinations ρ, η, ξ and $\xi\delta$ of the couplings, the Michel parameters, can be determined from the decay angles of leptonic τ decays and their correlations in $e^+e^- \to \tau^+\tau^-$. To give an example, the decay lepton spectrum of a tau with average polarization $\mathcal{P}_\tau$ can be expressed as

$$\frac{1}{\Gamma}\frac{d\Gamma}{dx} = h_0(x) + \eta h_\eta(x) + \rho h_\rho(x) - \mathcal{P}_\tau \ (\xi h_\xi(x) + \xi\delta h_{\xi\delta}(x)) \qquad (5.16)$$

The intervening Michel parameters are [393]

$$\rho \ = \ \frac{3}{16}\left(|g^S_{RR}|^2 + |g^S_{LR}|^2 + |g^S_{RL}|^2 + |g^S_{LL}|^2\right)$$

$$+\frac{3}{4}\left(|g^V_{RR}|^2+|g^V_{LR}|^2+|g^T_{RL}|^2+|g^T_{LL}|^2+\mathrm{Re}(g^S_{LR}g^{*T}_{LR}+g^S_{RL}g^{*T}_{RL})\right) \quad (5.17)$$

$$\eta = \frac{1}{2}\mathrm{Re}(6g^V_{RL}g^{*T}_{LR}+6g^V_{LR}g^{*T}_{RL}+g^S_{RR}g^{*V}_{LL}+g^S_{RL}g^{*V}_{LR}+g^S_{LR}g^{*V}_{LR}+g^S_{LL}g^{*V}_{RR}) \quad (5.18)$$

$$\xi = -\frac{1}{4}\left(|g^S_{RR}|^2+|g^S_{LR}|^2-|g^S_{RL}|^2+|g^S_{LL}|^2\right)-\left(|g^V_{RR}|^2-|g^V_{LL}|^2-3|g^V_{LR}|^2+3|g^V_{RL}|^2\right)$$
$$+5\left(|g^T_{LR}|^2-|g^T_{RL}|^2\right)-4\mathrm{Re}(g^S_{LR}g^{*T}_{LR}-g^S_{RL}g^{*T}_{RL}) \quad (5.19)$$

$$\xi\delta = -\frac{3}{16}\left(|g^S_{RR}|^2+|g^S_{LR}|^2-|g^S_{RL}|^2+|g^S_{LL}|^2\right)-\frac{3}{4}\left(|g^V_{RR}|^2-|g^V_{LL}|^2\right)$$
$$+\frac{3}{4}\left(|g^T_{LR}|^2+|g^T_{RL}|^2\right)-\frac{3}{4}\mathrm{Re}(g^S_{LR}g^{*T}_{LR}-g^S_{RL}g^{*T}_{RL}) \quad (5.20)$$

up to a common normalization factor. At Born level, the spectral functions $h_i(x)$ are polynomials [351] in the reduced energy of the charged lepton, $x = E_l/E_\tau \simeq E_l/E_b$, which do not contain any couplings. The values expected for the Michel parameters with a pure $V-A$ charged current are listed in Tab. 5.1.

Also for hadronic τ decays, an analogous decomposition into spectral functions can be made [391]

$$\frac{1}{\Gamma}\frac{d\Gamma}{dx} = g_0(x) + \mathcal{P}_\tau\xi_h g_1(x) \quad (5.21)$$

where ξ_h is the chirality parameter, which in principle could be different for each decay mode, and g_i are the corresponding spectral functions of $x = E_{had}/E_\tau$, the scaled hadron energy. In models which admit only V and A type interactions, ξ_h is given by the average ν_τ helicity. The Standard Model thus gives $\xi_h = 2h_\nu = -1$ for all hadronic decays.

It follows from the above formulae that single decay spectra, not using the correlation between the two tau decays in an event, will not be able to disentangle the complete set of Michel parameters. If we instead consider the full information from observing both decay products A and B in $\mathrm{e^+e^-} \to \tau^+\tau^- \to \mathrm{A^+B^-} + \nu$'s, mixed terms allow to extract the maximum information. The double differential decay distribution is of the form

$$\frac{1}{\Gamma}\frac{d^2\Gamma}{dx_A dx_B} = H_0^{(A)}(x_A)H_0^{(B)}(x_B)+H_1^{(A)}(x_A)H_1^{(B)}(x_B)$$
$$+\mathcal{P}_\tau\left(H_1^{(A)}(x_A)H_0^{(B)}(x_B)+H_0^{(A)}(x_A)H_1^{(B)}(x_B)\right) \quad (5.22)$$

The functions H for leptons are

$$H_0^{(l)} = h_0(x)+\eta h_\eta(x)+\rho h_\rho(x) \quad (5.23)$$

$$H_1^{(l)} = \xi h_\xi(x)+\xi\delta h_{\xi\delta}(x) \quad (5.24)$$

with the same leptonic spectral functions h_i as above. For hadrons ($j = \pi, \rho$) one finds

$$H_0^{(j)} = g_0^{(j)}(x) \quad (5.25)$$

$$H_1^{(j)} = \xi_h g_1^{(j)}(x) \quad (5.26)$$

These Born level spectra have to be radiatively corrected and detector acceptance and resolution must be taken into account. A maximum likelihood fit to the observed doubly differential

	ARGUS [105,394]	ALEPH [186]	L3 [214]	EPS95 [394]	$\mu \to e\nu\nu$ [252]	$V-A$
ρ	0.74 ± 0.04	0.75 ± 0.05	0.81 ± 0.05	0.750 ± 0.023	0.7518 ± 0.0026	3/4
η	$+0.03 \pm 0.22$	-0.04 ± 0.19	$+0.10 \pm 0.23$	$+0.02 \pm 0.12$	-0.007 ± 0.013	0
ξ	0.97 ± 0.14	1.18 ± 0.16	0.95 ± 0.25	1.04 ± 0.10	1.0027 ± 0.0085	1
$\xi\delta$	0.65 ± 0.12	0.88 ± 0.13	0.73 ± 0.19	0.75 ± 0.08	0.751 ± 0.007	3/4
ξ_h	-1.02 ± 0.04	-1.01 ± 0.04	-1.02 ± 0.08	-1.01 ± 0.03		-1

Table 5.1: The Michel parameters from leptonic tau decays and the chirality parameter from hadronic tau decays, compared to the world average for muon decays [252] and the expectations for a pure $V-A$ current. The errors correspond to statistical and systematic errors added in quadrature. Note that correlations among the parameters and to the simultaneously measured tau polarization are not negligible. The average labeled EPS95 was evaluated for the 1995 EPS-HEP conference [394].

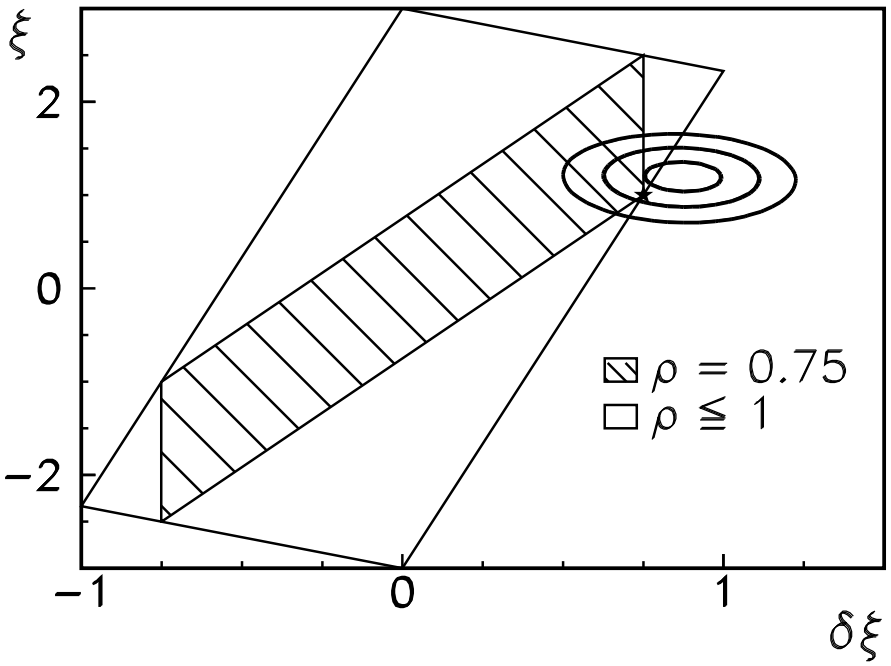

Figure 5.9: Confidence ellipses in the ξ-$\xi\delta$ plane from ALEPH data [186] corresponding to 39, 63 and 78% confidence levels. The open trapezoid encloses the physical region for the parameters, the hatched area delimits the region allowed for $\rho = 3/4$. The Standard Model expectation is marked by a star.

distributions can then give a measurement of the Michel parameters and the mean tau polarization (if present).

ALEPH [186] and ARGUS [105] have recently published an analysis of this type, and preliminary data from L3 are also available [214]. Table 5.1 summarizes the results. Clearly all data are in excellent agreement with the Standard Model assignment of a pure $V-A$ charged current for the τ lepton. This conclusion is also true when correlations among the Michel parameters and with the tau polarization are taken into account. Fig. 5.9 shows the allowed region in the ξ-$\xi\delta$ plane as defined by the ALEPH data [186]. For comparison, the corresponding world average values of the Michel parameters from muon decay are also shown in Tab. 5.1. It is obvious that the measurement accuracy for the tau lepton decay structure has a way to

go before it can compete with the precision reached in muon decays.

5.3 Tau decays and the hadronic charged current

In analogy to the purely leptonic tau decays, the invariant amplitude for semileptonic tau decays can be written in the form of a current-current interaction

$$\mathcal{M}(\tau^- \to h^- \nu_\tau) = \frac{G_F}{\sqrt{2}} |V_h| L_\mu J^\mu \tag{5.27}$$

where h^- stands for a given hadronic system, V_h is the corresponding element of the Cabibbo-Kobayashi-Maskawa matrix (V_{ud} for non-strange h, V_{us} for strange h). L_μ describes the leptonic τ current

$$L_\mu = \bar{v}_{\nu_\tau} \gamma_\mu (1 - \gamma_5) u_\tau \tag{5.28}$$

The hadronic transition current J_μ is the piece of interest here. It describes how the hadronic system h is formed, from the vacuum, by the weak charged current. Restricting to a $V - A$ structure, one can write

$$J_\mu = < h | V_\mu(0) - A_\mu(0) | 0 > \tag{5.29}$$

With a non-strange current, hadronic systems of spin-parity $J^P = 0^-$, 0^+, 1^- or 1^+ can be produced. The vector part of the current leads to final states with even G-parity, e.g. an even number of pions, while the axialvector part couples to odd G-parity states, i.e. an odd number of pions. The Conserved Vector Current hypothesis (CVC) limits the vector part to produce only vector states. The vector current can then be related to the cross section for $e^+e^- \to h'$, where h' is a hadronic system related to h by an isospin rotation.

Taking this factorized invariant amplitude, the tau width into $h^- \nu_\tau$ can be expressed in a form-factor ansatz [395,396]

$$d\Gamma(\tau^- \to h^- \nu_\tau) = \frac{G_F^2}{4 m_\tau} |V_h|^2 L_{\mu\nu} H^{\mu\nu} d\mathrm{PS} \tag{5.30}$$

with the leptonic and hadronic tensors $L_{\mu\nu}$ and $H_{\mu\nu}$ and the Lorentz invariant phase space element dPS. In the rest system of h^-, the tensor product simplifies to a sum over structure functions W_i and kinematic factors [395].

For the long-lived hadronic states $h^- = \pi^-/\mathrm{K}^-$, the structure functions reduce to delta functions such that the tau partial widths are directly related to the corresponding weak decay rate

$$\Gamma(\tau^- \to \pi^- \nu_\tau) = \frac{G_F^2}{16\pi} f_\pi^2 |V_{ud}|^2 m_\tau^3 \left(1 - \frac{m_\pi^2}{m_\tau^2}\right)^2 \tag{5.31}$$

where the pion decay constant f_π is defined by the pion decay width

$$\Gamma(\pi^- \to \mu^- \bar{\nu}_\mu) = \frac{G_F^2}{8\pi} f_\pi^2 |V_{ud}|^2 m_\pi m_\mu^2 \left(1 - \frac{m_\mu^2}{m_\pi^2}\right)^2 \tag{5.32}$$

Radiative corrections to these relations are small [370, 397–399]. The corresponding relations for $\tau^- \to \mathrm{K}^- \nu_\tau$ follow by replacing the masses and $f_\pi |V_{ud}|$ by $f_\mathrm{K} |V_{us}|$.

Mode		WA94 BR (%)	Theory
$h^-\nu$		11.77 ± 0.14	11.67 ± 0.06
	$\pi^-\nu$	11.09 ± 0.15	10.95 ± 0.06
	$K^-\nu$	0.68 ± 0.04	0.72 ± 0.01
$h^-\pi^0\nu$		25.36 ± 0.21	25.1 ± 0.6
	$\pi^-\pi^0\nu$	24.91 ± 0.21	24.9 ± 0.7
	$K^*\nu$	1.36 ± 0.08	1.1 ± 0.1
$h^-2\pi^0\nu$		9.18 ± 0.14	
	$\pi^-2\pi^0\nu$	9.09 ± 0.14	
	$K^-2\pi^0\nu$	0.09 ± 0.03	0.12 ± 0.04
$h^-3\pi^0\nu$		1.15 ± 0.15	
	$\pi^-3\pi^0\nu$		1.08 ± 0.05
$h^-4\pi^0\nu$		0.16 ± 0.07	
$h^-K^0\nu$		1.03 ± 0.09	
	$K^-K^0\nu$	0.13 ± 0.04	0.12 ± 0.03
$h^-\pi^0K^0\nu$		0.53 ± 0.06	
	$\pi^-\pi^0K^0\nu$	0.41 ± 0.07	
	$K^-\pi^0K^0\nu$	0.12 ± 0.04	
$h^-K^0K^0\nu$		0.08 ± 0.04	0.044 ± 0.032
$h^-\pi^0\eta\nu$		0.18 ± 0.03	
	$\pi^-\pi^0\eta\nu$		0.130 ± 0.018
$h^-\omega\nu$		2.12 ± 0.07	
	$\pi^-\omega\nu$		1.79 ± 0.14
$h^-\omega\pi^0\nu$		0.35 ± 0.12	
$\sum$ 1 prong excl.		84.66 ± 0.38	
$\sum$ 1 prong incl.		85.41 ± 0.23	
$3h\nu$		9.24 ± 0.21	
	$\pi^-\pi^+\pi^-\nu$	8.64 ± 0.24	
	$K^-\pi^+\pi^-\nu$	0.40 ± 0.09	
	$K^-K^+\pi^-\nu$	0.20 ± 0.07	0.20 ± 0.07
$3h\pi^0\nu$		4.45 ± 0.14	
	$2\pi^-\pi^+\pi^0\nu$		4.20 ± 0.29
$3h2\pi^0\nu$		0.51 ± 0.05	
$3h \geq 3\pi^0\nu$		0.20 ± 0.07	
$\sum$ 3 prong excl.		14.40 ± 0.27	
$\sum$ 3 prong incl.		14.49 ± 0.23	
$5h\nu$		0.073 ± 0.007	
$5h\pi^0\nu$		0.021 ± 0.006	
	$3\pi^-2\pi^+\pi^0\nu$		0.027 ± 0.005
$\sum$ 5 prong excl.		0.09 ± 0.01	
$\sum$ 5 prong incl.		0.10 ± 0.01	
$\sum$ 7 prong incl.		< 0.012 (95%CL)	
$\sum$ all excl.		99.15 ± 0.46	

Table 5.2: The world average branching fractions of the tau lepton compiled at the 1994 Workshop on Tau Lepton Physics [400], compared to theoretical predictions [6, 401–404]. h^- stands for π^- or K^-. The π^- branching fraction have been obtained from the semi-inclusive h^- numbers by subtracting the K^- branching fraction where available.

The description of hadronic resonance production in tau decays by this ansatz is complicated by the structure of such resonances itself. However, for the even G-parity states, only the vector current contributes and CVC gives a convenient way to relate the decay width to the cross section for $e^+e^- \to$ hadrons [405,406]. Thus for the hadronic systems with $J^{PG} = 1^{-+}$, $h^- = 2n\pi, \omega\pi, \eta\pi\pi$ etc, predictions can be based on e^+e^- data. One finds [401]

$$\frac{d\Gamma}{dq^2} = \frac{G_F^2 |V_{ud}|^2}{32\pi^2 m_\tau^3}(m_\tau^2 - q^2)(m_\tau^2 + 2q^2)\frac{q^2}{4\pi\alpha^2}\sigma^{I=1}_{e^+e^-}(q^2) \qquad (5.33)$$

up to small radiative corrections [370]. The analysis of the e^+e^- data is not straight forward since one requires that only the (strong) isovector part of the cross section be measured [401, 402]. To give an example, the measured cross section for $e^+e^- \to \pi^+\pi^-$ can be used to predict the width for $\tau^- \to \pi^-\pi^0\nu_\tau$, only after the contribution from $e^+e^- \to \omega \to \pi^+\pi^-$ has been subtracted including interference.

An excellent survey of recent experimental results on the hadronic branching fractions of the tau lepton has been prepared by Heltsley for the 1994 Workshop on Tau Lepton Physics [400]. His overview of new world average branching fractions is reproduced in Table 5.2, obtained using the error scaling method of the Particle Data Group [252]. New results that became available since then are summarized in Table 5.3. The results are to a large extent dominated by the recent ALEPH results.

Many results have only recently become available, especially in the strange sector. This has been made possible by the advances in detector technology (RICH, accurate TOF and dE/dx measurements) to identify charged kaons, fine grain electromagnetic calorimeters able to resolve electromagnetic showers from high energy π^0 and hadronic calorimeters to find and separate off showers from K^0. Attention has to be payed to the way in which semi-inclusive branching ratios are split for exclusive ones. While the Particle Data Group used to advise experimentalists to group modes with a K^0_L into the semi-inclusive mode without K^0, new efforts to actually see and classify these modes allow to properly account for them.

Because of the complex dynamics involved in decays to $K\bar{K}$ final states, predictions for the branching fractions are non trivial. A cascade of resonances can contribute, e.g. $W \to a_1 \to \pi(\rho, \omega, \Phi) \to K\bar{K}$ or $W \to a_1 \to KK^* \to \bar{K}\pi$. Recently, Finkemeier and Mirkes [404] have derived predictions for a complete set of two and three meson final states, based on form factors predicted by chiral Lagrangians and accounting for low lying resonances. The agreement with measured branching fractions is generally satisfactory [404].

It is evident from the tables that the strive of recent experiments, especially ALEPH, to cover and classify all decay modes of the tau lepton has successfully removed doubts about substantial branching fractions into unobserved modes. Their method to classify all final states into generic classes and extract the branching fractions by careful cross-feed corrections was pioneered by CELLO [115] and successfully applied at LEP [170]. The exclusive branching fractions now sum up to the corresponding topological ones without apparent loss. The total sum of exclusive modes falls short of one by less than a percent, with an error of half a percent. Rare decay modes at the level of less than 10^{-4} can of course only be observed by the high statistics sample of CLEO until new data from B- and τC-factories become available.

Hadronic decay modes beyond $\tau^- \to \pi^-\nu_\tau$ and $\tau^- \to K^-\nu_\tau$ are dominated by the production of hadronic resonances. Examples of hadronic mass distributions are shown in Fig. 5.10, 5.11

Mode		Experiment	BR (%)
	$e^-\nu\nu$	OPAL	18.04 ± 0.33
	$e^-e^+e^-\nu\nu$	CLEO	$2.7 \pm 1.4\ 10^{-3}$
	$\mu^-\nu\nu$	OPAL	17.36 ± 0.27
	$\mu^-e^+e^-\nu\nu$	CLEO	$< 3.1\ 10^{-3}$ (90% CL)
$h^-\nu$		DELPHI	11.84 ± 0.56
		OPAL	14.96 ± 0.24
	$K^-\nu$	OPAL	0.59 ± 0.08
	$\pi^-\pi^0\nu$	DELPHI	24.09 ± 0.67
	$\pi^-K^0\nu$	L3	0.95 ± 0.16
	$\pi^-K^0\pi^0\nu$	L3	0.41 ± 0.12
	$\pi^-K^0_S \geq 0\pi^0\nu$	OPAL	0.72 ± 0.08
	$\pi^-K^*\nu$	ARGUS	0.25 ± 0.11
	$\pi^-\Phi\nu$	ARGUS	< 0.035 (90% CL)
	$K^-\pi^0\nu$	DELPHI	0.69 ± 0.25
	$K^- \geq 1\pi^0\nu$	OPAL	0.55 ± 0.10
	$K^-K^*\nu$	ARGUS	0.20 ± 0.06
	$K^-K^0_S \geq 0\pi^0\nu$	OPAL	0.20 ± 0.06
$h^-K^0_S\nu$		ALEPH	0.43 ± 0.05
		DELPHI	0.80 ± 0.12
$h^-K^0_S \geq 0\pi^0\nu$		DELPHI	0.72 ± 0.12
$h^-K^-K^+ \geq 0\pi^0\nu$		DELPHI	0.20 ± 0.09
$h^-K^0_S\pi^0\nu$		ALEPH	0.30 ± 0.04
$h^-K^0_SK^0_L\nu$		ALEPH	0.13 ± 0.04
	$\pi^-K^0K^0\nu$	L3	0.31 ± 0.13
	$\pi^-\eta\nu$	CLEO	< 0.025 (95% CL)
	$K^-\eta\nu$	CLEO	0.026 ± 0.06
	$\pi^-\pi^0\eta\nu$	CLEO	0.17 ± 0.03
		ALEPH	0.23 ± 0.06
	$\pi^-\omega\nu$	CLEO	1.95 ± 0.13
$3h\nu$		OPAL	9.87 ± 0.26
		CLEO	9.51 ± 0.21
	$\pi^-\pi^+\pi^-\nu$	DELPHI	8.35 ± 0.42
$3h\pi^0\nu$		OPAL	4.57 ± 0.25
		CLEO	4.23 ± 0.23
$3h > 1\pi^0\nu$		OPAL	5.09 ± 0.25

Table 5.3: New branching fraction measurements that appeared since the 1994 Workshop on Tau Lepton Physics [212,375,407–420].

and 5.12. The mode $\tau^- \to \pi^-\pi^0\nu_\tau$ appears saturated by the ρ^- resonance, just like the decay $\tau^- \to K^-\pi^0\nu_\tau$ is dominated by the K^* resonance. The three prong decay $\tau^- \to \pi^-\pi^+\pi^-\nu_\tau$ shows the broad peak in the mass spectrum corresponding to the a_1 resonance.

Hadronic tau decays can thus probe the dynamics of the hadronic charged current in substantial detail, far beyond the simple decay rate measurement. Model independent methods to determine the structure functions have been developed especially for the decay $\tau^- \to$

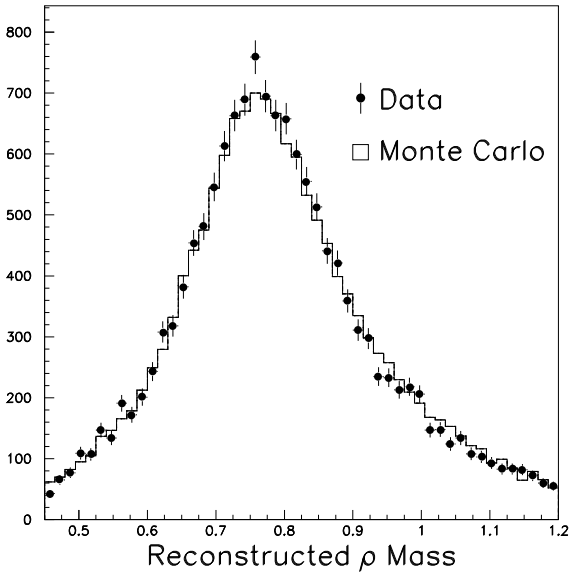

Figure 5.10: Hadronic mass distribution in candidate events for $\tau^- \to \pi^-\pi^0\nu_\tau$ from L3. The data (dots) are compared to a Monte Carlo Calculation with ρ dominance for this channel (histogram), including background.

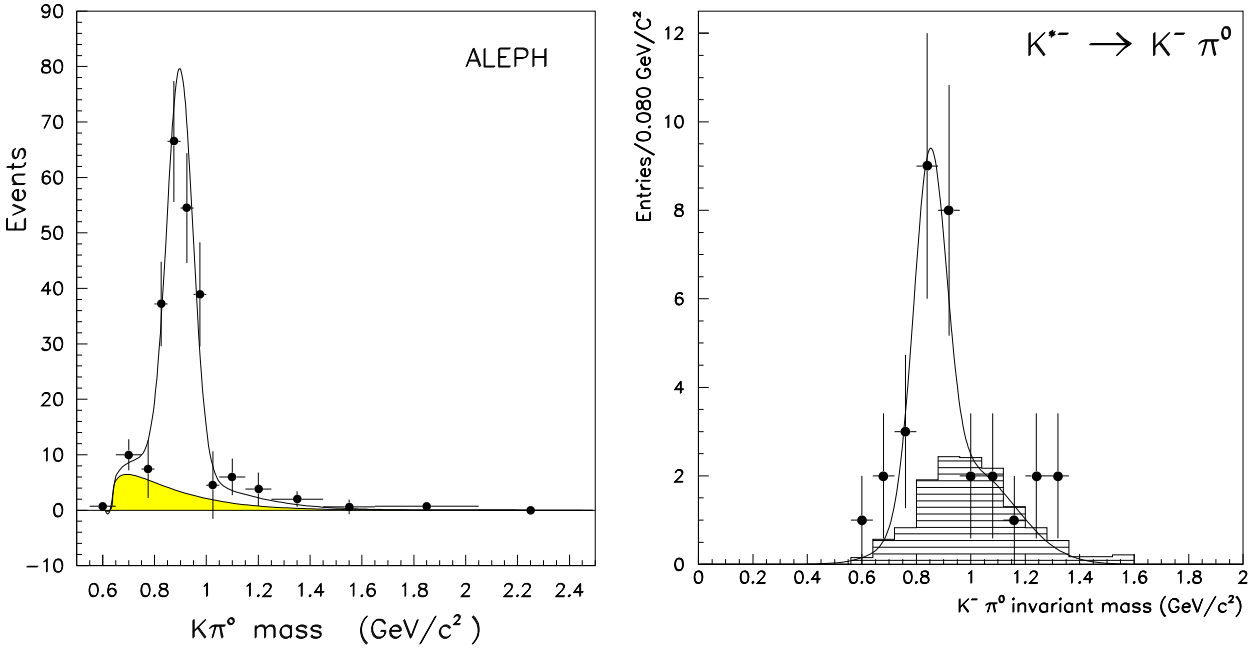

Figure 5.11: Hadronic mass distribution in candidate events for $\tau^- \to K^-\pi^0\nu_\tau$ from ALEPH (left) [182] and DELPHI (right) [198]. The data (dots) are compared to a fit (line) to the K^* resonance and background.

$\pi^-\pi^+\pi^-\nu_\tau$ [380, 395, 421, 422]. ARGUS [103, 105] and OPAL [242] have recently analyzed tau decays to a_1 along these lines. Fig. 5.13 shows the four structure functions W_i, compared to the model predictions of Kühn et al. [422] and Isgur et al. [421]. This analysis then allows to fix the parameters of the a_1 resonance as introduced in the respective model.

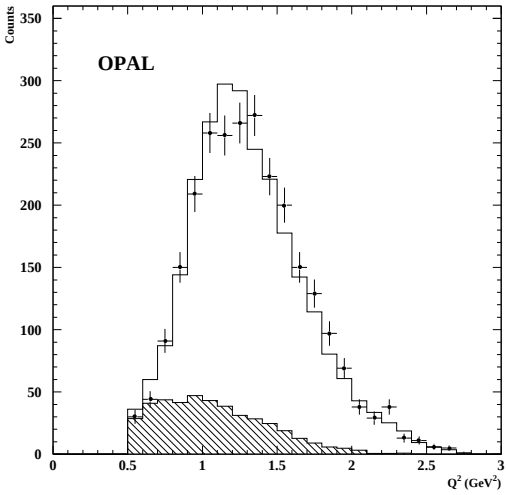

Figure 5.12: Hadronic mass distribution in candidate events for $\tau^- \rightarrow \pi^-\pi^+\pi^-\nu_\tau$ from OPAL [242]. The data (dots) are compared to a Monte Carlo with a_1 dominance (histogram) and background (hatched histogram).

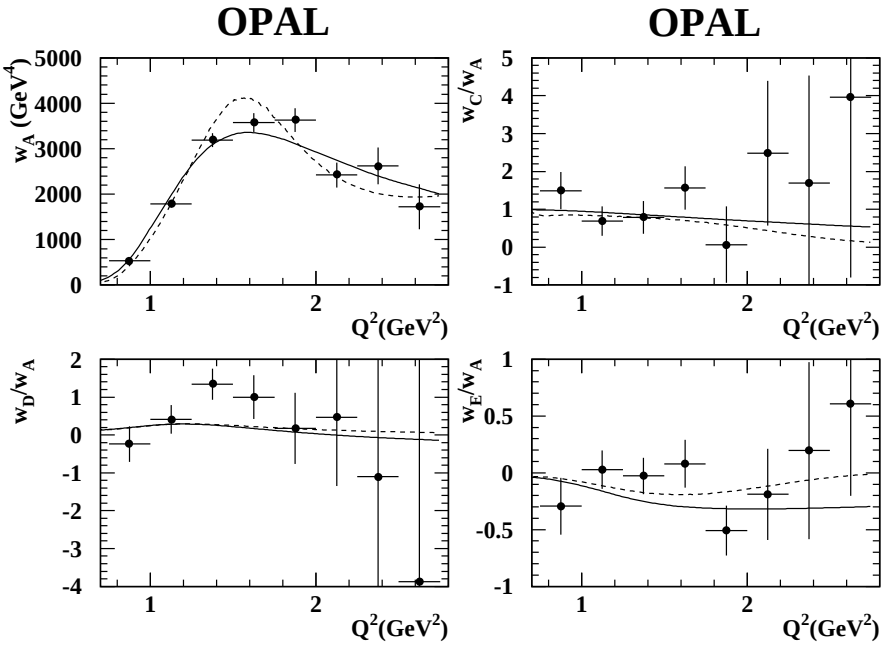

Figure 5.13: Structure functions W_i measured in the decay $\tau^- \rightarrow \pi^-\pi^+\pi^-\nu_\tau$ by OPAL [242]. The data (dots) are compared to the model calculations of Isgur et al. (dashed line) [421] and Kühn et al. (solid line) [422].

It is clear that analysis of this kind are far from conclusive at this stage but have just scratched the surface of this field. However the power of tau decays in understanding the low q^2 hadronic charged currents starts to become evident. One can thus predict a lively future for this topic in tau physics.

Chapter 6

Strong interactions and τ decay

The τ is the only lepton heavy enough to decay into hadrons. Since its mass is substantially larger than $\Lambda_{\rm QCD}$, it makes sense to try and determine the QCD running coupling constant from its hadronic decays. As usual, the more inclusive the measurement, the better the measurement of α_s is expected to be, since hadronization details of the final state play a lesser rôle. For τ decays, the most inclusive measurement is the total hadronic decay width which receives substantial perturbative QCD corrections, analogous to the total hadronic rate in e^+e^- reactions. The perturbative series for this quantity has been calculated up to order $\mathcal{O}(\alpha_s^3)$ and non perturbative corrections have been estimated [423–426]. Experimentally, the hadronic width is readily derived from the total width and leptonic branching fractions (see Chapter 5). The main interest to determine α_s at low momentum transfer is that it provides a long lever arm when compared to analogous measurements at $q^2 = M_Z^2$ and thus allows to directly observe the running of the coupling using only inclusive measurements.

On a somewhat less inclusive level, the spectral moments of hadron mass distributions have also been calculated to order $\mathcal{O}({\alpha_{\rm s}}^3)$ and measured with high precision. We will shortly discuss the main features of both methods for a determination of $\alpha_{\rm s}$ and some problems involved, referring to recent reviews for a more extensive discussion [427–429]. Since the mass of the τ is not far beyond the hadronic scale, there is no theoretical consensus yet on the estimate of the theoretical error in the determination of $\alpha_{\rm s}$ from τ decays and its extrapolation to higher momentum transfers.

6.1 Strong coupling from the total hadronic width

An inclusive measurement of the strong coupling constant can be achieved using the quantity R_τ

$$R_\tau = \frac{\Gamma(\tau \to \nu_\tau + \text{hadrons})}{\Gamma(\tau \to \nu_\tau e \bar{\nu_e})} \tag{6.1}$$

where the denominator is the leptonic width calculated according to Equ. 5.13. This quantity is thus defined in analogy with the ratio between the total hadronic and leptonic cross sections in e^+e^-, $R = \sigma(e^+e^- \to \text{hadrons})/\sigma(e^+e^- \to \mu^+\mu^-)$.

Since only $u\bar{d}$ and $u\bar{s}$ states can contribute to hadronic tau decays, the naive quark-parton model predicts $R_\tau = N_c(|V_{ud}|^2 + |V_{us}|^2) \simeq 3$, with the number of colors N_c and the contributing CKM matrix elements. The experimental value of $R_\tau = 3.6174 \pm 0.034$ [252] shows a deviation of $\sim 20\%$ from this prediction, due to final state strong interactions. The extraction of α_s from this measurement has been extensively studied in a series of papers by Braaten, Narison and Pich [426], Le Diberder [430–432] and more recently by Altarelli, Nason and Ridolfi [433], Neubert [434] and Ball, Beneke and Braun [435]. We refer to these papers for a complete review.

The theoretical expression for R_τ can be written as an integral over the squared hadronic mass, s [426]:

$$R_\tau = 6\pi i \int\limits_{|s|=m_\tau^2} \frac{ds}{m_\tau^2}(1 - \frac{s}{m_\tau^2})^2[(1 + 2\frac{s}{m_\tau^2})\Pi^{(1)}(s) + \Pi^{(0)}(s)] \tag{6.2}$$

where $\Pi^{(J)}$ is the hadronic spectral function for a hadron of spin J. In terms of correction factors to the quark parton result, this can be written as

$$R_\tau = N_c(|V_{ud}|^2 + |V_{us}|^2)\delta_{ew}[1 + \delta_p(\alpha_s(\mathrm{m}_\tau)) + \delta_{np} + \delta'_{ew}] \tag{6.3}$$

where $\delta_{ew} = 1.0194$ and $\delta'_{ew} = 0.010$ are electroweak corrections [426].

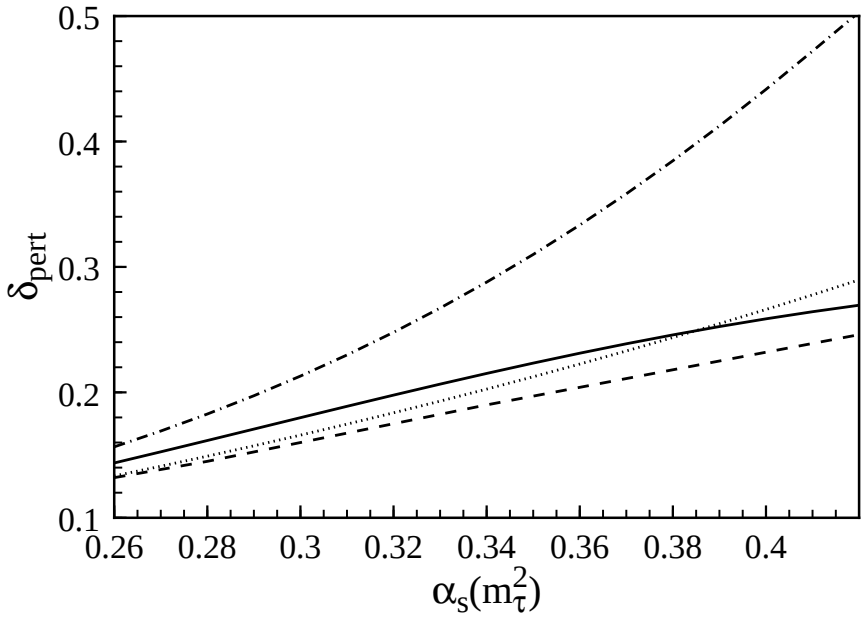

Figure 6.1: The theoretical predictions for the quantity δ_p (solid line) [434]; principle value of the Borel integral (dash-dotted line) [435]; resummation of Le Diberder and Pich (dashed line) [431]; exact order $\alpha_s{}^3$ result (dotted line) [434].

The perturbative term δ_p is known up to terms of order $\alpha_s{}^3$. Published theoretical predictions differ mainly in the treatment of the missing higher order ($\alpha_s{}^4$ and higher) terms [431,433–435] (see Fig. 6.1). The non perturbative corrections δ_{np}, classified according to the operator product expansion along the line of the SVZ [436] approach, are quite small [426], since the first power correction (excluding the small effects proportional to powers of the quark masses) is already suppressed by 4 powers of m_τ.

Experiment	R_τ	$\alpha_s(\mathrm{m}_\tau)$
PDG94 [252]	3.522 ± 0.035	0.306 ± 0.024
ALEPH [439]	3.645 ± 0.017	0.369 ± 0.028
CLEO [83]	3.559 ± 0.035	0.327 ± 0.025
DELPHI [193]	3.44 ± 0.24	$0.26^{+0.09}_{-0.12}$
L3 [384]	3.656 ± 0.039	0.373 ± 0.046
OPAL [239]	3.654 ± 0.038	$0.375^{+0.032}_{-0.025}$

Table 6.1: The ratio R_τ of hadronic and leptonic decay width and the corresponding value of the strong coupling constant. The error includes experimental errors and the experiments' assessment of theoretical errors. Potential additional uncertainties as discussed in the text are not included.

It has been argued [433,437,438] that certain ambiguities in the resummation of the perturbative expansion (the so called ultraviolet renormalons) behave effectively as a power correction of the order $1/m_\tau^2$. Attempts to circumvent this problem generally enlarge the error in the α_s determination. Thus, the method used in ref. [433] yields a theoretical error $\delta\alpha_\mathrm{s}(m_\tau) = 0.06$ due to this source. According to ref. [434], the error should be $\delta\alpha_\mathrm{s}(m_\tau) = 0.05$. In ref. [435], a range $\delta\alpha_\mathrm{s}(m_\tau) = 0.035$ is proposed, but with their method the central value is shifted downward by an amount roughly equal to the error. In ref. [431], a method is proposed which resums part of the perturbative expansion, enhanced by powers of π, but ignores the infrared renormalon problem, leading to the smaller error $\delta\alpha_\mathrm{s}(m_\tau) = 0.03$.

At this stage we can thus only conclude that the theoretical error coming from missing higher orders lies between an optimistic value of $\delta\alpha_s(\mathrm{m}_\tau) = 0.03$ and an error that is the envelope of all other determinations, $\delta\alpha_s(\mathrm{m}_\tau) = 0.06$. The error in α_s is reduced by a factor of 10 when evolving from $q^2 = m_\tau^2$ to $q^2 = m_Z^2$.

Experimentally, R_τ can be derived from the leptonic branching fractions as

$$R_\tau = \frac{1 - \mathrm{BR}(\tau \to \mathrm{e}\nu_e\nu_\tau) - \mathrm{BR}(\tau \to \mu\nu_\mu\nu_\tau)}{\mathrm{BR}(\tau \to \mathrm{e}\nu_e\nu_\tau)} \tag{6.4}$$

Alternatively, since the agreement of the leptonic width with electroweak theory has been verified (see Chapter 5), the leptonic widths can be substituted by their predicted values $\Gamma_{SM}(\tau \to l\bar{\nu}_l\nu_\tau)$. R_τ then follows from the total width $\Gamma_{tot} = 1/\tau_\tau$ as

$$R_\tau = \frac{(1/\tau_\tau) - \Gamma_{SM}(\tau \to \mathrm{e}\nu_e\nu_\tau) - \Gamma_{SM}(\tau \to \mu\nu_\mu\nu_\tau)}{\Gamma_{SM}(\tau \to \mathrm{e}\nu_e\nu_\tau)} \tag{6.5}$$

Measurements of this type are summarized in Tab. 6.1. The agreement among the recent experiments is good. The lack of agreement to the value deduced on the basis of the Particle Data Group's 1994 averages reflect the deviation of recent precision measurements of lifetime and leptonic branching fractions (see Fig. 5.8).

6.2 Strong coupling from spectral moments

Additional information is contained in the shape of the hadronic spectrum and can be exploited taking moments of the q^2 or hadronic mass distribution. If the QCD predictions holds for the integrated quantity R_τ, it should also be valid for its moments R_τ^{kl} and its normalized moments D_τ^{kl} [432]:

$$R_\tau^{kl} \equiv \int_0^{m_\tau^2} ds \left(1 - \frac{s}{m_\tau^2}\right)^k \left(\frac{s}{m_\tau^2}\right)^l \frac{d\Gamma_{had}}{ds} \tag{6.6}$$

$$D^{kl} \equiv \frac{R_\tau^{kl}}{R_\tau} \tag{6.7}$$

The comparison of these predictions with data permits to extract α_s and non perturbative power terms simultaneously. For the normalized moments, this determination of $\alpha_s(m_\tau)$ is independent of the one based on the total hadronic width and depends on different systematics. Again, if all hadronic final states are summed over, non perturbative corrections are expected to be small and can in fact be estimated experimentally.

An extraction of $\alpha_s(m_\tau)$ from the measured spectral moments has been carried out by the ALEPH [175, 439] and CLEO [83, 439] collaborations. Due to different acceptances and resolutions for the different hadronic decay channels, the reconstruction of the inclusive hadronic mass spectrum is quite complex. First, hadronic decay channels are classified according to their apparent topology. Acceptance, background and cross feed are then corrected and the resolution unfolded. Finally, the mass distributions are added up using the τ branching fractions to form an inclusive spectrum. The resulting spectra from ALEPH and CLEO are reported in Fig. 6.2 and agree with each other quite well, although the reconstruction techniques for π^0 and the cross feed corrections differ substantially. The lowest moments of these distributions are summarized in Tab. 6.2. They are found to be in excellent agreement among the two experiments.

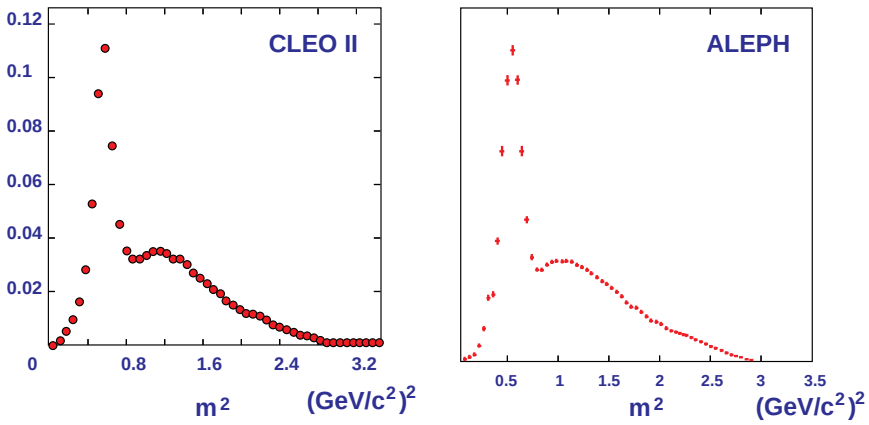

Figure 6.2: Inclusive distribution of invariant mass squared from CLEO and ALEPH [439] for hadronic τ decays, with the exception of $\tau \to \pi\nu$, after unfolding detector effects.

Moment	CLEO [83]	ALEPH [439]
$D_\tau^{1,0}$	0.7283 ± 0.0037	0.7217 ± 0.0063
$D_\tau^{1,1}$	0.1553 ± 0.0013	0.1556 ± 0.0019
$D_\tau^{1,2}$	0.0559 ± 0.0007	0.0570 ± 0.0013
$D_\tau^{1,3}$	0.0249 ± 0.0004	0.0259 ± 0.0008

Table 6.2: The measured normalized moments of the hadronic invariant mass squared distributions from ALEPH and CLEO. The errors correspond to statistical and systematic errors added in quadrature.

The measured values of R_τ and the spectral moments ($D^{1l}, l = 0,3$) are used in a global fit to extract a value of the strong coupling constant together with three non perturbative expansion coefficients. The resulting CLEO values for α_s are

$$\alpha_s(\mathrm{m}_\tau) = 0.306 \pm 0.024 \tag{6.8}$$

where the PDG94 value of R_τ (see Tab. 6.1) is used for normalization. ALEPH obtains

$$\alpha_s(\mathrm{m}_\tau) = 0.355 \pm 0.021 \tag{6.9}$$

with R_τ taken from their own measurement (see Tab. 6.1). Both errors include theoretical and experimental uncertainties, with the exception of the perturbative uncertainty discussed above which exceeds the quoted errors. The discrepancy of about two standard deviations between these two results is due to the discrepant values of R_τ, since the spectral moments are in perfect agreement.

The extrapolation of α_s to the Z mass, for ALEPH data, yields:

$$\alpha_s(\mathrm{m_Z}) = 0.121 \pm 0.002(\mathrm{theo+exp}) \pm 0.001(\mathrm{ext}) \tag{6.10}$$

where the first error sums experimental and theoretical uncertainties with exception of the perturbative uncertainty. The second error estimates the uncertainty due to the extrapolation from $q^2 = m_\tau^2$ to $q^2 = m_Z^2$. For CLEO one obtains

$$\alpha_s(\mathrm{m_Z}) = 0.114 \pm 0.003(\mathrm{theo+exp}) \pm 0.001(\mathrm{ext}) \tag{6.11}$$

The discrepancy of the two values is amplified by extrapolation, which lets the errors shrink by about a factor of 10. To account for the additional perturbative uncertainty, a theoretical error of between 0.003 and 0.006 should be added.

Conclusions are thus hampered by both experimental and theoretical uncertainties. The evolution of world average values for R_τ, together with an increased accuracy, significantly affects the deduced values of α_s. Theoretical errors are known only up to a factor of two, might be as large as 0.006 and thus dominate experimental errors. Comparing to other inclusive determinations of the strong coupling, one notices that the higher ALEPH result is in excellent agreement with the value deduced from the total hadronic Z width, $\alpha_s(\mathrm{m_Z}) = 0.125 \pm 0.004(\mathrm{stat+syst}) \pm 0.002(m_H)$, where the second error is due to the uncertainty in the Higgs boson mass [362]. The smaller CLEO value agrees better with the strong coupling deduced from deep inelastic scattering experiments, $\alpha_s(\mathrm{m_Z}) = 0.112 \pm 0.002(\mathrm{stat+syst}) \pm 0.004(q^2)$,

where the second error estimates the scale uncertainty [252]. The tau measurement, even though its value is surprisingly accurate given the low scale at which it applies, thus fails to remove the apparent discrepancy between these two values. More work is needed, on the theoretical as well as on the experimental side, to fully exploit these excellent measurements.

Chapter 7

New physics with τ leptons

Tau lepton final states are almost ubiquitous in the searches for new interactions and new particles [440]. This is especially true in searches for Higgs bosons, since these couple to mass and thus prefer to decay to heavy final states. Moreover, most experimental signatures for new particle production involve missing energy and/or multiple leptons, for which tau lepton production is an important background.

Instead of discussing these searches by artificially reducing to signatures involving tau leptons, we will restrict ourselves to two particular subjects which are more specific to the physics of the τ lepton proper: leptonic $\mathcal{CP}$ violation and lepton number or lepton flavor violation in tau production and decay. The main reason is that although neither of the two is predicted by the Minimal Standard Model, both effects could be quite readily accommodated. The observation of $\mathcal{CP}$ violation in leptonic charged currents could restore symmetry between the quark and the lepton sector by introducing a mixing matrix for leptons analogous to the CKM matrix [441] (see also Section 3.3). However, $\mathcal{CP}$ violation in neutral currents would be an unambiguous sign of new physics. Flavor conservation in the Standard Model is not protected by a gauge symmetry and in fact absent in hadronic charged currents. It thus makes sense to concentrate the discussion on these two somewhat less solid points of the Standard Model.

7.1 $\mathcal{CP}$ violation in τ production

The violation of $\mathcal{CP}$ symmetry, where $\mathcal{C}$ stands for charge conjugation and $\mathcal{P}$ for parity is still one of the fundamental mysteries in particle physics. So far, $\mathcal{CP}$ violation has been observed only in the decay of neutral kaons [442]. In the Standard Model, the $\mathcal{CP}$ violation of electroweak interactions with three fermion families is described by a phase in the CKM mixing matrix [441], which enters into the weak charged current coupling among quarks. In neutral current reactions, violation of $\mathcal{CP}$ symmetry has not been observed and the Standard Model does not predict any observable effect. However, extensions to the Standard Model have been proposed that can generate $\mathcal{CP}$ violations [443]. Formally $\mathcal{CP}$ violation can be introduced in a process, if the produced fermions possess an electric (d_τ) or a weak (d_τ^{weak}) dipole moment, without any a priori connection between their magnitudes. In extensions to the Standard Model, the dipole

moments are expected (see Section 3.4) to scale with the third power of the fermion mass, thus favoring the search with heavy leptons.

As discussed earlier (see Section 3.4) limits on the electric dipole moment can be obtained searching for anomalous photon radiation from $\tau^+\tau^-$ final states. In the context of $\mathcal{CP}$ violation, $\mathcal{CP}$ odd observables can be constructed in addition and their expectation values measured to obtain more stringent limits [444–446]. These are then normally expressed as limits on the weak dipole moment of the tau lepton.

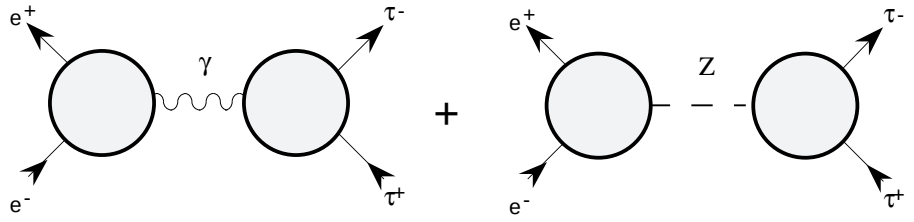

Figure 7.1: Form factor ansatz for the vertices $\tau\bar{\tau}\gamma$ and $\tau\bar{\tau}$Z

In analogy to the electromagnetic form factors introduced in Equ. 3.11, the neutral current Lagrangian $\mathcal{L}_{SM}$ of the Standard Model can be extended, in a model independent way, by an effective $\mathcal{CP}$ violating term, affecting the $\tau\bar{\tau}\gamma$ and $\tau\bar{\tau}$Z vertices. Taking into account operators with dimension ≤ 6 one finds

$$\mathcal{L}_{CP} = -\frac{i}{2}\bar{u}\sigma^{\mu\nu}\gamma_5 u(d_\tau F_{\mu\nu} + d_\tau^{weak} Z_{\mu\nu}) \tag{7.1}$$

(see Fig. 7.1), where $F_{\mu\nu}$ and $Z_{\mu\nu}$ are the electromagnetic and weak field tensors. The strength of $\mathcal{CP}$ violating amplitudes is governed by the two form factors, d_τ and d_τ^{weak}, which are complex and depend on q^2. The first d_τ (see Section 3.4), describes the τ coupling to the photon, the second d_τ^{weak}, the weak dipole form factor, describes the $\mathcal{CP}$ violating coupling of the τ lepton to the Z. On the Z peak, the photon contribution is negligible and the weak dipole moment $d_\tau^{weak}(q^2 = m_Z^2)$ is dominating.

Deviations from the Standard Model are thus encountered both by $\mathcal{CP}$ conserving cross section modification proportional to $|\mathcal{L}_{\mathcal{CP}}|^2$ and by interference between $\mathcal{L}_{SM}$ and $\mathcal{L}_{\mathcal{CP}}$, which is $\mathcal{CP}$ violating. The cross section modification [445]:

$$\Delta\Gamma_{\tau\tau} \approx |d_\tau^{weak}|^2 \frac{m_Z^3}{24\pi} \tag{7.2}$$

is in itself not a $\mathcal{CP}$ violating effect, but indirectly limits d_τ^{weak} when one assumes that it is the only deviating contribution to the partial Z width. Using recent results from LEP [447], $\Gamma_{\tau\tau} = (84.26 \pm 0.34)$ MeV, and the corresponding width expected from the Standard Model, $\Gamma_{\tau\tau}^{SM} = 83.7 \pm 0.4$ MeV [448], one obtains a limit of $|d_\tau^{weak}| < 2.3 \times 10^{-17} e$ cm at 95 % C.L.

7.1.1 $\mathcal{CP}$ violating observables

Direct limits on $\mathcal{CP}$ violation can be obtained by measuring the expectation value of $\mathcal{CP}$ odd observables. Any non zero value would indicate $\mathcal{CP}$ violation and thus be a sign for new physics.

Such observables can be constructed from the kinematic variables characterizing τ production

$$e^+(\vec{p}_+) + e^-(\vec{p}_-) \rightarrow \tau^+(\vec{k}_+) + \tau^-(\vec{k}_-) \tag{7.3}$$

where $\vec{p}_i$ are the momenta of the unpolarized beams and $\vec{k}_j$ the τ momenta. For double one prong tau decays

$$\tau^+\tau^- \rightarrow A(\vec{q}_-) + \bar{B}(\vec{q}_+) + X \tag{7.4}$$

the momenta $\vec{q}_-, \vec{q}_+$ are used in addition.

$\mathcal{CP}$ odd observables can then be constructed from the unit vectors $\hat{\vec{k}} = \vec{k}/k$ and the spin vectors $\vec{S}$ of both tau leptons. Since these are not directly observed, the momenta $\vec{q}$ of the decay products or their directions $\hat{\vec{q}} = \vec{q}/q$ can be substituted. The observables can be arranged as a traceless tensor [445]

$$T_{ij} = (\vec{q}_- - \vec{q}_+)_i(\vec{q}_- \times \vec{q}_+)_j + (i \leftrightarrow j) \tag{7.5}$$

or its normalized form

$$\hat{T}_{ij} = (\hat{\vec{q}}_- - \hat{\vec{q}}_+)_i \frac{(\hat{\vec{q}}_- \times \hat{\vec{q}}_+)_j}{|\hat{\vec{q}}_- \times \hat{\vec{q}}_+|} + (i \leftrightarrow j) \tag{7.6}$$

where the indices i, j $(1 \leq i, j \leq 3)$ label the Cartesian coordinates with the third component along the beam axis. The expectation values $< T_{ij} >_{A\bar{B}}$ change sign under $\mathcal{CP}$ transformation and are directly related to the weak dipole moment by

$$< T_{ij} >_{A\bar{B}} = d_\tau^{weak} C_{A\bar{B}} \frac{m_Z}{e} \begin{pmatrix} -\frac{1}{6} & 0 & 0 \\ 0 & -\frac{1}{6} & 0 \\ 0 & 0 & \frac{1}{3} \end{pmatrix} \tag{7.7}$$

The proportionality constants $C_{A\bar{B}}$ [445] depend on the τ decay mode and are related to the sensitivity of the decay mode as a τ spin analyzer. The third component, $< T_{33} >_{A\bar{B}}$, is a particularly sensitive observable and also the least influenced by systematic effects.

The OPAL collaboration, measuring $< T_{33} >$ on a sample of $\tau^+\tau^-$ decaying semi-inclusively to lepton-lepton, lepton-hadron or hadron-hadron pairs, first deduced a limit of [225]:

$$|d_\tau^{weak}| \leq 7.0 \times 10^{-17} e\text{cm} \quad 95\% C.L. \tag{7.8}$$

The ALEPH Collaboration, using $< \hat{T}_{33} >$ on a sample with exclusively identified decay modes $\tau \rightarrow e\nu\nu$, $\tau \rightarrow \mu\nu\nu$, $\tau \rightarrow \pi(\mathrm{K})\nu$ and $\tau \rightarrow \rho(\mathrm{K}^*)\nu$, obtained [173]:

$$|d_\tau^{weak}| \leq 3.7 \times 10^{-17} e\text{cm} \quad 95\% C.L. \tag{7.9}$$

This limits has been recently improved, using a larger sample, a better selection and including the τ decay into a_1, to [185]:

$$|d_\tau^{weak}| \leq 1.5 \times 10^{-17} e\text{cm} \quad 95\% C.L. \tag{7.10}$$

Using the same method, DELPHI obtained a preliminary limit of [201]

$$|d_\tau^{weak}| \leq 2.1 \times 10^{-17} e\text{cm} \quad 95\% C.L. \tag{7.11}$$

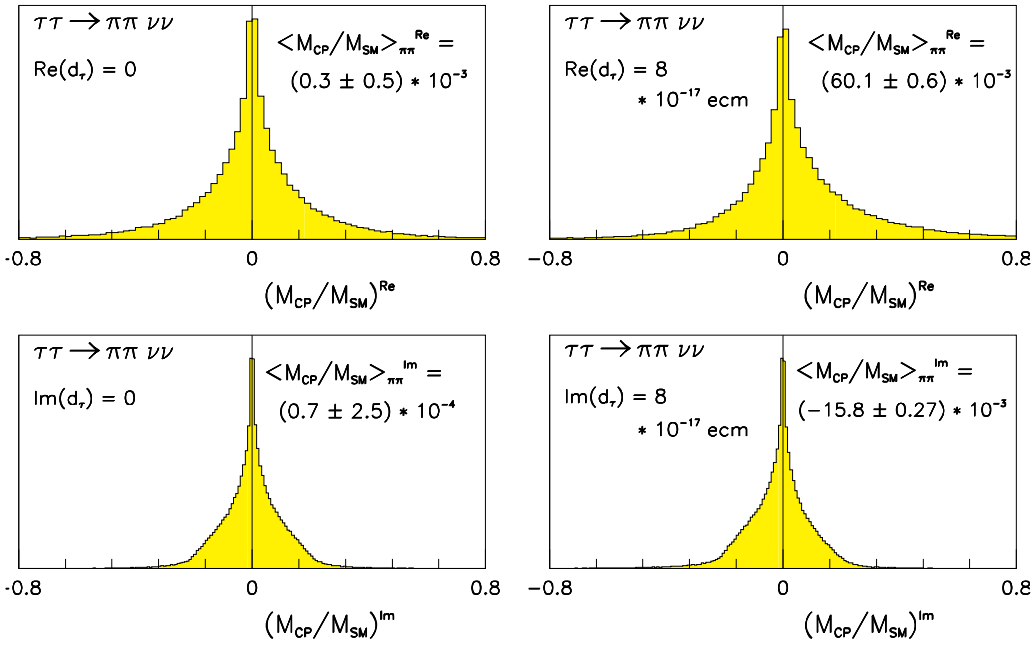

Figure 7.2: Monte Carlo simulation for $\frac{\mathcal{M}_{\mathcal{CP}}}{\mathcal{M}_{SM}}$ in the $\tau^+\tau^- \to \pi^+\pi^-\nu_\tau\bar{\nu}_\tau$ decay for zero d_τ^{weak} (left side) and $\mathrm{Re}(d_\tau^{weak}) = \mathrm{Im}(d_\tau^{weak}) = 8 \times 10^{-17} e$ cm (right side). [237]

A new method based on optimal $\mathcal{CP}$ odd observables constructed from the τ flight and spin directions has recently been introduced by OPAL [237]. The result achieved was a more sensitive measurement of the real part and, for first time, the imaginary part of the weak dipole moment. The new observables, one $\mathcal{CP}$ odd and $\mathcal{T}$ odd ($\mathcal{T}^-$) and an another $\mathcal{CP}$ odd and $\mathcal{T}$ even ($\mathcal{T}^+$), are constructed by taking the ratios of the respective amplitudes:

$$\mathcal{O}^{\mathcal{T}^+} = \frac{\mathcal{M}_{\mathcal{CP}}^{Re}}{\mathcal{M}_{SM}} \qquad \mathcal{O}^{\mathcal{T}^-} = \frac{\mathcal{M}_{\mathcal{CP}}^{Im}}{\mathcal{M}_{SM}} \tag{7.12}$$

These amplitudes can be expressed as:

$$\mathcal{M}_{\mathcal{CP}}^{Re} = (\hat{\vec{k}}_+ \cdot \hat{\vec{q}}_-)(\hat{\vec{k}}_+ \times (\vec{S}_+ - \vec{S}_-) \cdot \hat{\vec{q}}_-) \tag{7.13}$$

$$\mathcal{M}_{\mathcal{CP}}^{Im} = (\hat{\vec{k}}_+ \cdot \hat{\vec{q}}_-)[(\hat{\vec{k}}_+ \cdot \vec{S}_+)(\hat{\vec{q}}_- \cdot \vec{S}_-) - (\hat{\vec{k}}_+ \cdot \vec{S}_-)(\hat{\vec{q}}_- \cdot \vec{S}_+)] \tag{7.14}$$

$$\mathcal{M}_{SM} = 1 + (\hat{\vec{k}}_+ \cdot \hat{\vec{q}}_-)^2 + \vec{S}_+ \cdot \vec{S}_-(1 - (\hat{\vec{k}}_+ \cdot \hat{\vec{q}}_-)^2) - 2(\hat{\vec{q}}_- \cdot \vec{S}_+)(\hat{\vec{q}}_- \cdot \vec{S}_-) \tag{7.15}$$

$$+2(\hat{\vec{k}}_+ \cdot \hat{\vec{q}}_-)[(\hat{\vec{k}}_+ \cdot \vec{S}_+)(\hat{\vec{q}}_- \cdot \vec{S}_-) + (\hat{\vec{k}}_+ \cdot \vec{S}_-)(\hat{\vec{q}}_- \cdot \vec{S}_+)] \tag{7.16}$$

where $\hat{\vec{q}}_-$ is the direction of the electron beam, $\hat{\vec{k}}_+$ is the flight direction of the positive τ and the $\vec{S}_\pm$ are the spin vectors of the $\tau^\pm$ leptons in their respective rest frame. Neither the $\tau^\pm$ direction nor its spin can be measured directly. The reconstruction is thus complex [237] and described in detail elsewhere [449].

The mean values of these observables, $< \mathcal{O}^{\mathcal{T}^+} >$ and $< \mathcal{O}^{\mathcal{T}^-} >$, are related to the real and imaginary parts of the weak dipole moment

$$< \mathcal{O}^{\mathcal{T}^-} >_{A\bar{B}} = \frac{m_Z}{e} d_{A\bar{B}} Re(d_\tau^{weak}) \tag{7.17}$$

$$< \mathcal{O}^{\mathcal{T}^+} >_{A\bar{B}} = \frac{m_Z}{e} f_{A\bar{B}} Im(d_\tau^{weak}) \tag{7.18}$$

The dimensionless proportionality constants $d_{A\bar{B}}$ and $f_{A\bar{B}}$ are sensitivities (as $C_{A\bar{B}}$ in Equ. 7.7) and depend on the decay channel. A non zero expectation value for $< \mathcal{O}^+ >$ or $< \mathcal{O}^- >$, that would correspond to a non vanishing weak dipole moment, would be observed as an asymmetric tail in the $\mathcal{O}$ distribution. This is verified by Monte Carlo calculation, see Fig. 7.2.

The measured distribution of $\mathcal{CP}$ odd observables are symmetric (see Fig. 7.3) with no evidence for a non zero expectation value. Consequently, real and imaginary part of d_τ^{weak} are found to be compatible with zero for all decay modes and angular regions. Fig. 7.4 shows this for real part alone. An upper limit on the weak dipole moment is then set by a weighted mean over all these channels:

$$|\mathrm{Re}(d_\tau^{weak})| \leq 7.8 \times 10^{-18} e\mathrm{cm} \quad (7.19)$$

$$|\mathrm{Im}(d_\tau^{weak})| \leq 4.5 \times 10^{-17} e\mathrm{cm} \quad (7.20)$$

at 95% confidence level.

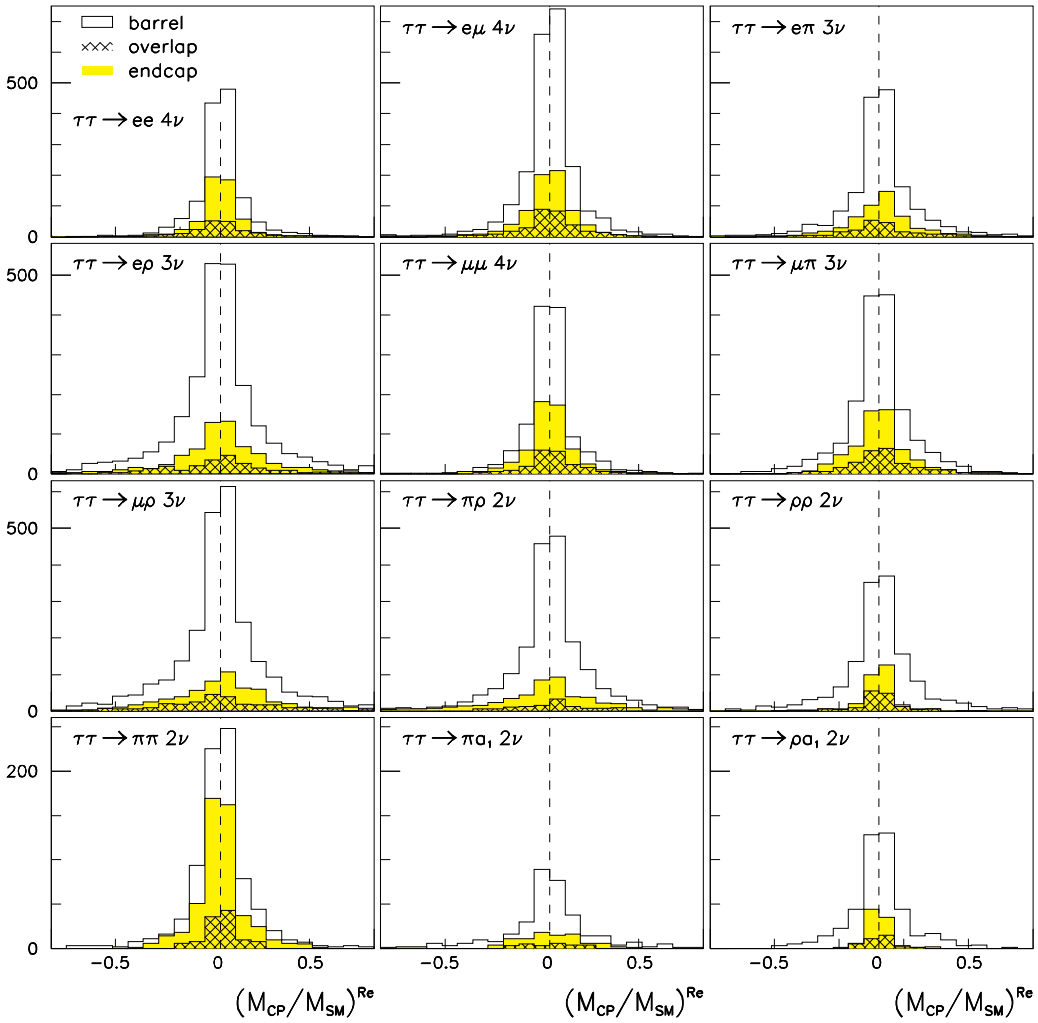

Figure 7.3: Distribution of the measured $\mathcal{CP}$ odd, $\mathcal{T}$ odd observables in $Z \to \tau^+\tau^-$ events from OPAL [237].

In summary, no $\mathcal{CP}$ violating effects have been detected in $Z \to \tau^+\tau^-$ neutral current processes. The current experimental limits come close to the range where $\mathcal{CP}$ violating effects are expected from models beyond the Standard Model.

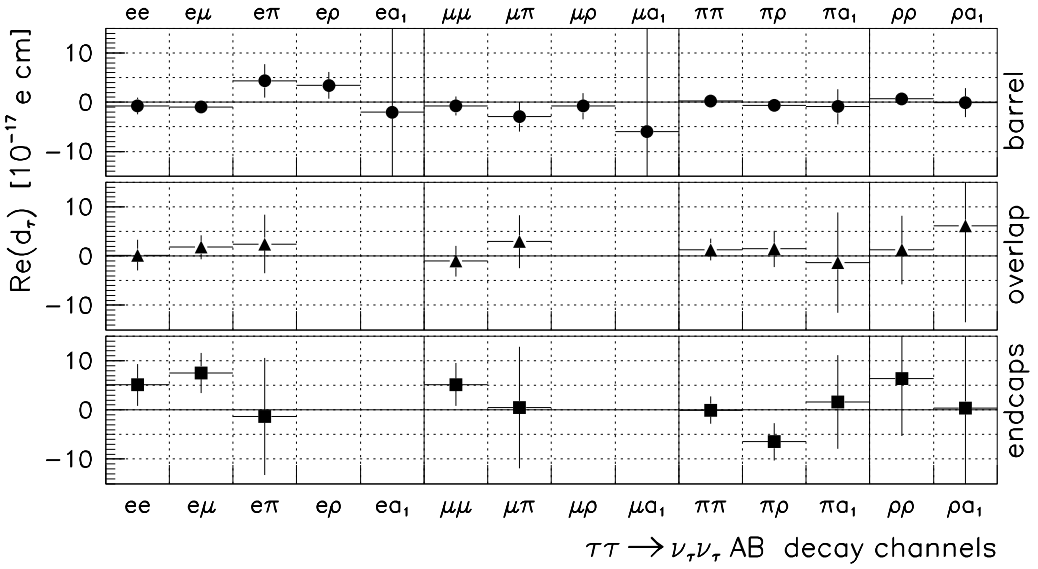

Figure 7.4: The real part of the weak dipole moment extracted from different τ decay channels in different geometrical regions of the OPAL detector [237].

7.2 Lepton number and lepton flavor violation

In the Standard Model, lepton flavor is strictly conserved, in charged as well as in neutral currents. In particular, the Z only couples to pairs of leptons carrying the same flavor (see Fig. 7.5a). Since, however, lepton flavor conservation is not protected by a gauge symmetry, extensions to the Standard Model can accommodate flavor changing transitions (see fig 7.5b), either directly or indirectly, such as models with neutral heavy leptons, left-right symmetric models, SUSY and superstring models [450–465]. The Z branching fractions to τe or $\tau\mu$ are in fact predicted to be quite large as shown in Tab. 7.1.

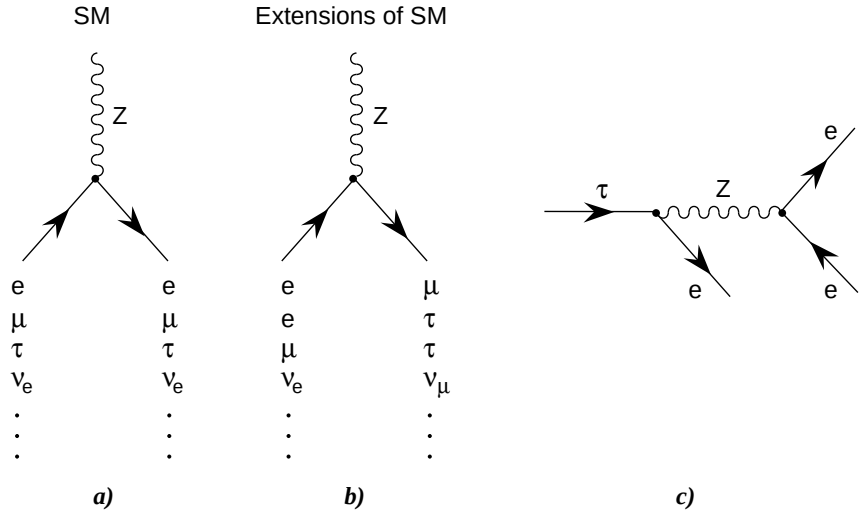

Figure 7.5: a) Standard Model neutral currents; b) lepton flavor violating Z decays; c) lepton flavor violating decay $\tau \rightarrow$ eee.

Flavor changing neutral currents would manifest themselves both in Z decays to different

Reference	Model	Br(Z$\rightarrow$ eτ)	Br (Z $\rightarrow \mu\tau$)
[461]	Superstrings,E_6 grand unified theory (new exotic family-blind fermions)	$\leq 3.4 \times 10^{-4}$	$\leq 4.2 \times 10^{-4}$
[463]	Scalar triplet model (Majorons)	$\leq 7.9 \times 10^{-6}$	$\leq 5.9 \times 10^{-6}$
[462]	Superstring inspired Standard Model (new neutral leptons)	$\sim 10^{-7} - 10^{-6}$	$\sim 10^{-7} - 10^{-6}$
[464]	Lepton flavor violation by neutral gauge couplings (extra exotic gauge bosons: Z'-Z mixing)	$< (4-6) \times 10^{-7}$	$< 3 \times 10^{-9}$
[465]	Soft supersymmetry breaking terms (scalar lepton mixing)	$\sim 10^{-9} - 10^{-8}$	$\sim 10^{-9} - 10^{-8}$

Table 7.1: Theoretical predictions for branching ratios $Z \rightarrow e\tau$ and $Z \rightarrow \mu\tau$

lepton flavors (Fig. 7.5b) and in flavor violating lepton decays (Fig. 7.5c). Factorization requires that the two rates are related. Best limits on muon and electron flavor violations thus come from muon decays. The measured limit on $\mu \rightarrow$ eee, Br($\mu \rightarrow$ eee) $< 1.0 \times 10^{-12}$ at 90% CL [466], sets an upper limit on the corresponding Z decay, Z$\rightarrow$ eμ of [467]:

$$\mathrm{Br}(\mathrm{Z} \rightarrow \mathrm{e}\mu) < 0.74 \times 10^{-12} \quad (90\%\mathrm{CL}) \tag{7.21}$$

much below the accessible range for direct observation of this process in Z decays. For τ flavor changing neutral currents, on the other hand, the sensitivity of the search in Z decays and τ decays are of comparable sensitivity.

7.2.1 Lepton flavor violation in Z decays

Z decays into eτ and $\mu\tau$ would be observed as a peak at the end point of the momentum spectrum in candidates for Z$\rightarrow \tau^+\tau^- \rightarrow$ e/μX. As an example, Fig. 7.6 shows the electron and muon spectra in $\tau\tau$ candidate events from L3 [468] near the endpoint. The expected monochromatic contribution from lepton flavor violation is also indicated, with a normalization corresponding to an arbitrary branching fraction. Clearly, no indication for such a process is observed.

The corresponding preliminary limits on lepton flavor changing neutral currents [216] are given in Table 7.2, which summarizes the status of direct limits on lepton flavor violation in Z decays. Common limits can be estimated [467] from the current LEP measurements [468], at 95% CL:

$$\mathrm{Br}(\mathrm{Z} \rightarrow \mathrm{e}\mu) < 0.62 \times 10^{-6} \tag{7.22}$$

$$\mathrm{Br}(\mathrm{Z} \rightarrow \mathrm{e}\tau) < 4.4 \times 10^{-6} \tag{7.23}$$

$$\mathrm{Br}(\mathrm{Z} \rightarrow \mu\tau) < 6.6 \times 10^{-6} \tag{7.24}$$

The present and future limits on Z$\rightarrow$ eμ are obviously not competitive to those obtained from muon number violating decay processes. However, for τ flavor violation the sensitivity reaches the level where extensions to the Standard Model predict observable branching fractions.

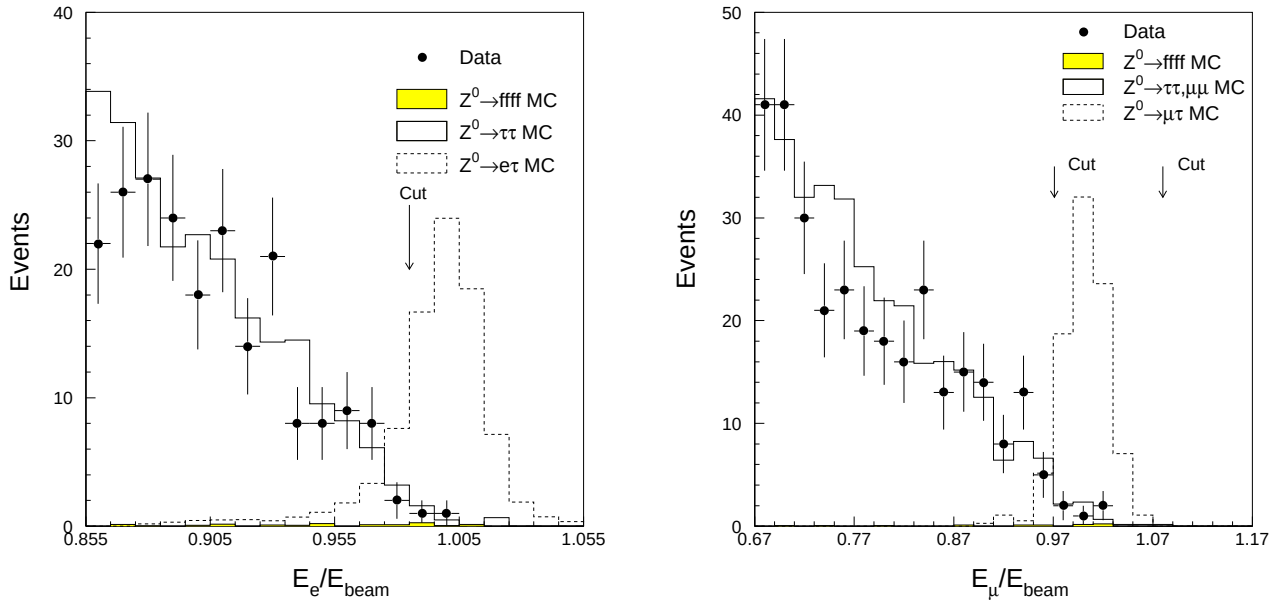

Figure 7.6: Left: Distribution of the electron energy in Z$\to$ eτ candidates. Right: Distribution of the muon energy for Z$\to$ $\mu\tau$ candidates [210].

Experiment	Br(Z$\to$ eμ)	Br(Z$\to$ eτ)	Br(Z$\to$ $\mu\tau$)
ALEPH [467]	$< 3.7 \times 10^{-6}$	$< 17 \times 10^{-6}$	$< 35 \times 10^{-6}$
DELPHI [202]	$< 4 \times 10^{-6}$	$< 36 \times 10^{-6}$	$< 15 \times 10^{-6}$
L3 [216]	$< 2.0 \times 10^{-6}$	$< 7.3 \times 10^{-6}$	$< 10 \times 10^{-6}$
OPAL [240]	$< 1.7 \times 10^{-6}$	$< 9.8 \times 10^{-6}$	$< 17 \times 10^{-6}$

Table 7.2: Direct experimental limits for branching ratios of Z$\to$ eμ, Z$\to$ eτ and Z$\to$ $\mu\tau$

7.2.2 Neutrinoless τ decays

The search for flavor changing lepton decays is another way to probe the basic assumptions of the Standard Model. In extensions to the Standard Model, neutrinoless lepton decay rates are enhanced for heavy leptons. In some models, the rate for flavor changing τ decays is even increased by a factor $(m_\tau/m_\mu)^5$ with respect to muon decay [460]. The expected decay rate of each channel depends however strongly on the model considered. As an example, the branching ratio [460] for the decays $\tau \to \gamma\mu$, $\tau \to l\pi$, $\tau \to 3l$ and $\tau \to l\eta$ in a model with heavy neutral leptons has a strong dependence on the heavy lepton mass and ranges from $\simeq 10^{-10}$, corresponding to a few tens of GeV mass, to $\simeq 10^{-6}$ for masses above 4 TeV. The predictions also depend on unknown coupling constants.

A particularly interesting case is the radiative decay $\tau^- \to \mu^-\gamma$ since its branching ratio is related to the rate of $\mu^- \to e^-\gamma$. The latter has been searched for in dedicated experiments at TRIUMF [469] and LAMPF [470], yielding an upper limit for its branching fraction of Br($\mu^- \to e^-\gamma$) $< 4.9 \times 10^{-11}$ at 90% C.L. The expected enhancement factor for $\tau^- \to \mu^-\gamma$, primarily due to the mass dependent coupling, ranges between 10^5 and 10^6, making this channel particularly

attractive to pursue experimentally. SUSY model predictions for this decay are [457]

$$\frac{\mathrm{Br}(\tau \to \mu\gamma)}{\mathrm{Br}(\mu \to \mathrm{e}\gamma)} \approx (\frac{m_\tau}{m_\mathrm{e}})^2 \frac{1}{5} \approx 10^6 \tag{7.25}$$

In string models [458], the same factor is approximately 2×10^5. The corresponding branching fraction for $\tau^- \to \mu^-\gamma$ should thus be of order 10^{-6} and close to being observable. The same conclusion holds for predictions from left right symmetric theories [455]. The limit obtained by CLEO for this decay [74] is more stringent than many theoretical estimations for lepton flavor violations:

$$\mathrm{Br}(\tau^- \to \mu^-\gamma) < 4.2 \times 10^{-6} \quad 90\% C.L. \tag{7.26}$$

This limit improves on a previous one obtained by ARGUS [99] ($< 3.4 \times 10^{-5}$ at 90% C.L.) by a factor of eight. Similar results have been obtained by DELPHI [202].

New bounds have been recently been set by CLEO [81] also on others forbidden lepton flavor and number violating τ decays. A search has been made for 22 neutrinoless modes, with a lepton plus two other charged particles in final state. No significant signal has been found. The results are summarized in Tab. 7.3 together with the corresponding values reported by the Particle Data Group [252]. The improvement reached in many cases is impressive. The limits on branching ratios for channels containing additional neutrals still come from older ARGUS [99] and Crystal Ball [107] studies.

The channels $\tau^- \to \mu^+(\mathrm{e}^+)h^-h^+$, $\tau^- \to \pi^-\gamma$ and $\tau^- \to \pi^-\pi^0$ limit lepton number violations, while all other modes are testing for lepton flavor violations. Neither effect has been observed at the level of a few times 10^{-6}. Simultaneous lepton and baryon number violations have also been searched for by ARGUS [99]; limits are of the order 10^{-3} only.

By factorization, the limits for $\tau^- \to \mathrm{e}^-\mathrm{e}^+\mathrm{e}^-$ and $\tau^- \to \mu^-\mathrm{e}^+\mathrm{e}^-$ can be translated into corresponding limits on Z$\to \mu\tau$ and Z$\to \mathrm{e}\tau$. One obtains [467]:

$$\mathrm{Br}(\mathrm{Z} \to \mathrm{e}\tau) < 14 \times 10^{-6} \tag{7.27}$$

$$\mathrm{Br}(\mathrm{Z} \to \mu\tau) < 18 \times 10^{-6} \tag{7.28}$$

at 90% CL, less stringent than the direct limits obtained at LEP (see Tab. 7.2).

Channel	Experiment	Upper Limit $[10^{-6}]$	Particle Data Group $[10^{-6}]$
$\tau^- \to e^-e^+e^-$	CLEO	<3.3	< 13
$\tau^- \to \mu^-e^+e^-$	CLEO	<3.4	<14
$\tau^- \to \mu^+e^-e^-$	CLEO	<3.4	< 14
$\tau^- \to e^-\mu^+\mu^-$	CLEO	<3.6	< 19
$\tau^- \to e^+\mu^-\mu^+$	CLEO	<3.5	<16
$\tau^- \to \mu^-\mu^+\mu^-$	CLEO	<4.3	< 17
$\tau^- \to e^-\pi^+\pi^-$	CLEO	<4.4	<27
$\tau^- \to e^-K^+\pi^-$	CLEO	<4.6	<58
$\tau^- \to e^-\pi^+K^-$	CLEO	<7.7	<29
$\tau^- \to e^+\pi^-\pi^-$	CLEO	<4.4	<17
$\tau^- \to e^+e^-\pi^-K^-$	CLEO	<4.5	<20
$\tau^- \to \mu^+\mu^-\pi^+\pi^-$	CLEO	<7.4	<36
$\tau^- \to \mu^+\mu^-K^+\pi^-$	CLEO	<15	<77
$\tau^- \to \mu^+\mu^-\pi^+K^-$	CLEO	<8.7	<77
$\tau^- \to \mu^+\pi^-\pi^-$	CLEO	<6.9	<39
$\tau^- \to \mu^+\pi^-K^-$	CLEO	<20	<40
$\tau^- \to e^-\rho^0$	CLEO	<4.2	<19
$\tau^- \to e^-K^{*0}$	CLEO	<6.3	<38
$\tau^- \to e^-\bar{K}^{*0}$	CLEO	<11	-
$\tau^- \to \mu^-\rho^0$	CLEO	<5.7	<29
$\tau^- \to \mu^-K^{*0}$	CLEO	<9.4	<45
$\tau^- \to \mu^-\bar{K}^{*0}$	CLEO	<8.7	-
$\tau^- \to \mu^-\gamma$	CLEO [74]	<4.2	<4.2
$\tau^- \to \mu^-\pi^0$	ARGUS	<44	<44
$\tau^- \to e^-\gamma$	ARGUS	<120	< 120
$\tau^- \to e^-\pi^0$	Crystal Ball [107]	<140	<140
$\tau^- \to \pi^-\gamma$	ARGUS	<280	< 280
$\tau^- \to \pi^-\pi^0$	ARGUS	<370	< 370
$\tau^- \to e^-\eta$	ARGUS	<63	< 63
$\tau^- \to \mu^-\eta$	ARGUS	<73	<73
$\tau^- \to \bar{p}\gamma$	ARGUS	<290	<290
$\tau^- \to \bar{p}\pi^0$	ARGUS	<656	<656
$\tau^- \to \bar{p}\eta$	ARGUS	<1290	<1290

Table 7.3: Upper limits (95 % CL) for neutrinoless τ decays, from CLEO [81], ARGUS [99] and Crystal Ball [107]. For comparison, the limits from the Data Particle Group [252] are also listed.

Chapter 8

Conclusions and outlook

Tau physics has entered the short list of precision subjects in particle physics, such that results on tau leptons are now gauged against muon physics results. This has been made possible by the tremendous progress in accelerator and detector technology that the recent generation of experiments has profited from. The main experimental break-throughs may be characterized as follows:

- *Static properties:* The mass of the tau lepton is now, twenty years after its discovery, known with sub-MeV precision. This measurement removes substantial freedom in the interpretation of tau physics results and makes high precision tests of electroweak theory possible. Although the tau neutrino yet remains to be seen through its interactions with matter, its mass is known to be less than 24 MeV. It is not excluded that the tau neutrino has a mass, and that it oscillates to other neutrino species.
- *Electroweak properties:* The tau lepton has pointlike electroweak vertices up to $q^2 = m_Z^2$. Its couplings to the electroweak currents are the same as those of electron and muon with permill precision.
- *Hadronic decays:* Nearly all expected tau decays with branching fractions down to a few times 10^{-5} have actually been observed. On one hand, more and more exclusive analysis and improved particle identification technology has allowed to differentiate more and more decay modes. On the other hand, semi-inclusive classification of final states has allowed to verify the completeness of observed final states with percent precision. The structure of the hadronic charged current at large distances has become a subject of study on its own.
- *New physics:* Tau leptons provide a powerful tool for the search of deviation from the current orthodoxy. Their high mass often enhances expected effects with respect to the first two lepton generation. No unexplained effects have, however, been detected to date. Especially, the tau and its neutrino seem to indeed have their own lepton flavor, conserved to the level of a few times 10^{-6}.

In conclusion, one is thus entitled to say that, for all we know, the tau is just another sequential lepton. There has thus been little progress in understanding why nature has provided replicas

of the lowest lying fermion family.

However, as impressive as recent progress in tau physics may be, the field has still a long way to go until precision really matches the scale set by muon physics. Moreover, we have only just scratched the surface of the rich field of study opened up by the possibility to produce resonant hadronic final states out of the vacuum. It thus stays true that when one looked without finding anything, one just has not looked hard enough.

In fact the prospects for looking more closely at the physics of tau leptons appear excellent. The CLEO and the LEP experiments are still taking high statistics data with excellent detector technology and first class analysis techniques. The experiments at future B-factories will multiply the world statistics of observed tau leptons by a large factor [471]. Last but not least, feasibility studies for a facility dedicated to this physics, a τ-charm factory [472] are being conducted and are endorsed by the physics community. With all the effort going into this fascinating subject, we will surely find out what (if anything) is "wrong" with the tau lepton, and we might finally understand why it exists at all.

Acknowledgments

We wish to thank Prof. J. Dumarchez, P. Nason and J. Kühn for helpful discussions on theoretical aspects of tau physics. The constructive criticism from Drs. M. Grünewald and A. Kunin and I. Vorobiev was also very valuable. We gratefully acknowledge the work done by the LEP electroweak working group, and especially Drs. J. Mnich and M. Grünewald. We also thank our many colleagues from the LEP, SLC, PEP, PETRA, CESR and DORIS collaborations who have been very helpful in putting the data together for this review. Last but not least we have greatly benefited from the contributions and summaries presented at the 1994 Workshop on Tau Lepton Physics in Montreux, Switzerland, organized by Prof. L. Rolandi.

Bibliography

[1] S. Glashow, Nucl. Phys. **22** (1961) 579;
S. Weinberg, Phys. Rev. Lett. **19** (1967) 1264;
A. Salam, in Elementary Particle Theory, N. Svartholm ed., Almqvist and Wiksell, Stockholm (1968) 367.

[2] SLAC-LBL Collab., M.L. Perl *et al.*, Phys. Rev. Lett. **35** (1975) 1489.

[3] M.L. Perl, Rept. Prog. Phys. **55** (1992) 653.

[4] B.C. Barish and R. Stroynowski, Phys. Rep. **157** (1988) 1.

[5] A. Pich, *Tau Physics*, in *Heavy Flavors*, A.J. Buras and M. Lindner edts., Advanced Series on Directions in High Energy Physics, Vol. 10, World Scientific, Singapore, 1992, p. 375.

[6] A.J. Weinstein and R. Stroynowski, Ann. Rev. Nucl. Part. Sci. **43** (1993) 457.

[7] UA1 Collab., C. Albajar *et al.*, Phys. Lett. **B 185** (1987) 233.

[8] UA2 Collab., J. Alitti *et al.*, Z. Phys. **C 52** (1991) 209.

[9] CDF Collab., F. Abe *et al.*, Phys. Rev. Lett. **68** (1992) 3398.

[10] MARK III Collab., J. Adler *et al.*, Phys. Rev. Lett. **59** (1987) 1517.

[11] CLEO Collab., R. Giles *et al.*, Phys. Rev. Lett. **50** (1983) 877.

[12] HRS Collab., K.K. Gan *et al.*, Phys. Lett. **153 B** (1985) 116.

[13] HRS Collab., S. Abachi *et al.*, Phys. Rev. **D 40** (1989) 902.

[14] MAC Collab., E. Fernandez *et al.*, Phys. Rev. Lett. **54** (1985) 1620.

[15] MARK II Collab., M.E. Levi *et al.*, Phys. Rev. Lett. **51** (1983) 1941.

[16] CELLO Collab., H.J. Behrend *et al.*, Phys. Lett. **114 B** (1982) 282.

[17] CELLO Collab., H.J. Behrend *et al.*, Phys. Lett. **B 222** (1989) 163.

[18] JADE Collab., W. Bartel *et al.*, Phys. Lett. **161 B** (1985) 188.

[19] JADE Collab., W. Bartel *et al.*, Z. Phys. **C 30** (1986) 371.

[20] JADE Collab., S. Hegner *et al.*, Z. Phys. **C 46** (1990) 547.

[21] MARK J Collab., D.P. Barber *et al.*, Phys. Rev. Lett. **43** (1979) 1915.

[22] MARK J Collab., D.P. Barber *et al.*, Phys. Rev. Lett. **46** (1981) 1663.

[23] MARK J Collab., B. Adeva *et al.*, Phys. Rep. **109** (1984) 131.

[24] MARK J Collab., B. Adeva *et al.*, Phys. Lett. **B 179** (1986) 177.

[25] MARK J Collab., B. Adeva *et al.*, Phys. Rev. **D 38** (1988) 2665.

[26] PLUTO Collab., Ch. Berger *et al.*, Phys. Lett. **99 B** (1981) 489.

[27] PLUTO Collab., Ch. Berger *et al.*, Z. Phys. **C 28** (1985) 1.

[28] TASSO Collab., R. Brandelik *et al.*, Phys. Lett. **92 B** (1980) 199.

[29] TASSO Collab., R. Brandelik *et al.*, Phys. Lett. **110 B** (1982) 173.

[30] TASSO Collab., M. Althoff *et al.*, Z. Phys. **C 26** (1985) 421.

[31] TASSO Collab., W. Braunschweig *et al.*, Z. Phys. **C 43** (1989) 549.

[32] AMY Collab., A. Bacala *et al.*, Phys. Lett. **B 218** (1989) 112.

[33] AMY Collab., C. Velissaris *et al.*, Phys. Lett. **B 331** (1994) 227.

[34] TOPAZ Collab., I. Adachi *et al.*, Phys. Lett. **B 208** (1988) 319.

[35] TOPAZ Collab., B. Howell *et al.*, Phys. Lett. **B 291** (1992) 206.

[36] VENUS Collab., K. Abe *et al.*, Z. Phys. **C 48** (1990) 13.

[37] L3 Collab., B. Adeva *et al.*, Phys. Lett. **B 236** (1990) 109.

[38] L3 Collab., B. Adeva *et al.*, Phys. Lett. **B 250** (1990) 183.

[39] L3 Collab., B. Adeva *et al.*, Z. Phys. **C 51** (1991) 179.

[40] L3 Collab., O. Adriani *et al.*, Phys. Lett. **B 309** (1993) 451.

[41] L3 Collab., M. Acciarri *et al.*, Z. Phys. **C 62** (1994) 551.

[42] SLAC-LBL Collab., M.L. Perl *et al.*, Phys. Lett. **63B** (1976) 466.

[43] SLAC-LBL Collab., G.J. Feldman *et al.*, Phys. Rev. Lett. **38** (1977) 117.

[44] SLAC-LBL Collab., M.L. Perl *et al.*, Phys. Lett. **70B** (1977) 487.

[45] SLAC-LBL Collab., F.B. Heile *et al.*, Phys. Lett. **B 138** (1978) 189.

[46] SLAC-LBL Collab., J.A. Jaros *et al.*, Phys. Rev. Lett. **40** (1978) 1120.

[47] DELCO Collab., W. Bacino *et al.*, Phys. Rev. Lett. **41** (1978) 13.

[48] MARK II Collab., J.M. Dorfan *et al.*, Phys. Rev. Lett. **46** (1981) 215.

[49] MARK II Collab., C.A. Blocker *et al.*, Phys. Lett. **109 B** (1982) 119.

[50] MARK II Collab., K.G. Hayes *et al.*, Phys. Rev. **D 25** (1982) 2869.

[51] MARK II Collab., C.A. Blocker *et al.*, Phys. Rev. Lett. **48** (1982) 1586.

[52] MARK III Collab., D. Coffman *et al.*, Phys. Rev. **D 36** (1987) 2185.

[53] DASP Collab., R. Brandelik *et al.*, Phys. Lett. **70 B** (1977) 125.

[54] DASP Collab., R. Brandelik *et al.*, Phys. Lett. **73 B** (1978) 109.

[55] DASP Collab., R. Brandelik *et al.*, Z. Phys. **C 1** (1979) 233.

[56] PLUTO Collab., J. Burmester *et al.*, Phys. Lett. **68 B** (1977) 297.

[57] PLUTO Collab., J. Burmester *et al.*, Phys. Lett. **68 B** (1977) 301.

[58] PLUTO Collab., G. Alexander *et al.*, Phys. Lett. **73 B** (1978) 99.

[59] PLUTO Collab., G. Alexander *et al.*, Phys. Lett. **78 B** (1978) 162.

[60] PLUTO Collab., G. Alexander *et al.*, Phys. Lett. **81 B** (1979) 84.

[61] PLUTO Collab., W. Wagner *et al.*, Z. Phys. **C 3** (1980) 193.

[62] DESY-Heidelberg Collab., W. Bartel *et al.*, Phys. Lett. **77 B** (1978) 331.

[63] CLEO Collab., P. Hass *et al.*, Phys. Rev. **D 30** (1984) 1996.

[64] CLEO Collab., S. Behrends *et al.*, Phys. Rev. **D 32** (1985) 2468.

[65] CLEO Collab., C. Bebek *et al.*, Phys. Rev. **D 36** (1987) 690.

[66] CLEO Collab., P. Baringer *et al.*, Phys. Rev. Lett. **59** (1987) 1993.

[67] CLEO Collab., T. Bowcock *et al.*, Phys. Rev. **D 41** (1990) 805.

[68] CLEO Collab., M. Goldberg *et al.*, Phys. Lett. **B 251** (1990) 223.

[69] CLEO Collab., R. Ammar *et al.*, Phys. Rev. **D 45** (1992) 3976.

[70] CLEO Collab., M. Battle *et al.*, Phys. Lett. **B 291** (1992) 488.

[71] CLEO Collab., M. Artuso *et al.*, Phys. Rev. Lett. **69** (1992) 3278.

[72] CLEO Collab., D.S. Akerib *et al.*, Phys. Rev. Lett. **69** (1992) 3610.

[73] CLEO Collab., M. Procario *et al.*, Phys. Rev. Lett. **70** (1993) 1207.

[74] CLEO Collab., A. Bean *et al.*, Phys. Rev. Lett. **70** (1993) 138.

[75] CLEO Collab., R. Balest *et al.*, Phys. Rev. **D 47** (1993) R3671.

[76] CLEO Collab., D. Cinabro *et al.*, Phys. Rev. Lett. **70** (1993) 3700.

[77] CLEO Collab., D. Bortoletto *et al.*, Phys. Rev. Lett. **71** (1993) 1791.

[78] CLEO Collab., M. Artuso *et al.*, Phys. Rev. Lett. **72** (1994) 3762.

[79] CLEO Collab., D. Gibaut *et al.*, Phys. Rev. Lett. **73** (1994) 934.

[80] CLEO Collab., M. Battle *et al.*, Phys. Rev. Lett. **73** (1994) 1079.

[81] CLEO Collab., J. Bartelt *et al.*, Phys. Rev. Lett. **73** (1994) 1890.

[82] G. Eigen, Proceedings of the Third Workshop on Tau Lepton Physics, Montreux, Switzerland 1994, L. Rolandi edt., Nucl. Phys. B (Proc. Suppl.) 40 (1995) 281.

[83] T. Coan, *Measurement of α_s from τ decays*, CLNS preprint CLNS 95/1332, contributed to the EPS-HEP Conference, Brussels, Jul. 27 - Aug. 2, 1995.

[84] BES Collab., J.Z. Bai *et al.*, Phys. Rev. Lett. **69** (1992) 3021.

[85] BES Collab., Chen Hongfang *et al.*, High Energy Phys. and Nucl. Phys. **18** (1993) 135.

[86] BES Collab., *Final Result on the Mass of the τ Lepton from the BES Collaboration*, presented at 27th International Conference on High Energy Physics, Glasgow, 1994, quoted from J.R. Patterson, *Weak and Rare Decays*, Proceedings of the 27th International Conference on High Energy Physics, Glasgow, 1994, P.J. Bussey and I.G. Knowles edt., Inst. of Physics Publishing, p. 149.

[87] N. Qi, BES Collab., *Tau Lepton Experiment at BES Detector*, Proceedings of the Third Workshop on Tau Lepton Physics, Montreux, Switzerland 1994, L. Rolandi edt., Nucl. Phys. B (Proc. Suppl.) 40 (1995) 387.

[88] ARGUS Collab., H. Albrecht *et al.*, Phys. Lett. **163 B** (1985) 404.

[89] ARGUS Collab., H. Albrecht *et al.*, Z. Phys. **C 33** (1986) 7.

[90] ARGUS Collab., H. Albrecht *et al.*, Phys. Lett. **B 185** (1987) 223.

[91] ARGUS Collab., H. Albrecht *et al.*, Phys. Lett. **B 185** (1987) 228.

[92] ARGUS Collab., H. Albrecht *et al.*, Phys. Lett. **B 202** (1988) 149.

[93] ARGUS Collab., H. Albrecht *et al.*, Z. Phys. **C 41** (1988) 1.

[94] ARGUS Collab., H. Albrecht *et al.*, Z. Phys. **C 41** (1988) 405.

[95] ARGUS Collab., H. Albrecht *et al.*, Phys. Lett. **B 246** (1990) 278.

[96] ARGUS Collab., H. Albrecht *et al.*, Phys. Lett. **B 250** (1990) 164.

[97] ARGUS Collab., H. Albrecht *et al.*, Phys. Lett. **B 260** (1991) 259.

[98] ARGUS Collab., H. Albrecht *et al.*, Z. Phys. **C 53** (1992) 367.

[99] ARGUS Collab., H. Albrecht *et al.*, Z. Phys. **C 55** (1992) 179.

[100] ARGUS Collab., H. Albrecht *et al.*, Z. Phys. **C 56** (1992) 339.

[101] ARGUS Collab., H. Albrecht *et al.*, Phys. Lett. **B 292** (1992) 221.

[102] ARGUS Collab., H. Albrecht *et al.*, Phys. Lett. **B 316** (1993) 608.

[103] ARGUS Collab., H. Albrecht *et al.*, Z. Phys. **C 58** (1993) 61.

[104] ARGUS Collab., H. Albrecht *et al.*, Phys. Lett. **B 337** (1994) 383.

[105] ARGUS Collab., H. Albrecht *et al.*, *Determination of the Michel Parameters ξ and δ in Leptonic τ Decays*, DESY preprint DESY 95-011 (1995).

[106] ARGUS Collab., H. Albrecht *et al.*, *Search for Lepton-Flavor Violating τ Decays*, DESY preprint DESY 95-071 (1995).

[107] Crystal Ball Collab., S. Keh *et al.*, Phys. Lett. **B 212** (1988) 123.

[108] Crystal Ball Collab., H. Janssen *et al.*, Phys. Lett. **B 228** (1989) 273.

[109] Crystal Ball Collab., D. Antreasyan *et al.*, Phys. Lett. **B 259** (1991) 216.

[110] CELLO Collab., H.J. Behrend *et al.*, Nucl. Phys. **B 211** (1983) 369.

[111] CELLO Collab., H.J. Behrend *et al.*, Phys. Lett. **127 B** (1983) 270.

[112] CELLO Collab., H.J. Behrend *et al.*, Z. Phys. **C 16** (1983) 301.

[113] CELLO Collab., H.J. Behrend *et al.*, Z. Phys. **C 23** (1984) 103.

[114] CELLO Collab., H.J. Behrend *et al.*, Phys. Lett. **B 200** (1988) 226.

[115] CELLO Collab., H.J. Behrend *et al.*, Z. Phys. **C 46** (1990) 537.

[116] JADE Collab., W. Bartel *et al.*, Z. Phys. **C 31** (1986) 359.

[117] JADE Collab., W. Bartel *et al.*, Phys. Lett. **B 182** (1986) 216.

[118] JADE Collab., C. Kleinwort *et al.*, Z. Phys. **C 42** (1989) 7.

[119] MARK J Collab., D.P. Barber *et al.*, Phys. Lett. **95 B** (1980) 149.

[120] MARK J Collab., D.P. Barber *et al.*, Phys. Rep. **63** (1980) 339.

[121] TASSO Collab., M. Althof *et al.*, Phys. Lett. **141 B** (1984) 264.

[122] TASSO Collab., W. Braunschweig *et al.*, Z. Phys. **C 39** (1988) 331.

[123] DELCO Collab., G.B. Mills *et al.*, Phys. Rev. Lett. **52** (1984) 1944.

[124] DELCO Collab., G.B. Mills *et al.*, Phys. Rev. Lett. **54** (1985) 624.

[125] DELCO Collab., W. Ruckstuhl *et al.*, Phys. Rev. Lett. **56** (1986) 2132.

[126] MAC Collab., E. Fernandez *et al.*, Phys. Rev. Lett. **54** (1985) 1624.

[127] MAC Collab., W.W. Ash *et al.*, Phys. Rev. Lett. **55** (1985) 2118.

[128] MAC Collab., W.T. Ford *et al.*, Phys. Rev. **D 35** (1987) 408.

[129] MAC Collab., H.R. Band *et al.*, Phys. Rev. Lett. **59** (1987) 415.

[130] MAC Collab., W.T. Ford *et al.*, Phys. Rev. **D 36** (1987) 1971.

[131] MAC Collab., H.R. Band *et al.*, Phys. Lett. **B 198** (1987) 297.

[132] MARK II Collab., G.J. Feldman *et al.*, Phys. Rev. Lett. **48** (1982) 66.

[133] MARK II Collab., C.A. Blocker *et al.*, Phys. Rev. Lett. **49** (1982) 1369.

[134] MARK II Collab., J.A. Jaros *et al.*, Phys. Rev. Lett. **51** (1983) 955.

[135] MARK II Collab., C. Matteuzzi *et al.*, Phys. Rev. Lett. **52** (1984) 1869.

[136] MARK II Collab., P.R. Burchat *et al.*, Phys. Rev. Lett. **54** (1985) 2489.

[137] MARK II Collab., C. Matteuzzi *et al.*, Phys. Rev. **D 32** (1985) 800.

[138] MARK II Collab., J.M. Yelton *et al.*, Phys. Rev. Lett. **56** (1986) 812.

[139] MARK II Collab., W.B. Schmidke *et al.*, Phys. Rev. Lett. **57** (1986) 527.

[140] MARK II Collab., P.R. Burchat *et al.*, Phys. Rev. **D 35** (1987) 27.

[141] MARK II Collab., K.K. Gan *et al.*, Phys. Rev. Lett. **59** (1987) 411.

[142] MARK II Collab., K.K. Gan *et al.*, Phys. Lett. **B 197** (1987) 561.

[143] MARK II Collab., D. Amidei *et al.*, Phys. Rev. **D 37** (1988) 1750.

[144] MARK II Collab., D.Y. Wu *et al.*, Phys. Rev. **D 41** (1990) 2339.

[145] MARK II Collab., J.J. Gomez-Cardenas *et al.*, Phys. Rev. Lett. **66** (1991) 1007.

[146] HRS Collab., I. Beltrami *et al.*, Phys. Rev. Lett. **54** (1985) 1775.

[147] HRS Collab., C. Akerlof *et al.*, Phys. Rev. Lett. **55** (1985) 570.

[148] HRS Collab., S. Abachi *et al.*, Phys. Rev. Lett. **56** (1986) 1039.

[149] HRS Collab., B.G. Bylsma *et al.*, Phys. Rev. **D 35** (1987) 2269.

[150] HRS Collab., M. Derrick *et al.*, Phys. Lett. **B 189** (1987) 260.

[151] HRS Collab., S. Abachi *et al.*, Phys. Lett. **B 197** (1987) 291.

[152] HRS Collab., S. Abachi *et al.*, Phys. Rev. Lett. **59** (1987) 2519.

[153] HRS Collab., R. Tschirhart *et al.*, Phys. Lett. **B 205** (1988) 407.

[154] HRS Collab., K. Sugano *et al.*, Nucl. Phys. **A 478** (1988) 729c.

[155] HRS Collab., S. Abachi *et al.*, Phys. Lett. **B 226** (1989) 405.

[156] HRS Collab., S. Abachi *et al.*, Phys. Rev. **D 41** (1989) 1414.

[157] TPC Collab., H. Aihara *et al.*, Phys. Rev. **D 30** (1984) 2436.

[158] TPC Collab., H. Aihara *et al.*, Phys. Rev. Lett. **57** (1986) 1836.

[159] TPC Collab., H. Aihara *et al.*, Phys. Rev. **D 35** (1987) 1553.

[160] TPC Collab., H. Aihara *et al.*, Phys. Rev. Lett. **59** (1987) 751.

[161] TPC Collab., D.A. Bauer *et al.*, Phys. Rev. **D 50** (1994) 13.

[162] DELPHI Collab., P. Abreu *et al.*, Nucl. Phys. **B 417** (1994) 3.

[163] ALEPH Collab., D.Decamp *et al.*, Phys. Lett. **B 231** (1989) 519.

[164] ALEPH Collab., D. Decamp *et al.*, Phys. Lett. **B 234** (1990) 399.

[165] ALEPH Collab., D. Decamp *et al.*, Phys. Lett. **B 235** (1990) 399.

[166] ALEPH Collab., D. Decamp *et al.*, Z. Phys. **C 48** (1990) 365.

[167] ALEPH Collab., D. Decamp *et al.*, Phys. Lett. **B 263** (1991) 112.

[168] ALEPH Collab., D. Decamp *et al.*, Phys. Lett. **B 265** (1991) 430.

[169] ALEPH Collab., D. Decamp *et al.*, Z. Phys. **C 53** (1992) 1.

[170] ALEPH Collab., D. Decamp *et al.*, Z. Phys. **C 54** (1992) 211.

[171] ALEPH Collab., D. Decamp *et al.*, Phys. Lett. **B 279** (1992) 411.

[172] ALEPH Collab., D. Buskulic *et al.*, Phys. Lett. **B 297** (1992) 432.

[173] ALEPH Collab., D. Buskulic *et al.*, Phys. Lett. **B 297** (1992) 459.

[174] ALEPH Collab., D. Decamp *et al.*, Phys. Rep. **216** (1992) 253.

[175] ALEPH Collab., D. Buskulic *et al.*, Phys. Lett. **B 307** (1993) 209.

[176] ALEPH Collab., D. Buskulic *et al.*, Z. Phys. **C 59** (1993) 215.

[177] ALEPH Collab., D. Buskulic *et al.*, Z. Phys. **C 59** (1993) 369.

[178] ALEPH Collab., D. Buskulic *et al.*, Z. Phys. **C 60** (1993) 71.

[179] ALEPH Collab., D. Buskulic *et al.*, Phys. Lett. **B 308** (1993) 425.

[180] ALEPH Collab., D. Buskulic *et al.*, Z. Phys. **C 62** (1994) 539.

[181] ALEPH Collab., D. Buskulic *et al.*, Phys. Lett. **B 321** (1994) 168.

[182] ALEPH Collab., D. Buskulic *et al.*, Phys. Lett. **B 332** (1994) 209.

[183] ALEPH Collab., D. Buskulic *et al.*, Phys. Lett. **B 332** (1994) 219.

[184] ALEPH Collab., F. Cerutti *et al.*, Proceedings of the Third Workshop on Tau Lepton Physics, Montreux, Switzerland 1994, L. Rolandi edt., Nucl. Phys. B (Proc. Suppl.) 40 (1995) 71.

[185] ALEPH Collab., D. Buskulic *et al.*, Phys. Lett. **B 346** (1995) 371.

[186] ALEPH Collab., D. Buskulic *et al.*, Phys. Lett. **B 346** (1994) 379.

[187] ALEPH Collab., D. Buskulic *et al.*, *Improved Tau Polarization Measurement*, CERN preprint CERN-PPE/95-023, submitted to Z. Phys.

[188] ALEPH Collab., D.Buskulic *et al.*, *An upper limit for the τ neutrino mass from $\tau \to 5\pi(\pi^0)\nu_\tau$ decays*, CERN preprint CERN-PPE/95-03, submitted to Phys. Lett. B.

[189] DELPHI Collab., P. Aarnio *et al.*, Phys. Lett. **B 231** (1989) 539.

[190] DELPHI Collab., P. Aarnio *et al.*, Phys. Lett. **B 241** (1990) 425.

[191] DELPHI Collab., P. Abreu *et al.*, Nucl. Phys. **B 367** (1991) 511.

[192] DELPHI Collab., P. Abreu *et al.*, Phys. Lett. **B 267** (1991) 422.

[193] DELPHI Collab., P. Abreu *et al.*, Z. Phys. **C 55** (1992) 555.

[194] DELPHI Collab., P. Abreu *et al.*, Phys. Lett. **B 298** (1993) 247.

[195] DELPHI Collab., P. Abreu *et al.*, Nucl. Phys. **B 403** (1993) 3.

[196] DELPHI Collab., P. Abreu *et al.*, Phys. Lett. **B 302** (1993) 356.

[197] DELPHI Collab., P. Abreu *et al.*, Nucl. Phys. **B 418** (1994) 403.

[198] DELPHI Collab., P. Abreu *et al.*, Phys. Lett. **B 334** (1994) 435.

[199] DELPHI Collab., P. Abreu *et al.*, Z. Phys. **C 67** (1995) 183.

[200] DELPHI Collab., P. Abreu *et al.*, *A Measurement of the τ Leptonic Branching Fractions*, CERN preprint CERN-PPE/95-114, submitted to Phys. Lett. B.

[201] DELPHI Collab., M.C. Chen *et al.*, *Test of CP-violation in $e^+e^- \to Z \to \tau^+\tau^-$*, DELPHI 95-113 PHYS 548, submitted to the EPS-HEP Conference, Brussels, Jul. 27 - Aug. 2, 1995.

[202] DELPHI Collab., L. Brugge *et al.*, *Search for Lepton Flavor Number Violating Z Decays*, DELPHI 95-72 PHYS 507, submitted to the EPS-HEP Conference, Brussels, Jul. 27 - Aug. 2, 1995.

[203] L3 Collab., B. Adeva *et al.*, Phys. Lett. **B 231** (1989) 509.

[204] L3 Collab., B. Adeva *et al.*, Phys. Lett. **B 250** (1990) 205.

[205] L3 Collab., B. Adeva *et al.*, Phys. Lett. **B 265** (1991) 451.

[206] L3 Collab., B. Adeva *et al.*, Phys. Lett. **B 271** (1991) 453.

[207] L3 Collab., O. Adriani *et al.*, Phys. Lett. **B 294** (1992) 466.

[208] L3 Collab., O. Adriani *et al.*, Phys. Lett. **B 295** (1992) 337.

[209] L3 Collab., O. Adriani *et al.*, Phys. Rep. **236** (1993) 1.

[210] L3 Collab., O. Adriani *et al.*, Phys. Lett. **B 316** (1993) 427.

[211] L3 Collab., M. Acciarri *et al.*, Phys. Lett. **B 341** (1994) 245.

[212] L3 Collab., M. Acciarri *et al.*, Phys. Lett. **B 345** (1994) 93.

[213] L3 Collab., M. Acciarri *et al.*, Phys. Lett. **B 346** (1994) 190.

[214] L3 Collab., M. Acciarri *et al.*, *A Measurement of the Michel Parameters and the Chirality Parameter in* $e^+e^- \to \tau^+\tau^-$ *with the L3 Detector at LEP*, paper submitted to the EPS-HEP Conference, Brussels, Jul. 27 - Aug. 2, 1995.

[215] L3 Collab., M. Acciarri *et al.*, *A Preliminary Measurement of* A_τ *and* A_e *using 1994 Data*, paper submitted to the EPS-HEP Conference, Brussels, Jul. 27 - Aug. 2, 1995.

[216] L3 Collab., M. Acciarri *et al.*, *Search for Lepton Flavor Violation in Z Decays*, L3 Note 1798 (1995), submitted to the EPS-HEP Conference, Brussels, Jul. 27 - Aug. 2, 1995.

[217] OPAL Collab., M.Z. Akrawy *et al.*, Phys. Lett. **B 231** (1989) 530.

[218] OPAL Collab., M.Z. Akrawy *et al.*, Phys. Lett. **B 235** (1990) 379.

[219] OPAL Collab., M.Z. Akrawy *et al.*, Phys. Lett. **B 244** (1990) 135.

[220] OPAL Collab., M.Z. Akrawy *et al.*, Phys. Lett. **B 254** (1991) 203.

[221] OPAL Collab., G. Alexander *et al.*, Z. Phys. **C 52** (1991) 175.

[222] OPAL Collab., G. Alexander *et al.*, Phys. Lett. **B 266** (1991) 201.

[223] OPAL Collab., P.D. Acton *et al.*, Phys. Lett. **B 273** (1991) 355.

[224] OPAL Collab., P.D. Acton *et al.*, Phys. Lett. **B 273** (1991) 338.

[225] OPAL Collab., P.D. Acton *et al.*, Phys. Lett. **B 281** (1992) 405.

[226] OPAL Collab., P.D. Acton *et al.*, Phys. Lett. **B 287** (1992) 389.

[227] OPAL Collab., P.D. Acton *et al.*, Phys. Lett. **B 288** (1992) 373.

[228] OPAL Collab., P.D. Acton *et al.*, Phys. Lett. **B 311** (1993) 291.

[229] OPAL Collab., P.D. Acton *et al.*, Z. Phys. **C 58** (1993) 219.

[230] OPAL Collab., P.D. Acton *et al.*, Z. Phys. **C 59** (1993) 183.

[231] OPAL Collab., R. Akers *et al.*, Z. Phys. **C 60** (1993) 593.

[232] OPAL Collab., R. Akers *et al.*, Z. Phys. **C 61** (1994) 19.

[233] OPAL Collab., R. Akers *et al.*, Phys. Lett. **B 328** (1994) 207.

[234] OPAL Collab., R. Akers *et al.*, Z. Phys. **C 65** (1995) 183.

[235] OPAL Collab., R. Akers *et al.*, Z. Phys. **C 65** (1995) 1.

[236] OPAL Collab., R. Akers *et al.*, Phys. Lett. **B 338** (1994) 497.

[237] OPAL Collab., R. Akers *et al.*, Z. Phys. **C 66** (1995) 31.

[238] OPAL Collab., R. Akers *et al.*, Phys. Lett. **B 339** (1994) 278.

[239] OPAL Collab., R. Akers *et al.*, Z. Phys. **C 66** (1995) 543.

[240] OPAL Collab., R. Akers *et al.*, *A Search for Lepton Flavour Violating Z Decays*, CERN-PPE/95-43, submitted to Z. Phys.

[241] OPAL Collab., R. Akers *et al.*, *A Study of QCD Structure Constants and a Measurement of $\alpha_s(m_Z)$ at LEP using Event Shape Observables* , CERN-PPE/95-69, submitted to Z. Phys.

[242] OPAL Collab., R. Akers *et al.*, Z. Phys. **C 67** (1995) 45.

[243] OPAL Collab., R. Akers *et al.*, *Measurement of the Mass of the Tau Z Neutrino from $\tau \to 3\pi\nu_\tau$ Decays*, OPAL internal note PN193 (1994), contributed to the EPS-HEP Conference, Brussels, July 27 - August 2, 1995.

[244] OPAL Collab., R. Akers *et al.*, *Updated Measurement of the Tau Polarization Asymmetries*, OPAL internal note PN172 (1994), contributed to the EPS-HEP Conference, Brussels, July 27 - August 2, 1995.

[245] MARK II Collab., G.S. Abrams *et al.*, Phys. Rev. Lett. **63** (1989) 2780.

[246] MARK II Collab., G.S. Abrams *et al.*, Phys. Rev. Lett. **63** (1989) 2173.

[247] SLD Collab., K. Abe *et al.*, Phys. Rev. Lett. **73** (1994) 25.

[248] SLD Collab., K. Abe *et al.*, *Measurement of the Tau Lifetime at SLD*, SLAC preprint SLAC-PUB-95-6767 (1995), submitted to Phys. Rev. D.

[249] A.A. Zholentz *et al.*, Phys. Rev. Lett. **B 96** (1980) 214.

[250] A.A. Zholentz *et al.*, Sov. J. Nucl. Phys. **34** (1981) 814.

[251] M. Pohl, *τ Decay Results from LEP*, Proceedings of the 4th International Symposium on Heavy Flavor Physics, Orsay, France 1991, M. Davier and G. Wormser edt., Edition Frontieres, 1992, p. 331.

[252] Particle Data Group, L. Montanet *et al.*, Phys. Rev. **D 50** (1994) 1173.

[253] E.A. Kuraev and V.S. Fadin, Sov. J. Nucl. Phys. **41** (1984) 466.

[254] M.B. Voloshin, *Topics in Tau Physics at a Tau-Charm Factory*, University of Minnesota preprint TPI-MINN-89/33-T, unpublished.

[255] J. Timmermans, *Measurements of the τ Mass, Lifetime and Leptonic Branching Ratio*, presented at 27th International Conference on High Energy Physics, Glasgow, 1994, Proceedings of the 27th International Conference on High Energy Physics, Glasgow, 1994, P.J. Bussey and I.G. Knowles edt., Inst. of Physics Publishing, p. 1077.

[256] The LEP Collaborations ALEPH, DELPHI, L3, OPAL and the LEP Electroweak Working Group, *Combined Preliminary Data on Z Parameters from the LEP Experiments and Constraints on the Standard Model*, CERN Preprint CERN-PPE/94-187.

[257] E.W. Kolb and M.S. Turner, *The Early Universe* (Addison-Wesley, Redwood City, CA,1990), Chap. 5;
G.G.Raffelt, Phys. Rev. 198 (1990) 1;
S.Buldman, Phys. Rev. D45(1992);
J.Bahcall, *Neutrino Astrophysics* (Cambridge University Press,Cambridge, CB2 1RP).

[258] A.B. McDonald, *Neutrino Astronomy*, Proceedings of XXIII International Cosmic Ray Conference, Calgary, Alberta, Canada,19-30 July 1993, ed. World Scientific, Singapore, p. 115.

[259] D.R. Morrison, *Brief review of theory and experiments on the solar neutrino problem*, CERN-PPE/93-196, presented at the XXII Int. Symposium on Multiparticle Dynamics, Aspen, USA, 12-17 September 1993 and 3rd Nestor Workshop, Pylos, Greece, 19-21 October 1993.

[260] T. Gaisser and M. Goodman, *Neutrino oscillations experiments with atmospheric neutrinos*, Argonne Nat. Lab. preprint ANL-HEP-C-94-72.

[261] H.T.Wong, *Neutrino Oscillation experiments: Perspective and Prospects*, Proceeding of Les Rencontres de Physique de la Vallee d'Aoste, La Thuile, Aosta, March 6-14, 1994, Editions Frontiers, p. 77.

[262] P.Langacker et al., Nucl. Phys. B282 (1987) 589.

[263] H. Harari, Phys. Lett. **B 216** (1989) 413.

[264] G. Gyuk and M.S. Turner, Proceedings of the Third Workshop on Tau Lepton Physics, Montreux, Switzerland 1994, L. Rolandi edt., Nucl. Phys. B (Proc. Suppl.) 40 (1995) 557.

[265] G.F. Giudice, Phys. Lett. **B 251** (1990) 460.

[266] B. Pontecorvo, Zh. Eksp. Theor. Fiz. **33** (1957) 549.

[267] B. Pontecorvo, Zh. Eksp. Theor. Fiz. **34** (1958) 247.

[268] B. Pontecorvo, Zh. Eksp. Theor. Fiz. **53** (1967) 1717.

[269] C.Rubbia, *Renaissance of Experimental Neutrino Physics*, CERN preprint CERN-PPE/93-08, presented at Conversaciones de Madrid El Escorial, Madrid, Spain, September 5, 1992.

[270] P.Langacker and M.X.Luo, Phys. Rev. D44 (1991) 817.

[271] T. Yaganida, Prog.Theor. Phys. B135 (1978) 66.

[272] M. Gell-Mann, P. Ramond and R. Slansky, in Supergravity, eds. P.van Niewwenhuizen and D. Freedman (North Holland, Amsterdam 1979), p.315.

[273] H. Harari, *Intrinsic ν_τ properties*, presented at Third Workshop on Tau Lepton Physics, Montreux, Switzerland,19-22 September 1994, unpublished.

[274] R.Stroynowski, Proceedings of the Third Workshop on Tau Lepton Physics, Montreux, Switzerland 1994, L. Rolandi edt., Nucl. Phys. B (Proc. Suppl.) 40 (1995) 569.

[275] T. Kirsten, *Solar Neutrino Data*, Proceeding of Les Rencontres de Physique de la Vallee d'Aoste, La Thuile, Aosta, March 6-14, 1994, Editions Frontiers, p. 3.

[276] D.O. Caldwell, Nucl. Phys. B (Proc. Suppl.) **43** (1995) 126.

[277] R. Davis *et al.*, Proceedings of the XXIII International Cosmic Ray Conference, Calgary, Alberta, Canada, 19-30 July 1993, ed. World Scientific, Singapore.

[278] R. Davis, *The Status and Future of Solar Neutrino Reserach*, Brookhaven Nat. Lab. preprint BNL50879 (1978).

[279] SAGE Collab., *First results from Soviet-American Gallium Experiment*, Neutrino '90, Proceedings of 14th International Conference on Neutrino Physics and Astrophysics, CERN, Geneva, Switzerland, 10-15 June 1990, Nucl. Phys. B (Proc.Supl.) 19 (1991) 84.

[280] SAGE Collab., V.Garvint et al., *Latest results from Soviet-American Gallium Experiment*, Proceedings of XXVI International Conference on High Energy Physics, Dallas, 1992, Vol 1 p. 1101.

[281] O.L. Anosov *et al.*, Annals of the New York Academy of Science, 688 (1993) 598.

[282] T. Kirsten, *The Gallex Project of Solar Neutrino Detection*, in Advances in Nuclear Astrophysics, Editions Frontieres, 1986, p. 85.

[283] GALLEX Collab., P. Anselmann *et al.*, Phys. Rev. Lett. **B 285** (1992) 376.

[284] GALLEX Collab., P. Anselmann *et al.*, Phys. Rev. Lett. **B 285** (1992) 390.

[285] GALLEX Collab., P. Anselmann *et al.*, Phys. Lett. **B 314** (1993) 445.

[286] GALLEX Collab., P. Anselmann *et al.*, Phys. Lett. **B 327** (1994) 337.

[287] Kamiokande Collab., K.S. Hirata *et al.*, Phys. Rev. Lett. **65** (1990) 1297.

[288] Kamiokande Collab., K.S. Hirata *et al.*, Phys. Rev. **D 44** (1991) 2241.

[289] Kamiokande Collab., S.Kaneyuki, Proceedings of the Moriond Conference (1993).

[290] J.N. Bahcall and R.K Ulrich, Rev. Mod. Phys. **60** (1988) 297.

[291] J.N.Bahcall, Nucl.Phys.Proc.Supp., **B19** (1990) 94.

[292] J.N. Bahcall and R.K Ulrich, Rev. Mod. Phys. **64** (1992) 885.

[293] S.Turck-Chieze *et al.*,Astrophys.J. **335** (1988) 415.

[294] F. Beines *et al.*, Phys. Rev. Lett. **32** (1974) 180.

[295] S.A. Bludman, Phys. Rev. **D 45** (1992) 4720.

[296] L.Wolfenstein, Phys. Rev. **D17** (1978) 2369 and Phys. Rev. **D20** (1979) 2634; S.P. Mikheyev and A.Yu. Smirnov, Yad.Fiz. **44** (1985) 847 [Sov.J.Nucl.Phys. **42** (1985) 913].

[297] CDF Collab., F. Abe *et al.*, Phys. Rev. Lett. **73** (1994) 225.

[298] CDF Collab., F. Abe *et al.*, Phys. Rev. **D50** (1994) 2966.

[299] G. Ewan Nucl. Inst. Meth. **A314** (1992) 373; Phys in Canada **48** (1992) 112.

[300] M.Takita, Proceedings of the International Symposium on Neutrino Astrophysics, Takayama/Kamioka, Japan (1992), Tokyo, Universal Academy Press.

[301] J.P. Revol, Proceedings of International Symposium on Neutrino Astrophysics, Takayama/Kamioka, Japan (1992), Tokyo, Universal Academy Press.

[302] *BOREXINO at Gran Sasso, Proposal for a Real Time Detector for Low Energy Solar Neutrinos*, G. Bellini, M. Campanella, D. Guigni and R. Raghvan edts., August 1991.

[303] G. Barr, T.K. Gaisser and T. Stanev, Phys. Rev. **D39** (1989) 3532.

[304] T.K. Gaisser, Nucl. Phys. **B31 (Proc.Suppl.)** (1993) 399.

[305] Y. Fukuda *et al.*, Phys. Lett. **B335** (1994) 237.

[306] D. Casper *et al.*, Phys. Rev. Lett. **66** (1991) 2561.

[307] Kamiokande Collab., Y. Fukuda *et al.*, Phys. Lett. **B 335** (1994) 237.

[308] M. O. Goodman, *The atmospheric neutrino anomaly in Soudan 2*, Argonne Nat. Lab. preprint ANL-HEP-FR-94-56 (1994).

[309] Ch. Berger *et al.*, Phys. Lett. **B227** (1989) 489.

[310] Ch. Berger *et al.*, Phys. Lett. **B245** (1990) 305.

[311] NUSEX Collab., M. Aglietta *et al.*, Europhys. Lett. **8** (1989) 611.

[312] E.W. Beier and E.D. Frank, Proceedings of Royal Society Conference on Neutrino Astrophysics, London, 1993.

[313] BEBC Collab., O. Enriquez *et al.*, Phys. Lett. **102B** (1981) 73.

[314] BEBC WA66 Collab., H. Talebzadeh *et al.*, Nucl. Phys. **B291** (1987) 503.

[315] CCFR Collab., I.E. Stockale *et al.*, Z. Phys. **C 27** (1985) 53.

[316] CDHS Collab., F. Dydak *et al.*, Phys. Lett. **B134** (1984) 281.

[317] CHARM Collab., F. Begsam *et al.*, Phys. Lett. **B142** (1984) 103.

[318] CHARM II Collab., M. Gruwé *et al.*, Phys. Lett. **B 309** (1993) 463.

[319] E531 Collab., N. Ushida *et al.*, Phys. Rev. Lett. **57** (1986) 2897.

[320] CHORUS Collab., *A New Search For* $\nu_\mu \rightarrow \nu_\tau$ *Oscillations*, CERN-PPE/93-131.

[321] G. Rosa, Proceedings of the Third Workshop on Tau Lepton Physics, Montreux, Switzerland 1994, L. Rolandi edt., Nucl. Phys. B (Proc. Suppl.) 40 (1995) 85.

[322] NOMAD Collab., *Proposal to search for* $\nu_\mu \rightarrow \nu_\tau$, CERN-SPSLC/91-21, CERN-SPSLC/91-48, SPSC/P261 (1991).

[323] A. Rubbia, Proceedings of the Third Workshop on Tau Lepton Physics, Montreux, Switzerland 1994, L. Rolandi edt., Nucl. Phys. B (Proc. Suppl.) 40 (1995) 93.

[324] E803 Collab., *Muon neutrino to tau neutrino oscillations experiment E803 at Fermilab*, Proposal P-803, Fermilab, October 1990.

[325] N.W.Reay, ν_τ *at Fermilab*, presented at Third Workshop on Tau Lepton Physics, Montreux, Switzerland, 19-22 September 1994, unpublished.

[326] E822 Collab., *Progress report and revised E822 Proposal for Long Baseline Neutrino Oscillation Experiment from Fermilab to SOUDAN*, Fermilab, October 1993.

[327] E889 Collab., *Proposal for Long Baseline Neutrino Oscillation Experiment at AGS E-829*, Proposal Brookhaven Nat. Lab., BNL-Proposal-889 (1993).

[328] L.Cammilleri, *Neutrino oscillation experiments at accelerators*, CERN-PPE/94-87, talk given at 6th International Workshop on Neutrino Telescopes, Venice, Italy, 22-24 February 1994.

[329] E872 Collab., *Measurement of* τ *lepton production from process* $\nu_\tau + N \rightarrow \tau$, Fermilab Proposal P-872, 1994.

[330] R. Escribano and E. Masso, Phys. Lett. **B 301** (1993) 419.

[331] R. Escribano and E. Masso, Nucl. Phys. **B 429** (1994) 19.

[332] F. de Aguila and M. Sher, Phys. Lett. **B 252** (1990) 116.

[333] G. Couture, Phys. Lett. **B 272** (1991) 404.

[334] M.A. Samuel, L. Guowen and R. Mendel, Phys. Rev. Lett. **67** (1991) 669.

[335] D.J. Silverman and G.L. Shaw, Phys. Rev. Lett. **D 27** (1983) 1196.

[336] J.A. Grifols and A. Mendez, Phys. Lett. **B 255** (1989) 611.

[337] L. Vuillemier, University of Lausanne Thesis, 1994, unpublished.

[338] G. Domokos *et al.*, Phys. Rev. **D 32** (1985) 247.

[339] J. Bernabeu *et al.*, FTUC preprint **FTUC/94-43** (1994) 1.

[340] W.J. Marciano, Proceedings of the Third Workshop on Tau Lepton Physics, Montreux, Switzerland 1994, L. Rolandi edt., Nucl. Phys. B (Proc. Suppl.) 40 (1995) 3.

[341] A.V. Kyuldjiev, Nucl. Phys. **B 243** (1984) 387.

[342] M.B. Voloshin, M.I. Vysotsky and L.B. Okun, Sov. J. Nucl. Phys. **44** (1988) 440.

[343] G.G. Raffelt, Phys. Rep. **198** (1990) 460.

[344] A.M. Cooper *et al.*, Phys. Lett. **B 80** (1992) 153.

[345] N.G. Deshpande and K.V.L. Sarma, Phys. Rev. **D 43** (1991) 943.

[346] H. Grotch and R.W. Robinett, Z. Phys. **C 39** (1988) 553.

[347] T.M.Gould and I.Z. Rothstein, Phys. Lett. **B 333** (1994) 545.

[348] F. Behrends *et al.*, *Z Lineshape* in *Z Physics at LEP 1*, G. Altarelli, R. Kleiss and C. Verzegnassi edt., CERN Yellow Report CERN/89-08 (1989), Vol. 1, p. 89.

[349] M. Bohm *et al.*, *Forward-Backward Asymmetries* in *Z Physics at LEP 1*, G. Altarelli, R. Kleiss and C. Verzegnassi edt., CERN Yellow Report CERN/89-08 (1989), Vol. 1, p. 203.

[350] M. Consoli *et al.*, *Electroweak Radiative Corrections for Z Physics* in *Z Physics at LEP 1*, G. Altarelli, R. Kleiss and C. Verzegnassi edt., CERN Yellow Report CERN/89-08 (1989), Vol. 1, p. 7.

[351] S. Jadach *et al.*, *The Tau Polarization Measurement* in *Z Physics at LEP 1*, G. Altarelli, R. Kleiss and C. Verzegnassi edt., CERN Yellow Report CERN/89-08 (1989), Vol. 1, p. 235 and erratum.

[352] F. Jegerlehner, *Physics of Precision Experiments with Z's*, Prog. Part. Nucl. Phys. 27 (1991) 1.

[353] A. Litke, Harvard University PhD Thesis (1979) unpublished.

[354] B. Naroska, Phys. Rep. **148** (1987) 67.

[355] F. Dydak, CERN Preprint CERN-EP/86-121, Proceedings of the 1985 Les Houches Summer School (1985), p. 127.

[356] J. Mnich, *Test der elektroschwachen Wechselwirkung in* $e^+e^- \to \mu^+\mu^-$, PhD Thesis RWTH Aachen, PITHA 87/19 (1987).

[357] J. Mnich, *Experimental Tests of the Standard Model in* $e^+e^- \to f\bar{f}$ *at the Z Resonance*, Habilitation Thesis, RWTH Aachen (1995), to be published in Phys. Rep.

[358] M. Gruenewald, *Tau Physics at LEP*, Humbold University Berlin preprint HUB-IEP-95/13 (1995), submitted to Physica Scripta.

[359] D. Bardin *et al.*, Z. Phys. **C 44** (1989) 493.

[360] D. Bardin *et al.*, Nucl. Phys. **B 351** (1991) 1.

[361] D. Bardin *et al.*, Phys. Lett. **B 255** (1991) 290.

[362] The LEP Electroweak Working Group, *A Combination of Preliminary LEP Electroweak Results for the 1995 Summer Conferences*, Internal Note LEPEWWG/95-02 (1995).

[363] K. Hagiwara, A.D. Martin and D. Zeppenfeld, Phys. Lett. **B 235** (1990) 198.

[364] A. Rougé, Z. Phys. **C 48** (1990) 75.

[365] M. Davier *et al.*, Phys. Lett. **B 306** (1993) 411.

[366] D0 Collab., B. Klima, *Top Physics in D0*, Talk given at the 17^{th} International Symposium on Lepton Photon Interactions, Beijing, China 1995.

[367] CDF Collab., W.M. Yao, *Observation of Top Quark Production at the Tevatron*, Talk given at the 17^{th} International Symposium on Lepton Photon Interactions, Beijing, China 1995.

[368] J.D. Richman and P.R. Burchat, *Leptonic and Semileptonic Decays of Charm and Bottom Hadrons*, University of California preprint USCB-HEP-95-08 and Standford-HEP-95-01, to be published in Rev. Mod. Phys.

[369] W. Lerche *et al.*, Phys. Lett. **78 B** (1978) 510.

[370] W. Marciano and A. Sirlin, Phys. Rev. Lett. **61** (1988) 1815.

[371] Particle Data Group, M. Aguilar-Benitez *et al.*, Phys. Lett. **B 239** (1990) 1.

[372] C.G. White, Proceedings of the Third Workshop on Tau Lepton Physics, Montreux, Switzerland 1994, L. Rolandi edt., Nucl. Phys. B (Proc. Suppl.) 40 (1995) 311.

[373] F. Stichelbaut, *Tau Lifetime Measurements at LEP and SLC*, EPS-HEP Conference, Brussels, Jul. 27 - Aug. 2, 1995.

[374] C.E.K. Charlesworth, Proceedings of the Third Workshop on Tau Lepton Physics, Montreux, Switzerland 1994, L. Rolandi edt., Nucl. Phys. B (Proc. Suppl.) 40 (1995) 341.

[375] G. Rahal-Callot, *Tau Lepton Physics*, invited talk given at the EPS-HEP Conference, Brussels, Jul. 27 - Aug. 2, 1995.

[376] I. Ferrante, Proceedings of the Third Workshop on Tau Lepton Physics, Montreux, Switzerland 1994, L. Rolandi edt., Nucl. Phys. B (Proc. Suppl.) 40 (1995) 299.

[377] A. Andreazza, Proceedings of the Third Workshop on Tau Lepton Physics, Montreux, Switzerland 1994, L. Rolandi edt., Nucl. Phys. B (Proc. Suppl.) 40 (1995) 321.

[378] M. Biasini, Proceedings of the Third Workshop on Tau Lepton Physics, Montreux, Switzerland 1994, L. Rolandi edt., Nucl. Phys. B (Proc. Suppl.) 40 (1995) 331.

[379] P. Tsai and A.C. Hearn, Phys. Rev. **140** (1965) 721.

[380] J.H. Kuehn and F. Wagner, Nucl. Phys. **B 236** (1984) 16.

[381] J.H. Kuehn, Phys. Lett. **B 313** (1993) 458.

[382] M. Davier, Proceedings of the Third Workshop on Tau Lepton Physics, Montreux, Switzerland 1994, L. Rolandi edt., Nucl. Phys. B (Proc. Suppl.) 40 (1995) 395.

[383] M. Dam, Proceedings of the Third Workshop on Tau Lepton Physics, Montreux, Switzerland 1994, L. Rolandi edt., Nucl. Phys. B (Proc. Suppl.) 40 (1995) 227.

[384] J. Alcaraz, Proceedings of the Third Workshop on Tau Lepton Physics, Montreux, Switzerland 1994, L. Rolandi edt., Nucl. Phys. B (Proc. Suppl.) 40 (1995) 237.

[385] P. Watkins, Proceedings of the Third Workshop on Tau Lepton Physics, Montreux, Switzerland 1994, L. Rolandi edt., Nucl. Phys. B (Proc. Suppl.) 40 (1995) 247.

[386] D.I. Britton *et al.*, Phys. Rev. Lett. **68** (1992) 3000.

[387] C. Czapak *et al.*, Phys. Rev. Lett. **70** (1993) 17.

[388] T. Numao *et al.*, Mod. Phys. Lett. **A7** (1992) 3357.

[389] S. Jadach, B.F.L. Ward and Z. Was, *The Monte Carlo Program KORALZ*, CERN preprint CERN-TH/5994/91 (1991); Comp. Phys. Comm. 66 (1991) 276.

[390] W. Fetscher, H.-J. Gerber and K.F. Johnson, Phys. Lett. **B 173** (1986) 102.

[391] W. Fetscher, Phys. Rev. **D 42** (1990) 1544.

[392] L. Michel, Proc. Phys. Soc. **A 63** (1950) 514.

[393] A. Stahl, Phys. Lett. **B 324** (1994) 121.

[394] H. Thurn, *New Measurements of Michel Parameters and Neutrino Helicity in τ Decays*, talk given at EPS-HEP Conference, Brussels, Jul. 27 - Aug. 2, 1995.

[395] J.H. Kuehn and E. Mirkes, Z. Phys. **C 56** (1992) 661.

[396] J.H. Kuehn and E. Mirkes, Proceedings of the Third Workshop on Tau Lepton Physics, Montreux, Switzerland 1994, L. Rolandi edt., Nucl. Phys. B (Proc. Suppl.) 40 (1995) 181.

[397] R. Decker and M. Finkemeier, Phys. Rev. **D 48** (1993) 4203.

[398] R. Decker and M. Finkemeier, Phys. Lett. **B 316** (1993) 403.

[399] R. Decker and M. Finkemeier, Phys. Lett. **B 334** (1994) 199.

[400] B.K. Heltsley, Proceedings of the Third Workshop on Tau Lepton Physics, Montreux, Switzerland 1994, L. Rolandi edt., Nucl. Phys. B (Proc. Suppl.) 40 (1995) 413.

[401] S.I. Eidelman and V.N. Ivanchenko, Proceedings of the Third Workshop on Tau Lepton Physics, Montreux, Switzerland 1994, L. Rolandi edt., Nucl. Phys. B (Proc. Suppl.) 40 (1995) 131.

[402] R.J. Sobie, Proceedings of the Third Workshop on Tau Lepton Physics, Montreux, Switzerland 1994, L. Rolandi edt., Nucl. Phys. B (Proc. Suppl.) 40 (1995) 139.

[403] R. Decker, *Tau decays with kaons*, presented at Third Workshop on Tau Lepton Physics, Montreux, Switzerland, 19-22 September 1994, unpublished.

[404] M. Finkemeier and E. Mirkes, *Tau decays into kaons*, University of Wisconsin preprint MAD/PH/882 (1995).

[405] Y.S. Tsai, Phys. Rev. **D 4** (1971) 2821.

[406] H.B. Thacker and J.J. Sakurai, Phys. Lett. **B 36** (1971) 103.

[407] K.K.Gan, *New Results on Non-Strange Decays of the τ Lepton*, EPS-HEP Conference, Brussels, Jul. 27 - Aug. 2, 1995.

[408] F. Bossi, *Tau Decays into Kaons*, EPS-HEP Conference, Brussels, Jul. 27 - Aug. 2, 1995.

[409] ARGUS Collab., H. Albrecht *et al.*, *Tau decays into* K^* *mesons*, DESY preprint DESY 95-087 (1995).

[410] R. Balest, *Tau decays into three charged leptons and two neutrinos*, paper no. EPS0150 contributed to the EPS-HEP Conference, Brussels, Jul. 27 - Aug. 2, 1995.

[411] R. Balest, *Measurements of the decays* $\tau^- \to h^- h^+ h^- \nu_\tau$, CLNS preprint CLNS 95/1343, contributed to the EPS-HEP Conference, Brussels, Jul. 27 - Aug. 2, 1995.

[412] B. Barish, *First observation of the decay* $\tau^- \to K^- \eta \nu_\tau$, paper no. EPS0192 contributed to the EPS-HEP Conference, Brussels, Jul. 27 - Aug. 2, 1995.

[413] ALEPH Collab., D.Buskulic *et al.*, *Limit on the tau branching ratio into 7 or more particles and into undetected particles*, paper no. EPS045, contributed to the EPS-HEP Conference, Brussels, July 27 - August 2, 1995.

[414] ALEPH Collab., D.Buskulic *et al.*, *Measurement of the* $\tau \to \eta\pi\pi^0\nu_\tau$ *branching ratio using* $\eta \to \gamma\gamma$ *and* $\eta \to \pi^+\pi^-\pi^0$, paper no. EPS424, contributed to the EPS-HEP Conference, Brussels, July 27 - August 2, 1995.

[415] DELPHI Collab., L. Brugge *et al.*, *A measurement of τ decays into two charged kaons*, paper no. EPS0526, submitted to the EPS-HEP Conference, Brussels, Jul. 27 - Aug. 2, 1995.

[416] DELPHI Collab., L. Brugge *et al.*, *Measurements of* $\tau^\pm \to \nu_\tau K^0_s X^\pm$ *and* $\tau^\pm \to \nu_\tau K^0_s h^\pm \geq 0$ *neutrals*, paper no. EPS0526, submitted to the EPS-HEP Conference, Brussels, Jul. 27 - Aug. 2, 1995.

[417] L3 Collab., M. Acciarri *et al.*, Phys. Lett. **B 352** (1995) 497.

[418] OPAL Collab., R. Akers *et al.*, *Measurement of τ lepton decays to* K^0_s *accompanied by a charged pion or kaon*, paper no. EPS0298b contributed to the EPS-HEP Conference, Brussels, July 27 - August 2, 1995.

[419] OPAL Collab., R. Akers *et al.*, *Branching ratios of tau leptons to charged kaons in single prong decays*, paper no. EPS0298a contributed to the EPS-HEP Conference, Brussels, July 27 - August 2, 1995.

[420] OPAL Collab., R. Akers *et al.*, *Measurement of* $\tau^- \to h^- h^+ h^- \nu_\tau$ *and* $\tau^- \to h^- h^+ h^- \leq 1\pi^0\nu_\tau$ *branching ratios*, CERN preprint CERN-PPE/95-070, submitted to Z. Phys.

[421] N. Isgur, C. Morningstar and C. Reader, Phys. Rev. **D 39** (1989) 1357.

[422] J.H. Kuehn and A. Santamaria, Z. Phys. **C 48** (1990) 445.

[423] E. Braaten, Phys. Rev. Lett. **60** (1988) 1606.

[424] S. Narison and A. Pich, Phys. Lett. **B 211** (1988) 183.

[425] E. Braaten, Phys. Rev. **D 39** (1989) 1458.

[426] E. Braaten, S. Narison and A. Pich, Nucl. Phys. **B 373** (1992) 581.

[427] G. Altarelli, Proceedings of the Third Workshop on Tau Lepton Physics, Montreux, Switzerland 1994, L. Rolandi edt., Nucl. Phys. B (Proc. Suppl.) 40 (1995) 59.

[428] S.Narison, Proceedings of the Third Workshop on Tau Lepton Physics, Montreux, Switzerland 1994, L. Rolandi edt., Nucl. Phys. B (Proc. Suppl.) 40 (1995) 47.

[429] B.R. Webber,*QCD and Jet physics*, proceedings of XXVII International Conference on High Energy Physics (1994), P.J. Bussey I.G. Knowles edt., Institute of Physics Publishing, p. 213.

[430] S.Narison, *Simple but efficient tests of QCD from tau decays*, CERN preprint CERN-TH 7188/94 - PM94/08 talk given at the Symposium on Symmetry and Simplicity in Physics, Torino, 24-26 February 1994, published in Atti dell'Accademia delle Scienze di Torino.

[431] F.Le Diberder and A. Pich, Phys. Lett. **B 286** (1992) 147.

[432] F.Le Diberder and A. Pich, Phys. Lett. **B 289** (1992) 165.

[433] G.Altarelli,P.Nason and G.Ridolfi, *A Study of Ultraviolet Renormalon Ambiguities in the Determination of α_s from τ decays*, CERN preprint CERN-TH 7537/94 (1994).

[434] M.Neubert, *Resummation of Renormalon Chains for Cross Sections and Inclusive Decay Rates*, CERN-TH.7524/94, UM-TH-95-3, hep-ph/9502264 (1994), submitted to Phys. Rev. D.

[435] P.Ball, M. Beneke and V.M. Braun, *Resummation of $(\beta_0\alpha_s)^n$ Corrections in QCD: Techniques and Applications to the τ Hadronic Width and Heavy Quark Pole Mass*, CERN-TH/95-26, UM-TH-95-3, hep-ph/9502300 (1995).

[436] M.A.Shifman,A.L.Vainstein and V.I.Zakharov, Nucl. Phys. **B 147** (1979) 385.

[437] M. Beneke and V.I. Zakharov, Phys. Rev. Lett. **69** (1992) 2472.

[438] M. Beneke, Nucl. Phys. **B 385** (1992) 452.

[439] L.Duflot, Proceedings of the Third Workshop on Tau Lepton Physics, Montreux, Switzerland 1994, L. Rolandi edt., Nucl. Phys. B (Proc. Suppl.) 40 (1995) 37.

[440] M. Pohl, *Search for New Particles and New Interactions*, Proceedings of the XXVIIth International Conference on High Energy Physics, Glasgow Scotland 1994, P.J. Bussey and I.G. Knowles edt., Institute of Physics Publishing, 1994, p. 107.

[441] M. Kobayashi and T. Maskawa, Prog. Theor. Phys. **49** (1973) 652.

[442] J.H. Christenson *et al.*, Phys. Rev. Lett. **13** (1964) 138.

[443] *Introduction to $\mathcal{CP}$-Violation*, Advanced Series on Directions in High Energy Physics, Vol. 3, edt. C. Jarlskog, World Scientific (1989), p. 3;
R.N. Mohapatra, ibid. p. 348; R.N. Mohapatra, ibid. p. 436.

[444] W. Bernreuther and O. Nachtmann, Phys. Rev. Lett. **63** (1989) 2787.

[445] W. Bernreuther *et al.*, Z. Phys. **C 52** (1991) 567.

[446] W. Bernreuther *et al.*, Phys. Rev. **D 48** (1993) 78.

[447] D. Schaile, *Precision Tests of the Electroweak Interaction*, Proceedings of XXVII International Conference on High Energy Physics (1994), P.J. Bussey I.G. Knowles edt., Institute of Physics Publishing, p. 27.

[448] W. Hollik, Proceedings of XVI International Symposium on Lepton and Photon Physics (1993), P. Drell and D. Rubin edt., AIP, p. 354.

[449] A. Stahl, Proceedings of the Third Workshop on Tau Lepton Physics, Montreux, Switzerland 1994, L. Rolandi edt., Nucl. Phys. B (Proc. Suppl.) 40 (1995) 505.

[450] S.T. Petcov, Phys. Lett. **115 B** (1982) 402.

[451] J.D. Bjorken *et al.*, Phys. Rev. **D 16** (1977) 1474.

[452] V. Barger and D.V. Nanopoulos, Nuovo Cimento **A 44** (1978) 303.

[453] P. Minkowski, Phys. Lett. **67 B** (1977) 421.

[454] R.N. Mohapatra and X. Zhang, Phys. Rev. **D 46** (1992) 5331.

[455] R.N. Mohapatra, Phys. Rev. **D 46** (1992) 2990.

[456] R.N. Mohapatra *et al.*, Phys. Rev. **D 49** (1994) 2410.

[457] S. Kelley *et al.*, Nucl. Phys. **B 358** (1991) 27.

[458] R. Arnowitt and P. Nath, Phys. Rev. Lett. **66** (1991) 2708.

[459] J. Wu *et al.*, Phys. Rev. **D 47** (1993) 4006.

[460] M.C. Gonzales and J.W.F. Valle, Mod. Phys. Lett. **7** (1992) 477.

[461] G. Eilam and T.G. Rizzo, Phys. Lett. **B 188** (1987) 418.

[462] J. Bernabeu and A. Santamaria, Phys. Lett. **B 197** (1987) 418.

[463] J. Bernabeu *et al.*, Phys. Lett. **B 187** (1987) 303.

[464] T.K. Kuo and N. Nakagawa, Phys. Rev. **D 32** (1985) 306.

[465] M.J.S. Levine, Phys. Rev. **D 36** (1987) 1329.

[466] SINDRUM Collab., U. Bellgardt *et al.*, Nucl. Phys. **B 299** (1988) 1.

[467] I. Vorobiev, Proceedings of the Third Workshop on Tau Lepton Physics, Montreux, Switzerland 1994, L. Rolandi edt., Nucl. Phys. B (Proc. Suppl.) 40 (1995) 513.

[468] I. Vorobiev, private communication.

[469] G. Azuelos *et al.*, Phys. Rev. Lett. **51** (1983) 164.

[470] R.D. Bolton *et al.*, Phys. Rev. **D 38** (1988) 2077.

[471] Proceedings of the Workshop on Tau-Charm Factory in the Era of CESR and B-Factories, SLAC, Aug. 15-16, 1994, L.V. Beers and M.L. Perl edt., SLAC Report 451 (1994).

[472] Proceedings of the Third Workshop on the Tau-Charm Factory, J. Kirkby and R. Kirkby edt., Editions Frontière, Gif-sur-Yvette (1994).